Physics Letters B 816 (2021) 136204

Contents lists available at ScienceDirect

Physics Letters B

www.elsevier.com/locate/physletb

Measurement of the associated production of a Higgs boson decaying into b-quarks with a vector boson at high transverse momentum in pp collisions at $\sqrt{s} = 13$ TeV with the ATLAS detector

The ATLAS Collaboration *

ARTICLE INFO

Article history:
Received 6 August 2020
Received in revised form 3 February 2021
Accepted 5 March 2021
Available online 17 March 2021
Editor: M. Doser

ABSTRACT

The associated production of a Higgs boson with a W or Z boson decaying into leptons and where the Higgs boson decays to a $b\bar{b}$ pair is measured in the high vector-boson transverse momentum regime, above 250 GeV, with the ATLAS detector. The analysed data, corresponding to an integrated luminosity of 139 fb^{-1}, were collected in proton–proton collisions at the Large Hadron Collider between 2015 and 2018 at a centre-of-mass energy of $\sqrt{s} = 13$ TeV. The measured signal strength, defined as the ratio of the measured signal yield to that predicted by the Standard Model, is $0.72^{+0.39}_{-0.36}$ corresponding to an observed (expected) significance of 2.1 (2.7) standard deviations. Cross-sections of associated production of a Higgs boson decaying into b quark pairs with a W or Z gauge boson, decaying into leptons, are measured in two exclusive vector boson transverse momentum regions, 250–400 GeV and above 400 GeV, and interpreted as constraints on anomalous couplings in the framework of a Standard Model effective field theory.

1. Introduction

Since the discovery of the Higgs boson (H) [1–4] with a mass of around 125 GeV [5] by the ATLAS and CMS Collaborations [6,7] in 2012, the analysis of proton–proton (pp) collision data at centre-of-mass energies of 7 TeV, 8 TeV and 13 TeV delivered by the Large Hadron Collider (LHC) [8] has led to precise measurements of the main production cross-sections and decay rates of the Higgs boson, as well as measurements of its mass and its spin and parity properties. In particular, the observation of the decay of the Higgs boson into b-quark pairs provided direct evidence for the Yukawa coupling of the Higgs boson to down-type quarks [9,10]. Finally, a combination of 13 TeV results searching for the Higgs boson produced in association with a leptonically decaying W or Z boson established the observation of this production process [9]. A first cross-section measurement as a function of the vector-boson transverse momentum was also carried out by the ATLAS Collaboration [11].

The previous ATLAS analyses [9,11] in this channel were mainly sensitive to vector bosons with transverse momentum (p_{T}) in the range of approximately 100–300 GeV. These analyses considered a pair of jets with radius parameter of $R = 0.4$, referred to as small-radius (small-R) jets, to reconstruct the Higgs boson. For higher Higgs boson transverse momenta, the decay products can become close enough that they cannot be reconstructed with two small-R jets. To explore this 'boosted' regime, the Higgs boson is reconstructed as a single large-R jet with $R = 1.0$ [12]. This high-p_{T} regime is particularly interesting due to its sensitivity to physics beyond the Standard Model [13].

This Letter presents a measurement of cross-sections for the associated production of a high transverse momentum Higgs boson that decays into a $b\bar{b}$ pair with a leptonically decaying W or Z boson. The analysis uses pp collision data recorded between 2015 and 2018 by the ATLAS detector [14] during Run 2 at the LHC. This dataset corresponds to an integrated luminosity of 139 fb^{-1}. Events are selected in 0-, 1- and 2-lepton channels, based on the number of reconstructed charged leptons, ℓ (electrons or muons), in the final state to explore the $ZH \to \nu\nu b\bar{b}$, $WH \to \ell\nu b\bar{b}$ and $ZH \to \ell\ell b\bar{b}$ signatures, respectively. The Higgs boson is reconstructed as a single large-R jet and the b-quarks from its decay as a pair of jets, reconstructed with a p_{T}-dependent radius parameter, associated with the large-R jet and identified as containing a b-hadron.

The analysis using small-R jets and focusing on slightly lower Higgs boson transverse momentum regions was recently updated with the complete Run 2 dataset [15]. The large-R jet analysis significantly overlaps with the small-R jets analysis. The two results can therefore not be straightforwardly combined.

The dominant background processes after the event selection correspond to the production of V + jets, where V refers to either a W or Z boson, $t\bar{t}$, single-top and dibosons. The signal is extracted

* *E-mail address:* atlas.publications@cern.ch.

https://doi.org/10.1016/j.physletb.2021.136204

from a combined profile likelihood fit to the large-R jet mass, using several signal and control regions. The yield of diboson production VZ with $Z \to b\bar{b}$ is also measured using the same fit and provides a validation of the analysis. The cross-section measurements are performed within the simplified template cross-section (STXS) framework [16,17]. These measurements are then used to constrain anomalous couplings in a Standard Model effective field theory (SMEFT) [18].

2. ATLAS detector

The ATLAS detector [14] at the LHC is a multipurpose particle detector with a forward–backward symmetric cylindrical geometry and a near 4π coverage in solid angle.[1] It consists of an inner detector (ID) for tracking surrounded by a thin superconducting solenoid providing a 2 T axial magnetic field, electromagnetic and hadronic calorimeters, and a muon spectrometer. The ID covers the pseudorapidity range $|\eta| < 2.5$. It consists of silicon pixel, silicon microstrip, and transition radiation tracking detectors. An inner pixel layer, the insertable B-layer [19,20], was added at a mean radius of 3.3 cm during the long shutdown period between Run 1 and Run 2 of the LHC. Lead/liquid-argon (LAr) sampling calorimeters provide electromagnetic (EM) energy measurements with high granularity ($|\eta| < 3.2$). The hadronic calorimeter uses a steel/scintillator-tile sampling detector in the central pseudorapidity range ($|\eta| < 1.7$) and a copper/LAr detector in the region $1.5 < |\eta| < 3.2$. The forward regions ($3.2 < |\eta| < 4.9$) are instrumented with copper/LAr and tungsten/LAr calorimeter modules optimised for electromagnetic and hadronic measurements, respectively. A muon spectrometer with an air-core toroid magnet system surrounds the calorimeters. Three layers of high-precision tracking chambers provide coverage in the range $|\eta| < 2.7$, while dedicated fast chambers allow muon triggering in the region $|\eta| < 2.4$. The ATLAS trigger system consists of a hardware-based first-level trigger followed by a software-based high-level trigger [21].

3. Data and Monte Carlo simulation

The data were collected in pp collisions at $\sqrt{s} = 13$ TeV during Run 2 of the LHC. The data sample corresponds to an integrated luminosity of 139 fb^{-1} after requiring that all detector subsystems were operating normally and recording high-quality data [22]. The uncertainty in the combined 2015–2018 integrated luminosity is 1.7% [23], obtained using the LUCID-2 detector [24] for the primary luminosity measurements. Collision events considered for this analysis were recorded with a combination of triggers selecting events with high missing transverse momentum or with a high-p_{T} lepton, depending on the analysis channel. More details of the trigger selection are given in Section 5.

Monte Carlo (MC) simulated event samples processed with the ATLAS detector simulation [25] based on Geant 4 [26] are used to model the signal and background contributions, except for the multijet production, whose contribution is estimated with data-driven techniques as detailed in Section 6. A summary of all the signal and background processes with the corresponding generators used for the nominal samples is shown in Table 1. All simulated processes are normalised using the most precise theoretical predictions currently available of their cross-sections. In addition to the hard scatter, each event was overlaid with additional pp collisions (pile-up) generated with Pythia 8.1 [27] using the ATLAS A3 set of tuned parameters [28] and the NNPDF23LO [29] parton distribution function (PDF) set. Simulated events were then reconstructed with the same algorithms as those applied to data and are weighted to match the pile-up distribution observed in the data.

For the signal events, the AZNLO [30] model of parton showers and the underlying event (UE) was used. For the top-quark pair and single-top-quark production processes, the UE model was taken from the ATLAS A14 [31] set of tuned Pythia 8.1 [27] parameters and for the other backgrounds the default Sherpa [32–35] tune set was used. For all samples of simulated events, except for those generated using Sherpa, the EvtGen v1.2.0 program [36] was used to describe the decays of bottom and charm hadrons. The nominal PDF set used for W/Z+jets and diboson processes was NNPDF3.0NNLO [37] while for the top-quark pair and single-top production the NNPDF3.0NLO [37] set was used. Samples produced with alternative generators which are used to estimate modelling systematic uncertainties are described in Section 7.

All qq-initiated signal processes were simulated with up to one additional parton at next-to-leading-order (NLO) accuracy in QCD using the Powheg-Box v2 [41] and the GoSam [43] generator with the MiNLO (Multiscale Improved NLO) [44,45] procedure applied, interfaced to Pythia 8.212 for the simulation of the parton shower (PS), UE and multiple parton interactions. The $gg \to ZH$ contribution was simulated at leading order (LO) in QCD with Powheg-Box v2. The $gg \to ZH$ cross-section process was calculated at NLO in QCD including soft gluon resummation up to next-to-leading logarithms (NLL) [53–57]. Signal MC events were generated using the NNPDF3.0NLO PDF set and subsequently reweighted to the PDF4LHC15NLO PDF set [38]. The total inclusive cross-sections for all signal processes (WH and ZH) were calculated at next-to-next-to-leading-order (NNLO) QCD and NLO electroweak (EW) [46–52] accuracy, including photon-induced contributions calculated with Hawk [39,40].

The nominal top-quark pair production generator was Powheg-Box v2 with real and virtual corrections at NLO accuracy in QCD and interfaced to Pythia 8.230 for the parton showering. The nominal top-quark pair production cross-section is from a resummed NNLO and next-to-next-to-leading logarithm (NNLL) prediction [59].

Single top-quark production was also generated with Powheg-Box v2 interfaced to Pythia 8.230. The nominal cross-section normalisations for the single top-quark production s- and t-processes were estimated from resummed calculations at NLO, while for the Wt process approximate NNLO was used [61,62,64]. At higher orders in QCD, the definition of the Wt process can correspond to leading-order top-quark pair production processes. To account for these ambiguities and related interference effects when generating the processes separately, the diagram removal (DR) subtraction scheme was used [68].

The nominal W/Z+jets background samples used Sherpa 2.2.1 [33–35] for the matrix element (ME) and parton shower with virtual corrections at NLO accuracy for up to two additional jets and at LO for up to four additional jets using OpenLoops [32,34,35]. In these samples, the simulation of the emission of hard partons matched with a parton shower was based on the Catani–Seymour subtraction term [32,34,35] and the multi-parton ME was merged with the parton shower using an improved ckkw matching procedure extended to NLO accuracy using the MEPS@NLO prescription [66]. The nominal normalisation of this background was obtained from an NNLO fixed-order estimate [67].

The diboson nominal samples were generated using Sherpa 2.2.1 for the dominant qq-initiated processes for which zero or one additional parton was calculated at NLO in the ME, while two or

[1] ATLAS uses a right-handed coordinate system with its origin at the nominal interaction point in the centre of the detector. The positive x-axis is defined by the direction from the interaction point to the centre of the LHC ring, with the positive y-axis pointing upwards, while the beam direction defines the z-axis. Cylindrical coordinates (r, ϕ) are used in the transverse plane, ϕ being the azimuthal angle around the z-axis. The pseudorapidity η is defined in terms of the polar angle θ by $\eta = -\ln\tan(\theta/2)$. The angular distance is defined as $\Delta R \equiv \sqrt{(\Delta\eta)^2 + (\Delta\phi)^2}$. Rapidity is defined as $y = 0.5\ln[(E + p_z)/(E - p_z)]$ where E denotes the energy and p_z is the component of the momentum along the beam direction.

Table 1
Signal and background processes with the corresponding generators used for the nominal samples. If not specified, the order of the cross-section calculation refers to the expansion in the strong coupling constant (α_S). ($\star$) The events were generated using the first PDF in the NNPDF3.0NLO set and subsequently reweighted to the PDF4LHC15NLO set [38] using the internal algorithm in Powheg-Box v2. (†) The NNLO(QCD)+NLO(EW) cross-section calculation for the $pp \to ZH$ process already includes the $gg \to ZH$ contribution. The $qq \to ZH$ process is normalised using the cross-section for the $pp \to ZH$ process, after subtracting the $gg \to ZH$ contribution. An additional scale factor is applied to the $qq \to VH$ processes as a function of the transverse momentum of the vector boson, to account for electroweak (EW) corrections at NLO. This makes use of the VH differential cross-section computed with Hawk [39,40].

Process	ME generator	ME PDF	PS and hadronisation	UE model tune	Cross-section order
Signal ($m_H = 125$ GeV and $b\bar{b}$ branching fraction set to 58%)					
$qq \to WH \to \ell\nu b\bar{b}$	Powheg-Box v2 [41] + GoSam [43] + MiNLO [44,45]	NNPDF3.0NLO$^{(\star)}$ [37]	Pythia 8.212 [42]	AZNLO [30]	NNLO(QCD)+ NLO(EW) [46–52]
$qq \to ZH \to \nu\nu b\bar{b}/\ell\ell b\bar{b}$	Powheg-Box v2 + GoSam + MiNLO	NNPDF3.0NLO$^{(\star)}$	Pythia 8.212	AZNLO	NNLO(QCD)$^{(\dagger)}$+ NLO(EW)
$gg \to ZH \to \nu\nu b\bar{b}/\ell\ell b\bar{b}$	Powheg-Box v2	NNPDF3.0NLO$^{(\star)}$	Pythia 8.212	AZNLO	NLO+ NLL [53–57]
Top quark ($m_t = 172.5$ GeV)					
$t\bar{t}$	Powheg-Box v2 [41,58]	NNPDF3.0NLO	Pythia 8.230	A14 [31]	NNLO+NNLL [59]
s-channel	Powheg-Box v2 [41,60]	NNPDF3.0NLO	Pythia 8.230	A14	NLO [61]
t-channel	Powheg-Box v2 [41,60]	NNPDF3.0NLO	Pythia 8.230	A14	NLO [62]
Wt	Powheg-Box v2 [41,63]	NNPDF3.0NLO	Pythia 8.230	A14	Approximate NNLO [64]
Vector boson + jets					
$W \to \ell\nu$	Sherpa 2.2.1 [32–35]	NNPDF3.0NNLO	Sherpa 2.2.1 [65,66]	Default	NNLO [67]
$Z/\gamma^* \to \ell\ell$	Sherpa 2.2.1	NNPDF3.0NNLO	Sherpa 2.2.1	Default	NNLO
$Z \to \nu\nu$	Sherpa 2.2.1	NNPDF3.0NNLO	Sherpa 2.2.1	Default	NNLO
Diboson					
$qq \to WW$	Sherpa 2.2.1	NNPDF3.0NNLO	Sherpa 2.2.1	Default	NLO
$qq \to WZ$	Sherpa 2.2.1	NNPDF3.0NNLO	Sherpa 2.2.1	Default	NLO
$qq \to ZZ$	Sherpa 2.2.1	NNPDF3.0NNLO	Sherpa 2.2.1	Default	NLO
$gg \to VV$	Sherpa 2.2.2	NNPDF3.0NNLO	Sherpa 2.2.2	Default	NLO

three additional partons were included at LO in QCD. The subdominant gg-initiated processes were generated with Sherpa 2.2.2. For these samples, zero or one additional parton was calculated at LO in the ME. These generators also provided the nominal normalisation for this process.

4. Object reconstruction

Of all the reconstructed pp collision vertices with at least two reconstructed trajectories of charged particles in the ID (tracks) with $p_{\mathrm{T}} > 0.5$ GeV, the hard-scattering primary vertex is selected as the one with the highest sum of squared transverse momenta of associated tracks [69].

Leptons are used for event categorisation as described in Section 5. Electrons are reconstructed from tracks in the ID associated with topological clusters of energy depositions in the calorimeter [70,71]. The identification criteria closely follow those described in Ref. [9]. *Baseline* electrons are required to have $p_{\mathrm{T}} > 7$ GeV and $|\eta| < 2.47$, to be isolated from other tracks and energy deposit clusters, to meet loose likelihood selection criteria based on shower shapes and to satisfy $|d_0/\sigma(d_0)| < 5$ and $|z_0 \sin\theta| < 0.5$ mm, where d_0 and z_0 are the transverse and longitudinal impact parameters defined relative to the primary vertex position[2] and $\sigma(d_0)$ is the d_0 uncertainty. *Signal* electrons are a subset of the baseline electron set and are selected using a tighter likelihood requirement, which also includes tracking and track–cluster matching variables, and using a tighter calorimeter-based isolation criterion.

Muon candidates are identified by matching ID tracks to full tracks or track segments reconstructed in the muon spectrometer within the inner detector coverage and using only information from the muon spectrometer outside of that coverage. Muons are required to have $p_{\mathrm{T}} > 7$ GeV and $|\eta| < 2.7$ and to have $|d_0/\sigma(d_0)| < 3$ and $|z_0 \sin\theta| < 0.5$ mm. Two muon categories are used in the analysis: *baseline* muons are selected using the 'loose' identification criterion of Ref. [72] and a loose track isolation; *signal* muons are required to have $|\eta| < 2.5$, to satisfy the 'medium' identification criterion [72] and a tighter track-based isolation criterion.

The low-threshold (7 GeV) *baseline* leptons are used to define the three main channels requiring exactly zero, one and two leptons. The latter 1- and 2-lepton channels further require at least one *signal* lepton, with identification and isolation requirements chosen to optimise the suppression of the multijet background. Signal leptons must have a $p_{\mathrm{T}} > 27$ GeV (except in the 1-lepton muon sub-channel where a $p_{\mathrm{T}} > 25$ GeV is used).

Calorimeter jets are reconstructed from noise-suppressed topological clusters (topoclusters) of calorimeter energy depositions [73], using the anti-k_t algorithm [74] with radius parameter $R = 1.0$ (large-R jets) or $R = 0.4$ (small-R jets) implemented in FastJet [75]. Small-R jets are built from topoclusters calibrated at the electromagnetic scale [76], while large-R jets are built from topoclusters calibrated at the local hadronic scale [73]. Large-R jets are groomed using trimming [77,78] to improve the jet mass resolution and its stability with respect to pile-up by discarding the softer components of jets that originate from initial-state radiation, pile-up interactions, or the underlying event. This is done by reclustering the constituents of the initial large-R jet, using the k_t algorithm [79,80], into subjets with radius parameter $R_{\mathrm{sub}} = 0.2$ and removing any subjet that has a p_{T} less than 5% of the parent jet p_{T}. The large-R jet mass m_{J} is computed using tracking and calorimeter information [81]. A dedicated MC-based calibration, similar to the procedure used in Ref. [81], is applied to correct the p_{T} and mass of the trimmed jets to the particle level. Large-R jets are required to have $p_{\mathrm{T}} > 250$ GeV, $m_{\mathrm{J}} > 50$ GeV and $|\eta| < 2.0$, the last due to tracking acceptance.

Small-R jets are used in building the missing transverse momentum and event categorisation. They are calibrated with a series of simulation-based corrections and *in situ* techniques, including corrections to account for pile-up energy entering the jet area, as described in Ref. [76]. They are required to have $p_{\mathrm{T}} > 30$ GeV and $|\eta| < 4.5$. To reduce the number of small-R jets originating from

[2] For the computation of the impact parameters, the beam line is used to approximate the primary vertex position in the transverse plane.

pile-up interactions, small-R jets are required to pass the jet vertex tagger (JVT) [82] requirement if they are in the range $p_{\mathrm{T}} < 120$ GeV and $|\eta| < 2.5$ due to tracking acceptance.

Track-jets formed from charged-particle tracks are used to reconstruct a candidate two-body $H \to b\bar{b}$ decay within the large-R jet. Track-jets are built with the anti-k_t algorithm with a variable radius (VR) p_{T}-dependent parameter, from tracks reconstructed in the inner detector with $p_{\mathrm{T}} > 0.5$ GeV and $|\eta| < 2.5$ [83–85]. VR track-jets have an effective jet radius R_{eff} proportional to the inverse of the jet p_{T} in the jet finding procedure: $R_{\mathrm{eff}}(p_{\mathrm{T}}) = \rho/p_{\mathrm{T}}$, where the ρ-parameter is set to 30 GeV. There are two additional parameters, R_{min} and R_{max}, used to set the minimum and maximum cut-offs on the jet radius, and these are set to 0.02 and 0.4, respectively. Only VR track-jets with $p_{\mathrm{T}} > 10$ GeV, $|\eta| < 2.5$ and with at least two constituents are considered [86]. VR track-jets are matched to the large-R calorimeter jets via ghost-association [87]. Track-jets not associated with large-R jets are also used in the analysis for event categorisation as described in Section 5.

The 'truth' flavour labelling of track-jets in simulation is done by geometrically matching the jet to 'truth' hadrons, using 'truth' information from the generator's event record. If a b-hadron with p_{T} above 5 GeV is found within $\Delta R = 0.3$ of the direction of the track-jet, the track-jet is labelled as a b-jet. If the b-hadron is matched to more than one track-jet, only the closest track-jet is labelled as a b-jet. If no b-hadron is found, the procedure is repeated first for c-hadrons to label c-jets and then for τ-leptons to label τ-jets. As is the case for defining a b-jet, the labelling is also exclusive for c- and τ-jets. A jet for which no such matching can be made is labelled as a light-flavour jet.

To identify track-jets containing b-hadron decay products, track-jets are tagged using the multivariate algorithm MV2c10, which exploits the presence of large-impact-parameter tracks, the topological decay chain reconstruction and the displaced vertices from b-hadron decays [88,89]. The MV2c10 algorithm is configured to achieve an average efficiency of 70% for tagging jets labelled as b-jets in an MC sample of $t\bar{t}$ events. This requirement has corresponding rejection factors of 9 and 304 for jets labelled as c-jets and light-flavour jets, respectively, in simulated $t\bar{t}$ events. The tagging efficiencies per jet flavour are corrected in the simulation to match those measured in data [86,90,91].

Two additional corrections are applied to the large-R jets to improve the scale and the resolution of their energy and mass measurements. First, to account for semileptonic decays of the b-hadrons, the four-momentum of the closest reconstructed non-isolated muon candidate within $\Delta R = \min(0.4, 0.04 + 10\ \mathrm{GeV}/p_{\mathrm{T}}^{\mathrm{muon}})$ of a track-jet matched to the large-R jet by ghost association is added to the calorimeter-based component of the large-R jet four-momentum while its expected calorimeter energy deposits are removed [85]. This is known as the muon-in-jet correction. Non-isolated muons satisfy the 'medium' identification criterion [72], but no isolation or impact parameter criteria are applied. Second, in the 2-lepton channel only, a per-event likelihood uses the full reconstruction of the event kinematics to improve the estimate of the energy of the b-jets [92]. The kinematic fit constrains the $\ell^+\ell^- b\bar{b}$ system and the additional small-R jets in the event to be balanced in the transverse plane and the dilepton system to the Z boson mass, by scaling the four-momentum of the objects in the event including the large-R jet, additional small-R jets and leptons within their detector response resolutions. The large-R jet mass is then scaled by the ratio of the energies after and before the correction. For the event selection detailed in Section 5, the large-R jet mass resolution improves by 5% to 10% after the first correction (depending on the lepton channel), while the second correction brings an additional improvement in the 2-lepton channel of up to 40%.

The presence of neutrinos in the $WH \to \ell\nu b\bar{b}$ and $ZH \to \nu\nu b\bar{b}$ signatures can be inferred from a momentum imbalance in the transverse plane. The missing transverse momentum $\boldsymbol{E}_{\mathrm{T}}^{\mathrm{miss}}$ is reconstructed as the negative vector sum of the momenta of leptons and small-R jets in the event plus a 'soft term' built from additional tracks associated with the primary vertex [93]. Small-R jets used for the $\boldsymbol{E}_{\mathrm{T}}^{\mathrm{miss}}$ reconstruction are required to have $p_{\mathrm{T}} > 20$ GeV. The magnitude of $\boldsymbol{E}_{\mathrm{T}}^{\mathrm{miss}}$ is referred to as $E_{\mathrm{T}}^{\mathrm{miss}}$. To suppress non-collision and multijet backgrounds in the 0-lepton channel, an additional track-based missing transverse momentum estimator, $\boldsymbol{E}_{\mathrm{T,\,trk}}^{\mathrm{miss}}$, is built independently as the negative vector sum of the transverse momenta of all tracks from the primary vertex.

An overlap removal procedure is applied to avoid double-counting between reconstructed leptons [9], including hadronically decaying τ-leptons [94], and small-R jets [92].

5. Event selection

Events are categorised into the 0-, 1- and 2-lepton channels depending on the number of selected electrons and muons to target the $ZH \to \nu\nu b\bar{b}$, $WH \to \ell\nu b\bar{b}$ and $ZH \to \ell\ell b\bar{b}$ signatures, respectively.

The 0-lepton selection is applied to events selected with an $E_{\mathrm{T}}^{\mathrm{miss}}$ trigger with thresholds varying from 70 to 110 GeV depending on the data-taking period to cope with increasing trigger rates at higher instantaneous luminosities. In the 1-lepton channel, single-electron events are required to be triggered by at least one of several unprescaled single-electron triggers. The lowest E_{T} threshold of these unprescaled triggers varied with time from 24 to 26 GeV. Events in the single-muon channel were triggered using the same $E_{\mathrm{T}}^{\mathrm{miss}}$ trigger as used in the 0-lepton channel. Given that muons do not enter in the online $E_{\mathrm{T}}^{\mathrm{miss}}$ calculation and that uninstrumented regions affect the coverage of the muon spectrometer, the $E_{\mathrm{T}}^{\mathrm{miss}}$ triggers translate into a requirement on the transverse momentum of the lepton and neutrino pair, $p_{\mathrm{T}}^{\ell\nu}$, which is more efficient in the analysis phase space than the single-muon triggers. In the 2-lepton channel, the same trigger strategy as in the 1-lepton channel is adopted. The dielectron selection is applied to events triggered by at least one of the un-prescaled single-electron triggers. The dimuon selection is applied to events triggered by an $E_{\mathrm{T}}^{\mathrm{miss}}$ trigger. All triggers used in this analysis are fully efficient for the events selected using the requirements described below.

In all three channels, events are required to contain at least one large-R jet with $p_{\mathrm{T}} > 250$ GeV and $|\eta| < 2.0$. To select the Higgs boson candidate, the leading p_{T} large-R jet is chosen, at least two VR track-jets are required to be matched to it by ghost-association, and the two leading ones are required to be b-tagged. This jet is referred to as the 'Higgs-jet candidate' in the following. To avoid the ambiguous cases of concentric jets, events where the b-tagged VR track-jets overlap with other VR track-jets, satisfying $\Delta R/R_{\mathrm{s}} < 1$ (where ΔR corresponds to the distance among any pair of VR track-jets and R_{s} corresponds to the smaller radius of the considered pair), are removed. The reconstructed transverse momentum p_{T}^{V} of the vector boson corresponds to $E_{\mathrm{T}}^{\mathrm{miss}}$ in the 0-lepton channel, to the magnitude of the vector sum of $\boldsymbol{E}_{\mathrm{T}}^{\mathrm{miss}}$ and the charged-lepton transverse momentum in the 1-lepton channel, and to the transverse momentum of the 2-lepton system in the 2-lepton channel. The p_{T}^{V} is required to be above 250 GeV in all three channels. The event selection is detailed in Table 2, with further explanations provided below for the non-straightforward selection criteria.

The multijet background in the 0-lepton channel originates mainly from jet energy mismeasurements. To reduce this background to a negligible level, three dedicated selection criteria are applied. Events are removed if the missing transverse momentum is pointing towards the direction of the Higgs-jet candidate

Table 2
Event selection requirements for the boosted $VH, H \to b\bar{b}$ analysis channels and sub-channels.

Selection	0 lepton channel	1 lepton channel		2 leptons channel	
		e sub-channel	μ sub-channel	e sub-channel	μ sub-channel
Trigger	$E_{\mathrm{T}}^{\mathrm{miss}}$	Single electron	$E_{\mathrm{T}}^{\mathrm{miss}}$	Single electron	$E_{\mathrm{T}}^{\mathrm{miss}}$
Leptons	0 *baseline* leptons	1 *signal* lepton $p_{\mathrm{T}} > 27$ GeV no second *baseline* lepton	$p_{\mathrm{T}} > 25$ GeV -	2 *baseline* leptons among which ≥ 1 *signal* lepton, $p_{\mathrm{T}} > 27$ GeV both leptons of the same flavour opposite sign muons	
$E_{\mathrm{T}}^{\mathrm{miss}}$	> 250 GeV	> 50 GeV	-	-	
p_{T}^{V}	$p_{\mathrm{T}}^{V} > 250$ GeV				
Large-R jets	at least one large-R jet, $p_{\mathrm{T}} > 250$ GeV , $\lvert\eta\rvert < 2.0$				
Track-jets	at least two track-jets, $p_{\mathrm{T}} > 10$ GeV , $\lvert\eta\rvert < 2.5$, matched to the leading large-R jet				
b-tagged jets	leading two track-jets matched to the leading large-R must be b-tagged (MV2c10, 70%)				
m_{J}	> 50 GeV				
$\min[\Delta\phi(\boldsymbol{E}_{\mathrm{T}}^{\mathrm{miss}}, \text{small-}R \text{ jets})]$	$> 30°$	-			
$\Delta\phi(\boldsymbol{E}_{\mathrm{T}}^{\mathrm{miss}}, H_{\mathrm{cand}})$	$> 120°$	-			
$\Delta\phi\,(\boldsymbol{E}_{\mathrm{T}}^{\mathrm{miss}}, \boldsymbol{E}_{\mathrm{T,\,trk}}^{\mathrm{miss}})$	$< 90°$	-			
$\Delta y(V, H_{\mathrm{cand}})$	-	$\lvert\Delta y(V, H_{\mathrm{cand}})\rvert < 1.4$			
$m_{\ell\ell}$	-			66 GeV $< m_{\ell\ell} <$ 116 GeV	
Lepton p_{T} imbalance	-			$(p_{\mathrm{T}}^{\ell_1} - p_{\mathrm{T}}^{\ell_2})/p_{\mathrm{T}}^{Z} < 0.8$	

($\Delta\phi(\boldsymbol{E}_{\mathrm{T}}^{\mathrm{miss}}, H_{\mathrm{cand}}) > 120°$). Events are also removed if the calorimetric $\boldsymbol{E}_{\mathrm{T}}^{\mathrm{miss}}$ and the track $\boldsymbol{E}_{\mathrm{T,\,trk}}^{\mathrm{miss}}$ are far apart ($\Delta\phi(\boldsymbol{E}_{\mathrm{T}}^{\mathrm{miss}}, \boldsymbol{E}_{\mathrm{T,\,trk}}^{\mathrm{miss}}) < 90°$). The $\boldsymbol{E}_{\mathrm{T}}^{\mathrm{miss}}$ is required to be isolated from any calorimeter small-R jet with transverse momentum in excess of 70 GeV ($\min[\Delta\phi(\boldsymbol{E}_{\mathrm{T}}^{\mathrm{miss}}, \text{small-}R \text{ jets})] > 30°$). In this case, only small-R jets not overlapping with the Higgs-jet candidate within $\Delta R = 1.0$ are considered.

In the 1-lepton channel, the isolation requirements remove most of the non-prompt lepton background. An additional $E_{\mathrm{T}}^{\mathrm{miss}}$ requirement is applied in the electron sub-channel to reduce this background further. In order to reduce other backgrounds, such as top and W+jets production, a further selection on the rapidity difference between the Higgs-jet candidate and the vector boson is applied ($\lvert\Delta y(V, H_{\mathrm{cand}})\rvert < 1.4$). The W-boson rapidity is estimated assuming that $E_{\mathrm{T}}^{\mathrm{miss}}$ is the p_{T} of the neutrino and the longitudinal momentum of the neutrino is estimated using the W-boson mass constraint. This method leads to a quadratic equation for the longitudinal momentum of the neutrino. In case of two real solutions: the retained solution is the one that minimises the difference between the longitudinal boost of the W boson and the Higgs boson. In case of no real solution, the imaginary part is set to 0.[3]

In the 2-lepton channel, where two same-flavour leptons are required (in the dimuon sub-channel the two muons are further required to be of opposite sign, in the dielectron case this selection is not applied due to the comparatively higher charge misidentification), the rapidity difference ($\lvert\Delta y(V, H_{\mathrm{cand}})\rvert < 1.4$) effectively reduces the main Z+jets background. A requirement is imposed on the lepton p_{T} imbalance ($(p_{\mathrm{T}}^{\ell_1} - p_{\mathrm{T}}^{\ell_2})/p_{\mathrm{T}}^{Z} < 0.8$), which is sensitive to the Z boson polarisation [95]. Since the Z boson has different states of polarisation in the ZH signal and the Z+jets background, this selection further reduces this background.

Since the signal-to-background ratio increases for large Higgs boson transverse momenta [12,96], events are further split into two p_{T}^{V} bins with $250 < p_{\mathrm{T}}^{V} < 400$ GeV and with $p_{\mathrm{T}}^{V} \geq 400$ GeV.

[3] This procedure is equivalent to setting the reconstructed W transverse mass to the W mass.

The selection efficiency in the 0-, 1- and 2-lepton channels and two p_{T}^{V} bins ranges between approximately 6% and 16% for the WH and ZH processes where the W and Z bosons decay leptonically and the Higgs boson decays into a pair of b-quarks. The analysis does not explicitly select τ-leptons but they are accounted for in the case of leptonically decaying τ-leptons in the 1- and 2-lepton channels and hadronically decaying τ-leptons in the 0-lepton channel if they are misidentified as jets.

As discussed in Section 1 the overlaps between the event selections presented herein and those of Ref. [15] are non negligible. In the 250 GeV $< p_{\mathrm{T}}^{V} <$ 400 GeV region, approximately 40% of the signal events are selected by both sets of selections, and the fraction of signal events uniquely selected by the large-R jet analysis varies between 5% and 30% with increasing p_{T}^{V}. In the $p_{\mathrm{T}}^{V} >$ 400 GeV region, the overlap decreases progressively to reach approximately 15% and the unique large-R jet analysis signal events increase to 75% at a p_{T}^{V} of around 700 GeV.

The $t\bar{t}$ process is a major background in the 0- and 1-lepton channels. For $t\bar{t}$ events, the b-tagged track-jets associated with the Higgs-jet candidate are mainly a b- and a c-jet (the former from a top-quark decay and the latter from the hadronic W boson decay) and therefore the second b-jet from the other top-quark is often expected to be identified as an additional b-tagged track-jet not associated with the Higgs-jet candidate. Taking this into account, signal regions (SR) in the 0- and 1-lepton channels are defined by vetoing on b-tagged track-jets outside the Higgs-jet candidate and control regions (CR), enriched in $t\bar{t}$ events, are built from events which fail this veto. The SRs and CRs are accounted for in the same way in the fit, but CRs are dominated by backgrounds and are used to constrain specific background components.

Events in the 0- and 1-lepton channels are further categorised depending on the number of small-R jets not matched to the Higgs-jet candidate, i.e. with $\Delta R(H_{\mathrm{cand}}, \text{small-}R \text{ jet}) > 1.0$. Two categories are defined: a *high-purity* signal region (HP SR) with 0 small-R jets not matched to the Higgs-jet candidate and a *low-purity* signal region (LP SR) with ≥ 1 small-R jets not matched to the Higgs-jet candidate.

The ten SRs and the four CRs are summarised in Table 3.

Table 3
Summary of the definition of the analysis regions. Signal enriched regions are marked with the label SR. There are regions with relatively large signal purity (HP SR) and with low purity (LP SR). Background enriched regions are marked with the label CR. The shorthand "add" stands for additional small-R jets, i.e. number of small-R jets not matched to the Higgs-jet candidate.

Channel	Categories					
	$250 < p_{\mathrm{T}}^{V} < 400$ GeV			$p_{\mathrm{T}}^{V} \geq 400$ GeV		
	0 add. b-track-jets		≥ 1 add. b-track-jets	0 add. b-track-jets		≥ 1 add. b-track-jets
	0 add. small-R jets	≥ 1 add. small-R jets		0 add. small-R jets	≥ 1 add. small-R jets	
0-lepton	HP SR	LP SR	CR	HP SR	LP SR	CR
1-lepton	HP SR	LP SR	CR	HP SR	LP SR	CR
2-lepton	SR			SR		

6. Background composition and estimation

The background contribution in the SRs is different for each of the three channels. In the 0-lepton channel, the dominant background sources are $Z+$jets and $t\bar{t}$ events with a significant contribution from $W+$jets and diboson production. In the 1-lepton channel, the largest backgrounds are $t\bar{t}$ and $W+$jets production followed by the single-top background. In the 2-lepton channel, $Z+$jets production is the dominant background followed by the ZZ background. Contributions from $t\bar{t}V$ and $t\bar{t}H$ are negligible. The multijet background, due to semileptonic heavy-flavour-hadron decays or misidentified jets, is found to be negligible in the 0- and 2-lepton channels as well as in the 1-lepton muon sub-channel after applying the event selections described in Section 5, as confirmed using data-driven techniques. In the 1-lepton electron sub-channel its contribution is not neglected. All initial background distribution shapes prior to the fit (described in Section 8), except those for multijet, are estimated from the samples of simulated events. The multijet shape and normalisation are determined using data.

The W/Z+jets simulated event samples are split into 6 categories depending on the 'truth' labels of the track-jets ghost-associated to the Higgs-jet candidate: $W/Z+bb$, $W/Z+bc$, $W/Z+bl$, $W/Z+cc$, $W/Z+cl$ and $W/Z+ll$; in this notation l refers to a light-flavour jet.[4] The $W/Z+bb$ fraction corresponds to approximately 80% of the total W/Z+jets background. This categorisation is used in the uncertainties variations of the ratios $V+bc/V+bb$, $V+bl/V+bb$ and $V+cc/V+bb$ to cover uncertainties on the flavour composition in V+jets production, see Section 7.

In the statistical analysis described in Section 8, the components $W/Z+bb$, $W/Z+bc$, $W/Z+bl$ and $W/Z+cc$ are treated as a single background component denoted by W/Z+HF. The W+HF and Z+HF contributions, which together constitute 90% of V+jets background, are estimated separately, each with its own normalisation factor determined from the fit to data.

The $t\bar{t}$ production background arises from topologies with decays of W bosons into τ-leptons which then decay hadronically in the 0-lepton channel and from W bosons decaying into e/μ in the 1-lepton channel. In the 2-lepton channel the $t\bar{t}$ contribution is much smaller. For the 0- and 1-lepton channels, two independent normalisation factors are considered and left floating in the fit, where they are constrained by the CRs.

Single-top production contributes to the 0- and 1-lepton channels and Wt production is the dominant process (s- and t-channel processes amount to less than 1% globally and less than 5% of the single-top contribution).

The diboson background process consists of final states arising mostly from WZ and ZZ events, where a Z boson decays into a pair of b-quarks. This process has a topology very similar to that of the signal, exhibiting a peak in m_{J} at the mass of the hadronically decaying vector boson. Although it is a subdominant contribution, it provides an important reference for validation. Its normalisation is measured simultaneously with the VH signal.

In the 1-lepton channel, the multijet background originating from jets misidentified as leptons and/or due to semileptonic heavy-flavour-hadron decays cannot be neglected. Since MC simulation samples are statistically limited and are not expected to reproduce the multijet production in this corner of the phase space, it is estimated from a template fit using the data. The m_{J} templates in the electron and muon sub-channels are taken from dedicated CRs enriched in multijet background, obtained from the inversion of the tight lepton isolation requirements and the removal of the $E_{\mathrm{T}}^{\mathrm{miss}}$ requirement, and after subtraction of the other backgrounds. The multijet normalisations are estimated in the SRs from a fit to the transverse mass[5] distribution separately for the electron and muon sub-channels. The contribution of the multijet background is found to be negligible in the muon sub-channel. In the electron sub-channel it is approximately 2% of the total background, with an uncertainty of 55% estimated mainly from the statistical uncertainty of the transverse mass fit. This contribution and its associated uncertainty are taken into account in the signal extraction fit.

7. Systematic uncertainties

Systematic uncertainties can have an impact on the overall signal and background yields, on the shapes of the jet mass distributions, on the CR to SR extrapolations, and on the relative acceptances between the HP and LP SRs and between the p_{T}^{V} bins. Systematic uncertainties are discussed herein for three main categories: experimental, signal modelling, and background modelling.

7.1. Experimental systematic uncertainties

The uncertainties in the small-R jet energy scale and resolution have contributions from *in situ* calibration studies, from the dependency on the pile-up activity and on the flavour composition of the jets [76]. For large-R jets, the uncertainties in the energy and mass scales are based on a comparison of the ratio of calorimeter-based to track-based measurements in dijet data and simulation, as described in Ref. [81]. The impact of the jet energy scale and resolution uncertainties on the large-R jet mass are assessed by applying different calibration scales and smearings to

[4] When labelling jets in the $V+$jets backgrounds modelling, the labelling of τ-jets is omitted and the negligible τ-lepton contribution is included with light-flavour jets.

[5] The transverse mass m_{T} of the W boson candidate in the event is calculated using the lepton candidate and $E_{\mathrm{T}}^{\mathrm{miss}}$ according to $m_{\mathrm{T}} = \sqrt{2p_{\mathrm{T}}^{\ell}E_{\mathrm{T}}^{\mathrm{miss}}(1-\cos\Delta\phi(\ell, E_{\mathrm{T}}^{\mathrm{miss}}))}$.

the jet observables in the simulation, according to the estimated uncertainties. An absolute uncertainty of 2% is used for the jet energy resolution while a relative uncertainty of 20% is used for the jet mass resolution, consistent with previous studies for trimmed jets [97,98].

The b-tagging uncertainties are assessed from the calibration data in various kinematic regions and separately for b-, c-, and light-flavour jets. The uncertainties are then decomposed in each of the flavour categories into independent components. An additional uncertainty is included to account for the extrapolation to jets with p_{T} beyond the kinematic reach of the data calibration (the thresholds are 250 GeV, 140 GeV and 300 GeV for b-, c- and light-flavour jets, respectively) [86,90,91].

Other experimental systematic uncertainties with a smaller impact are those in the lepton energy and momentum scales, in lepton reconstruction and identification efficiency, and in the efficiency of the triggers. An uncertainty associated with the modelling of pile-up in the simulation is included to cover the difference between the predicted and measured inelastic cross-sections [99]. The uncertainties in the energy scale and resolution of the small-R jets and leptons are propagated to the calculation of $E_{\mathrm{T}}^{\mathrm{miss}}$, which also has additional uncertainties from the scale, resolution and reconstruction efficiency of the tracks used to compute the soft term, along with the modelling of the underlying event [93].

7.2. Signal modelling systematic uncertainties

The systematic uncertainties that affect the modelling of the signal are derived closely following the procedure outlined in Refs. [11,16,92] and in Refs. [100,101] for uncertainties specific to STXS. The systematic uncertainties in the calculations of the VH production cross-sections and the $H \to b\bar{b}$ branching fraction are assigned following the recommendations of the LHC Higgs Cross Section Working Group [56,57,102–104]. Acceptance and shape systematic uncertainties are derived to account for missing higher-order QCD and EW corrections, for PDF+α_{S} uncertainties, and for variations of the PS and UE models. Factorisation and renormalisation scales are varied by factors of 0.5 and 2. PDF-related uncertainties are derived following Ref. [38]. The effects of the uncertainties from missing higher-order EW corrections, PDF+α_{S} and QCD scale variations on the jet mass shape are negligible. The PS and UE uncertainty is evaluated by comparing the nominal signal Powheg-Box samples showered by Pythia 8 with alternative samples showered by Herwig 7 [105].

7.3. Background modelling systematic uncertainties

The principal additional modelling uncertainties for the backgrounds that were considered are the following: renormalisation and factorisation scale variations by factors of 0.5 and 2 for higher order in QCD corrections of the matrix element of the process; merging scale variations from multi-leg simulations; resummation scale or parton shower uncertainties; PDF uncertainties; and differences with alternative MC generators. The impact of these systematic uncertainties in terms of normalisation, shape, acceptance and extrapolation between analysis regions is then estimated and included in the fit model (described in Section 8). Given that the analysis is based on the fit of the m_{J} variable only, all shape uncertainties are estimated with respect to this observable.

The normalisations of the W/Z+HF backgrounds are free parameters in the fit. They are determined thanks to the use of the jet mass distributions in SRs once $t\bar{t}$ is constrained from CR enriched in $t\bar{t}$ events. In addition to scale variations within Sherpa 2.2.1, alternative samples for acceptance and shape variations generated with MadGraph interfaced to Pythia 8 were considered. Finally, variations in the $V+bc/V+bb$, $V+bl/V+bb$ and $V+cc/V+bb$ ratios are accounted for independently for the W- and Z-boson backgrounds.

For top-quark pair production modelling uncertainties, specific initial-state radiation (ISR) and final-state radiation (FSR) Pythia parameters are used to assess the related systematic uncertainties. In addition to the typical scale variations, alternative NLO samples using the MadGraph5_aMC@NLO and Herwig 7 generators were considered. The $t\bar{t}$ normalisation is free in the fit and mainly constrained in the CRs for the 0- and 1-lepton channel. For the 2-lepton channel it is constrained to its nominal predicted value with an uncertainty of 20%. Due to top decays not fully contained within the large-R jet, the relative number of events where exactly two and where three or more VR track-jets are ghost-associated to the large-R jet can modify the large-R jet mass template. This is accounted for by an additional uncertainty estimated from the impact on the $t\bar{t}$ background template of a 20% variation in this relative ratio.

The normalisations, acceptances and shapes of all single-top production processes are constrained to their predictions within the corresponding uncertainties. For the dominant Wt channel, ISR/FSR uncertainties as well as alternative generator samples, Herwig 7 and MadGraph5_aMC@NLO, are considered. Since the Wt channel has the same flavour composition and a similar shape in the 0- and 1-lepton channels, the modelling uncertainties were studied in the 1-lepton channel and then propagated to the 0-lepton channel. An associated extrapolation uncertainty is taken into account.

To account for the ambiguities in the interference between $t\bar{t}$ and single-top production, an alternative sample generated with Powheg-Box interfaced to Pythia 8, using the diagram subtraction (DS) scheme, is used [68]. The difference between the DS and DR schemes for the Wt single-top production is accounted for as an additional systematic uncertainty.

For diboson production, in addition to the scale variations for acceptance, extrapolation and shape systematic uncertainties, alternative diboson samples were generated using Powheg-Box interfaced to Pythia 8 and the difference with respect to the Sherpa nominal samples was used as an additional uncertainty.

8. Results

The results are obtained from a binned maximum-profile-likelihood fit to the data of the m_{J} distribution, using all the signal and control regions defined in Section 5. The fit is performed using the RooStats framework [106,107]. Signal and background m_{J} templates are determined from MC simulation (described in Section 3) in all cases except for the multijet background in the 1-lepton channel, which is extracted from the data as discussed in Section 6.

The likelihood function is constructed from the product of the Poisson probabilities of each bin of the mass distributions and auxiliary terms used to model systematic uncertainties. The likelihood function is described in more detail in Ref. [92]. The parameters of interest (POI) are the signal strengths μ, multiplication factors that scale the expected SM Higgs boson signal, in one or more subchannels, or the VZ process. The signal strength parameters are extracted simultaneously with the overall diboson signal strength μ_{VZ}^{bb} by maximising the likelihood.

Systematic uncertainties are modelled in the likelihood function by parameterised variations of the number of signal and background events, and of the templates through nuisance parameters (NP). Systematic variations of the templates that are subject to large statistical fluctuations are smoothed, and systematic uncertainties that have a negligible impact on the final results are pruned away region-by-region [108]. NPs corresponding to most

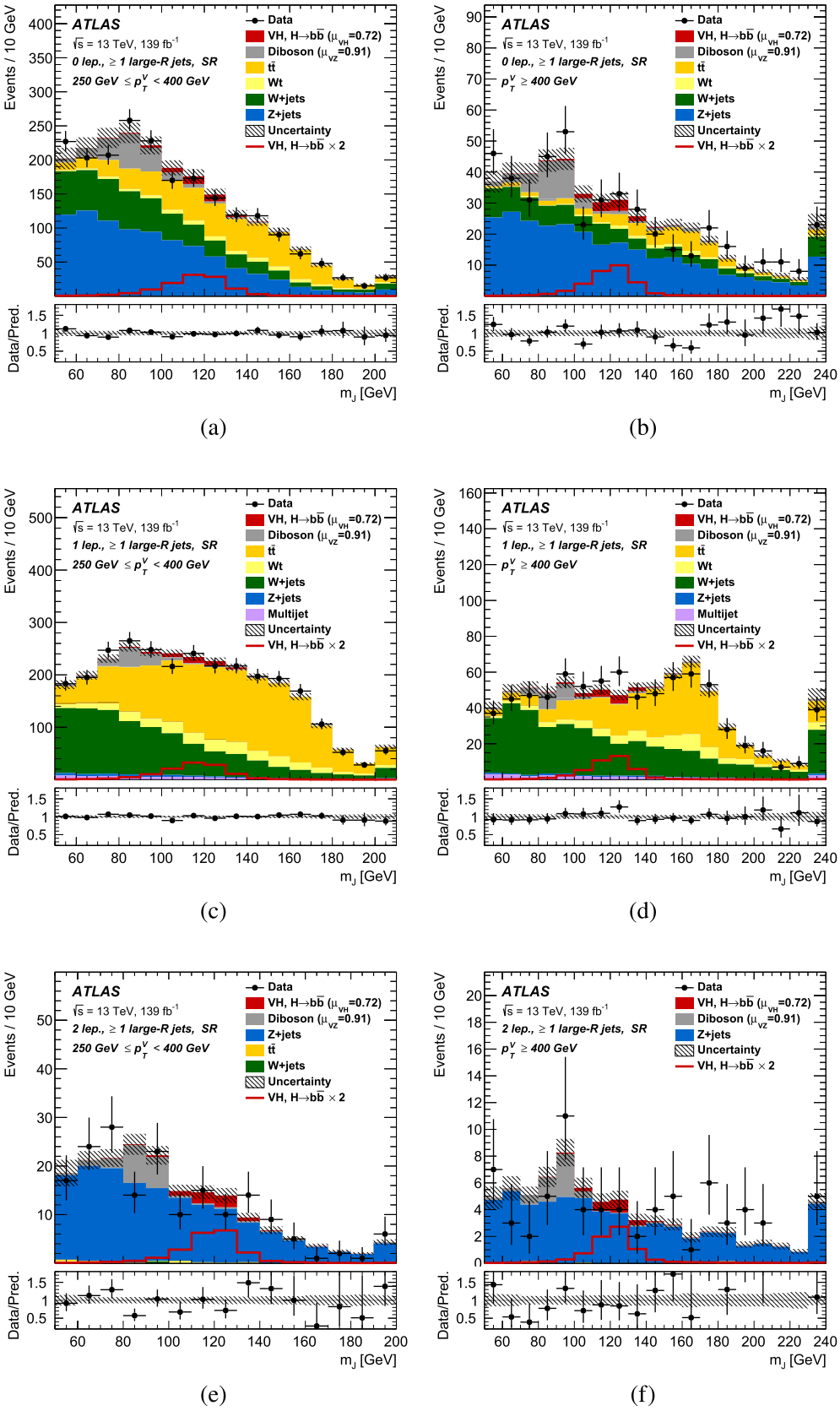

Fig. 1. The m_J post-fit distributions in (a, b) the 0-lepton, (c, d) 1-lepton and (e, f) 2-lepton signal regions for 2-b-tagged events for (a, c, e) 250 GeV $< p_T^V <$ 400 GeV and (b, d, f) $p_T^V \geq 400$ GeV. The low-purity and high-purity categories in the case of the 0-lepton and 1-lepton channels are merged in this figure. The background contributions after the likelihood fit are shown as filled histograms. The Higgs boson signal ($m_H = 125$ GeV) is shown as a filled histogram on top of the fitted backgrounds normalised to the signal yield extracted from data ($\mu_{VH}^{bb} = 0.72$), and unstacked as an unfilled histogram, scaled by the SM prediction times a factor of two. The size of the combined statistical and systematic uncertainty for the sum of the fitted signal and background is indicated by the hatched band. The highest bin in the distributions contains the overflow. The ratio of the data to the sum of the fitted signal and background is shown in the lower panel.

Table 4
Factors applied to the nominal normalisations of the $t\bar{t}$, $W+\text{HF}$ and $Z+\text{HF}$ backgrounds, as obtained from the likelihood fit. The errors represent the combined statistical and systematic uncertainties.

Process and category	Normalisation factor
$t\bar{t}$ 0-lepton	0.88 ± 0.10
$t\bar{t}$ 1-lepton	0.83 ± 0.09
$W+\text{HF}$	1.12 ± 0.14
$Z+\text{HF}$	1.32 ± 0.16

uncertainties discussed in Section 7 are constrained using Gaussian or log-normal probability density functions as auxiliary terms in the likelihood. The normalisations of the largest backgrounds, $t\bar{t}$ (in the 0- and 1-lepton channels), W+HF and Z+HF, are left unconstrained in the fit. The background normalisation factor values from the fit correspond to 0.88 ± 0.10 and 0.83 ± 0.09 for $t\bar{t}$, in the 0- and 1-lepton channels, respectively; 1.12 ± 0.14 for W+HF and 1.32 ± 0.16 for Z+HF and are also summarised in Table 4. The fit model uses a single normalisation factor for Z+HF and compatible results were found when using two different factors for the 0- and 2-lepton channels. To account for the uncertainty due to the limited size of the MC simulation samples, an NP is used for each bin of the templates [109].

The m_{J} distributions with signal strengths, background normalisations and all NPs set at their best-fit values, are shown in Fig. 1 for all three channels' SRs and in Fig. 2 for the CRs. The low-purity and high-purity categories in the case of the 0-lepton and 1-lepton channels are merged in Fig. 1. In all SRs and CRs a good agreement between the data and the prediction is observed.

For a Higgs boson mass of 125 GeV, when all lepton channels are combined, the observed excess with respect to the background-only hypothesis has a significance of 2.1 standard deviations, to be compared with an expectation of 2.7 standard deviations. The fitted μ_{VH}^{bb} value is:

$$\mu_{VH}^{bb} = 0.72^{+0.39}_{-0.36} = 0.72^{+0.29}_{-0.28}(\text{stat.})^{+0.26}_{-0.22}(\text{syst.}).$$

In this result, the largest uncertainties are statistical and include the impact from the floating background normalisations unconstrained in the fit. The latter component is subdominant. The impact of systematic uncertainties is almost as important as the total statistical uncertainty. The dominant source of systematic uncertainty is experimental and related to the large-R jet calibration, in particular in the m_{J} resolution, amounting to an impact of approximately 0.13 on μ_{VH}^{bb}. The second largest source of systematic uncertainty is the background modelling, which overall has an impact of approximately 0.10 on the result. The limited size of the MC simulation samples has a non-negligible impact of 0.09. Systematic uncertainties in the signal modelling have an impact of approximately 0.04, on par with uncertainties related to small-R jets. The breakdown of the systematic uncertainties in the measurement of the signal strength is displayed in Table 5.

The m_{J} distribution is shown in Fig. 3(a) summed over all channels and signal regions, weighted by their respective values of the ratio of the fitted Higgs boson signal to background yields and after subtraction of all backgrounds except for the WZ and ZZ diboson processes.

Fig. 3(b) shows the results of: a fit with six VH POIs measuring the individual signal strengths in each of the three channels and p_{T}^{V} bins separately; a three VH POI fit measuring the combined signal strengths in each channel; a two VH POI fit combining all channels in the two p_{T}^{V} bins separately; and the overall single VH POI combination.

For VZ production the fitted signal strength μ_{VZ}^{bb} is

$$\mu_{VZ}^{bb} = 0.91^{+0.29}_{-0.23} = 0.91 \pm 0.15(\text{stat.})^{+0.24}_{-0.17}(\text{syst.}),$$

Table 5
Breakdown of the absolute contributions to the uncertainty in μ_{VH}^{bb} inclusive in p_{T}^{V}. The sum in quadrature of the systematic uncertainties attached to the categories differs from the total systematic uncertainty due to correlations. The reported values represent the average between the positive and negative uncertainties on μ_{VH}^{bb}.

Source of uncertainty		Avg. impact
Total		0.372
Statistical		0.283
Systematic		0.240
Experimental uncertainties		
Small-R jets		0.038
Large-R jets		0.133
$E_{\text{T}}^{\text{miss}}$		0.007
Leptons		0.010
	b-jets	0.016
b-tagging	c-jets	0.011
	light-flavour jets	0.008
	extrapolation	0.004
Pile-up		0.001
Luminosity		0.013
Theoretical and modelling uncertainties		
Signal		0.038
Backgrounds		0.100
$\hookrightarrow$ Z + jets		0.048
$\hookrightarrow$ W + jets		0.058
$\hookrightarrow$ $t\bar{t}$		0.035
$\hookrightarrow$ Single top quark		0.027
$\hookrightarrow$ Diboson		0.032
$\hookrightarrow$ Multijet		0.009
MC statistical		0.092

in agreement with the SM prediction and the $W^{\pm}Z$ differential cross-section measurement performed by ATLAS at high transverse momentum of the Z boson ($p_{\text{T}}^{Z} > 220$ GeV) in the fully leptonic channel ($W^{\pm}Z \to \ell'\nu\ell^{+}\ell^{-}$) [110]. The simultaneous fit tests the performance of the analysis on an irreducible background, the known VZ production, with a topology similar to the VH signal. With all three lepton channels combined, a significance of 5.4 standard deviations is observed for the VZ process, compared to an expectation of 5.7 standard deviations. The correlation with the μ_{VH}^{bb} signal strength is approximately 11%. The statistical uncertainties amount to approximately 60% of the total uncertainty. The dominant source of systematic uncertainty is the background modelling, which has an impact of approximately 0.16 on the result. The source of systematic uncertainty related to the large-R jet reconstruction follows closely, with an impact of approximately 0.09 on μ_{VZ}^{bb}.

The cross-sections in the STXS framework are measured separately for ZH and WH production in two p_{T}^{V} regions, 250 GeV $< p_{\text{T}}^{V} <$ 400 GeV and $p_{\text{T}}^{V} \geq 400$ GeV. The analysis closely follows the strategy used in Ref. [11]. The expected signal distributions and acceptance times efficiencies for each STXS region are estimated from the simulated signal samples by selecting events using the generator's 'truth' information, in particular the 'truth' p_{T}^{V}, denoted by $p_{\text{T}}^{V,t}$. The likelihood function used is different from the one used to extract the μ_{VH}^{bb} and μ_{VZ}^{bb} results presented before. It has multiple POIs corresponding to the cross-sections in the four regions used in the analysis, multiplied by the $H \to b\bar{b}$ and $V \to$ leptons branching fractions. These four regions, i.e. ZH and WH production and the two $p_{\text{T}}^{V,t}$ bins, are known as reduced stage-1.2 regions in the STXS framework [111]. The sources of systematic uncertainty are identical to those defined in Section 7, except for the theoretical cross-section and branching fraction uncertainties, which are not included in the likelihood function because they affect the signal strength measurements but not the STXS measurements.

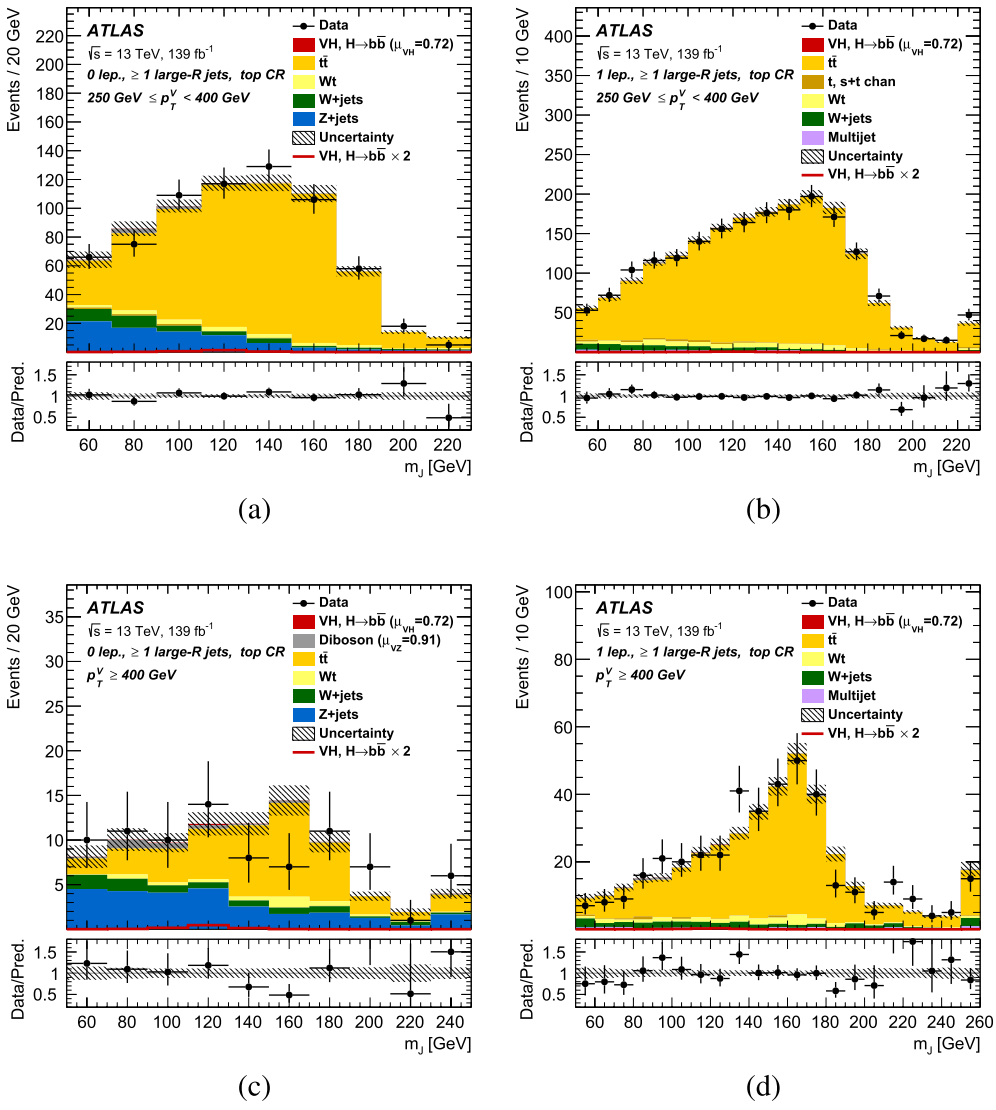

Fig. 2. The m_{J} post-fit distributions in the $t\bar{t}$ control region for (a, b) the 0-lepton channel and the 1-lepton channel for 250 GeV $< p_{\mathrm{T}}^{V} <$ 400 GeV and (c, d) the 0-lepton channel and the 1-lepton channel for $p_{\mathrm{T}}^{V} >$ 400 GeV. The background contributions after the likelihood fit are shown as filled histograms. The Higgs boson signal ($m_H = 125$ GeV) is shown as a filled histogram on top of the fitted backgrounds normalised to the signal yield extracted from data ($\mu_{VH}^{bb} = 0.72$), and unstacked as an unfilled histogram, scaled by the SM prediction times a factor of 2. The size of the combined statistical and systematic uncertainty for the sum of the fitted signal and background is indicated by the hatched band. The highest bin in the distributions contains the overflow. The ratio of the data to the sum of the fitted signal and background is shown in the lower panel.

The cross-sections are not constrained to be positive in the fit. The measured reduced stage-1.2 VH cross-section times branching fraction $\sigma \times B$ in each STXS bin, together with the SM predictions are summarised in Fig. 4 where the red error bands correspond to the theoretical uncertainty of the fiducial cross-section prediction in each bin. The measurements are also reported in Table 6 and are in agreement with the SM predictions from the signal MC sample. The principal sources of systematic uncertainties are similar to those affecting μ_{VH}^{bb}.

These results complement and extend those obtained by the small-R jets analysis [15] using the same dataset. The latter provides a more precise measurement of the cross-section in the inclusive $p_{\mathrm{T}}^{V} > 250$ GeV region. This can be attributed to the larger acceptance at lower p_{T}^{V} value, the usage of more precise physics objects calibration and to the use of multivariate analysis techniques. The results obtained by the two analyses in this region are compatible within one standard deviation.

9. Constraints on anomalous Higgs boson interactions

The STXS results presented in Section 8 are interpreted in an effective field theory approach where the scale of new physics is significantly larger than the SM electroweak scale so as to affect the measured observables at the LHC only through effective interactions among SM particles.

In this SMEFT approach, the SM Lagrangian is extended with higher-dimensional operators that capture the low-energy limit effects of a fundamental ultraviolet theory, without a priori knowledge of this theory [18]

$$\mathcal{L}_{\mathrm{SMEFT}} = \mathcal{L}_{\mathrm{SM}} + \sum_{d} \frac{1}{\Lambda^{d-4}} \left(\sum_{i} c_i^{(d)} \mathcal{O}_i^{(d)} \right),$$

where $\mathcal{O}_i^{(d)}$ are dimension-d operators and $c_i^{(d)}$ are the corresponding numerical coefficients called Wilson coefficients. All Wilson coefficients are assumed real. In the SM, all Wilson coefficients

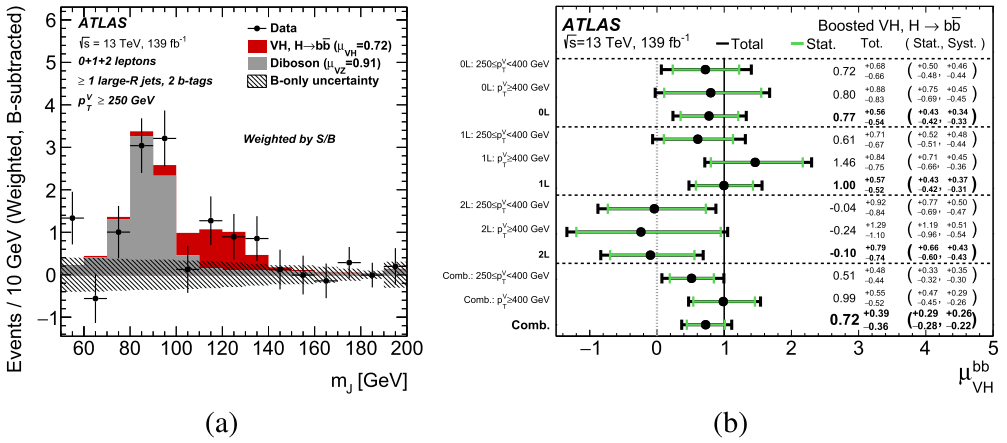

Fig. 3. (a) m_{J} distribution in data after subtraction of all backgrounds except for the WZ and ZZ diboson processes. The contributions from all lepton channels and signal regions are summed and weighted by their respective values of the ratio of fitted Higgs boson signal and background yields. The expected contribution of the associated WH and ZH production of a SM Higgs boson with $m_H = 125$ GeV is shown scaled by the measured combined signal strength ($\mu_{VH}^{bb} = 0.72$). The diboson contribution is normalised to its best-fit value of $\mu_{VZ}^{bb} = 0.91$. The size of the combined statistical and systematic uncertainty is indicated by the hatched band. This error band is computed from a full signal-plus-background fit including all the systematic uncertainties defined in Section 7, except for the VH/VZ experimental and theory uncertainties. (b) Fitted values of the Higgs boson signal strength parameter, μ_{VH}^{bb}, for $m_H = 125$ GeV for the 0-, 1- and 2-lepton channels in different p_{T}^{V} regions separately and for various combinations.

Table 6
Measured and predicted VH, $V \to$ leptons reduced stage-1.2 simplified template cross sections times the $H \to b\bar{b}$ and $V \to$ leptons branching fractions with corresponding uncertainties. All possible Z decays into neutral and charged leptons are considered.

STXS region ($\lvert y_H\rvert < 2.5$, $H \to b\bar{b}$)	SM prediction [fb]	Result	(Tot.)	(Stat.)	(Syst.) [fb]
$W \to \ell\nu$; $p_{\mathrm{T}}^{W,t} \in [250, 400]$ GeV	5.83 ± 0.26	3.3	$^{+4.8}_{-4.6}$	$^{+3.6}_{-3.4}$	$^{+3.2}_{-3.0}$
$W \to \ell\nu$; $p_{\mathrm{T}}^{W,t} \in [400, \infty]$ GeV	1.25 ± 0.06	2.1	$^{+1.2}_{-1.1}$	$^{+1.0}_{-0.9}$	$^{+0.6}_{-0.5}$
$Z \to \ell\ell, \nu\nu$; $p_{\mathrm{T}}^{Z,t} \in [250, 400]$ GeV	4.12 ± 0.45	1.4	$^{+3.1}_{-2.9}$	$^{+2.4}_{-2.3}$	$^{+1.9}_{-1.7}$
$Z \to \ell\ell, \nu\nu$; $p_{\mathrm{T}}^{Z,t} \in [400, \infty]$ GeV	0.72 ± 0.05	0.2	$^{+0.7}_{-0.6}$	$^{+0.6}_{-0.5}$	$^{+0.3}_{-0.3}$

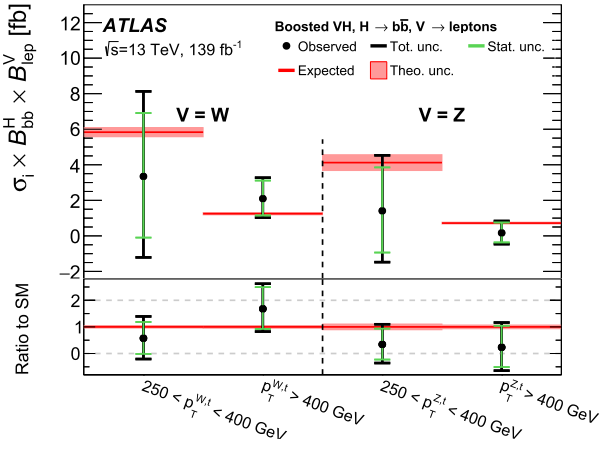

Fig. 4. Measured VH reduced stage-1.2 simplified template cross-sections times the $H \to b\bar{b}$ and $V \to$ leptons branching fractions.

Table 7
Wilson coefficients and their corresponding dimension-6 operators in the Warsaw formulation considered in this analysis [112,114].

Coefficient	Operator
$c_{H\Box}$	$(H^\dagger H)\Box(H^\dagger H)$
c_{HDD}	$(H^\dagger D^\mu H)^*(H^\dagger D_\mu H)$
c_{dH}	$(H^\dagger H)(\bar{q}_p d_r H)$
c_{HW}	$H^\dagger H W^I_{\mu\nu} W^{I\mu\nu}$
c_{HB}	$H^\dagger H B_{\mu\nu} B^{\mu\nu}$
c_{HWB}	$H^\dagger \tau^I H W^I_{\mu\nu} B^{\mu\nu}$
$c_{Hl}^{(1)}$	$H^\dagger i \overleftrightarrow{D}_\mu H(\bar{l}_p \gamma^\mu l_r)$
$c_{Hl}^{(3)}$	$H^\dagger i \overleftrightarrow{D}^I_\mu H(\bar{l}_p \tau^I \gamma^\mu l_r)$
$c_{He}^{(1)}$	$H^\dagger i \overleftrightarrow{D}_\mu H(\bar{e}_p \gamma^\mu e_r)$
$c_{Hq}^{(1)}$	$H^\dagger i \overleftrightarrow{D}_\mu H(\bar{q}_p \gamma^\mu q_r)$
$c_{Hq}^{(3)}$	$H^\dagger i \overleftrightarrow{D}^I_\mu H(\bar{q}_p \tau^I \gamma^\mu q_r)$
c_{Hu}	$H^\dagger i \overleftrightarrow{D}_\mu H(\bar{u}_p \gamma^\mu u_r)$
c_{Hd}	$H^\dagger i \overleftrightarrow{D}_\mu H(\bar{d}_p \gamma^\mu d_r)$
c'_{ll}	$(\bar{l}_p \gamma_\mu l_r)(\bar{l}_s \gamma^\mu l_t)$

are zero. The scale of new physics Λ is a free parameter set to 1 TeV. In this analysis, the Warsaw basis [112] of dimension $d = 6$ operators is used, taking into account only the lepton- and baryon-number-conserving ones. Furthermore, it only considers the CP-even terms respecting a $\mathrm{U}(3)^5$ flavour symmetry, which affect the $pp \to V(\to \text{leptons})H(\to b\bar{b})$ process [113]. The operators affecting the signal processes are listed in Table 7 [114].

The Wilson coefficients are used to parameterise the STXS and the Higgs boson decay rates [114] from leading-order predictions [113] and can be constrained using the STXS measurements presented in Section 8. The parameterisation of the STXS takes into account the linear terms originating from the interference between SM and non-SM amplitudes as well as the quadratic ones from the squared non-SM amplitudes. The former are of order $1/\Lambda^2$ and the latter of order $1/\Lambda^4$. Given that the current parameterisation takes neither next-to-leading-order effects nor the interference between SM and dimension-8 operators into account, the $1/\Lambda^4$ terms are incomplete. Where applicable, fit results will be shown for both the linear-only parameterisation and the case where quadratic terms are also included. Since the $gg \to ZH$ production cross-section is higher order in QCD, it is kept fixed to its

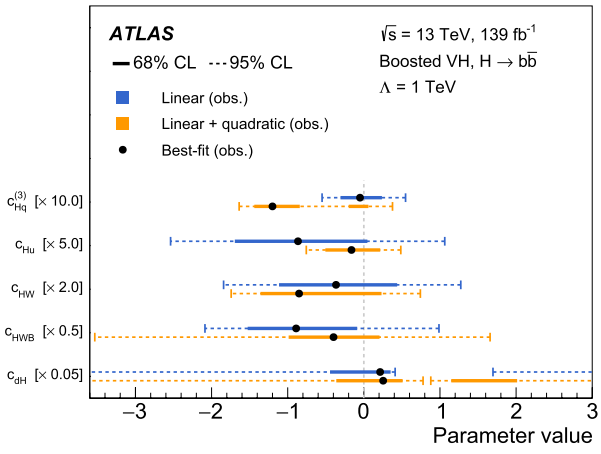

Fig. 5. Summary of the observed individual confidence interval at 68% (solid lines) and 95% (dashed lines) CL for the $c^{(3)}_{Hq}$, c_{Hu}, c_{HW}, c_{HWB} and c_{dH} Wilson coefficients from a fit of the STXS, using a linear-only parameterisation (in blue) and including quadratic terms (in orange).

SM expectation. The impact of the Wilson coefficients on the experimental analysis acceptance is not accounted for in this study. It was, however, verified that the impact was less than 20% of the SMEFT parameterisation in the kinematic range considered in this study.

Due to the limited number of STXS bins, not all Wilson coefficients can be measured simultaneously. The interpretations in the SMEFT framework are carried out with two different approaches. In the first, the four Wilson coefficients the analysis is most sensitive to (after removing degeneracies) in addition to the operator which affect the $H \to b\bar{b}$ decay, are varied individually, while the others are kept to their Standard Model value of 0. In the second approach, a principal component decomposition is performed which provides a set of four linear combinations (corresponding to the number of STXS measurements) of all the Wilson coefficients of Table 7 and the relative difference of the branching fraction of the Higgs boson into a pair of b-quarks with its Standard Model prediction ($\mathcal{I}_{BR}$). These combinations of Wilson coefficients, referred to as eigenvector combinations, are fitted simultaneously and their uncertainties are uncorrelated. The combinations are ordered in terms of experimental sensitivity.

In the first approach, the four leading Wilson coefficients are $c^{(3)}_{Hq}$, c_{Hu}, c_{HW}, and c_{HWB}. Operators with similar or degenerate effects were removed to get this list of coefficients. The operators $\mathcal{O}^{(1)}_{Hq}$ and $\mathcal{O}_{Hd}$ impact the analysis similarly to $\mathcal{O}_{Hu}$. Only c_{Hu} is therefore reported and can be considered as representative of this ensemble of Wilson coefficients. The $\mathcal{O}_{dH}$ operator was added to the list because it modifies the $H \to b\bar{b}$ vertex, which is specific to this analysis. The result of the fit is shown in Fig. 5, where both the linear-only and linear-and-quadratic parameterisations are shown. In the case of the $c^{(3)}_{Hq}$ coefficient the linear-and-quadratic fit slightly favours a negative value of $c^{(3)}_{Hq}$, but is also compatible with the SM value of 0 at the 68% confidence level (CL). The negative-log-likelihood one-dimensional profiles for the individual fits of the five aforementioned Wilson coefficients are shown in the Appendix.

The second approach aims at identifying the Wilson coefficients to which the measurements are most sensitive (those to which the measurements are not sensitive manifest themselves as flat directions in the likelihood) and determining a set of orthogonal linear combinations of Wilson coefficients. Only linear terms are considered and four coefficients denoted c_{EA}, c_{EB}, c_{EC}, and c_{ED}, corresponding to linear combinations of the Wilson coefficients according to the eigenvectors of the principal component decomposition, ordered in terms of their experimental sensitivity are extracted from the data. The parameterisation in terms of the main Wilson coefficients (reported in Table 7) and of the branching fraction of the Higgs boson to b-quarks, is given in Table 8 (coefficients less than 0.10 have been omitted for better readability). In contrast to the first approach where the STXS and the partial and total Higgs decay widths were parameterised independently, this second approach considers the full branching fraction $H \to bb$ as one linear parameter to remove redundancies in operators that only affect the total Higgs width. The leading combination c_{EA} is dominated by the $c^{(3)}_{Hq}$ Wilson coefficient as expected from the fact that it is also the most constrained from the individual fits. The next-to-leading c_{EB} combination is dominated by the $c^{(1)}_{Hq}$,

Table 8
Linear combinations of Wilson coefficients corresponding to the principal component decomposition eigenvectors (coefficients less than 0.10 have been omitted for better readability). The corresponding eigenvalues, representing in the Gaussian approximation the squared inverse uncertainty of the measured eigenvector, are also indicated.

Coefficient	Eigenvalue	Eigenvector combination
c_{EA}	1500.0	$0.99 \cdot c^{(3)}_{Hq} + 0.11 \cdot c_{Hu}$
c_{EB}	26.9	$0.82 \cdot c_{Hu} - 0.49 \cdot c^{(1)}_{Hq} - 0.24 \cdot c_{Hd} - 0.13 \cdot c^{(3)}_{Hq}$
c_{EC}	2.2	$0.67 \cdot \mathcal{I}_{BR} + 0.66 \cdot c_{HW} + 0.18 \cdot c^{(1)}_{Hq} - 0.16 \cdot c^{(3)}_{Hl} + 0.14 \cdot c_{HWB} + 0.12 \cdot c'_{ll}$
c_{ED}	0.1	$0.70 \cdot c^{(1)}_{Hq} + 0.52 \cdot c_{HWB} + 0.27 \cdot c_{Hu} - 0.27 \cdot c_{HW} - 0.24 \cdot c_{Hd} + 0.13 \cdot c_{HB}$

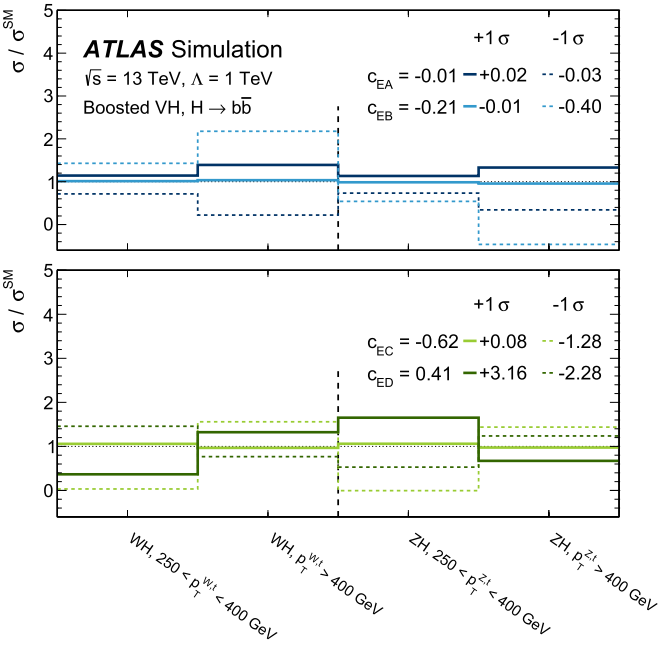

Fig. 6. The impact of the measured $+1\sigma$ (solid) and -1σ (dashed) variations of the four eigenvectors on the reduced STXS bins.

Table 9
Expected and observed best-fit values and associated uncertainties (68% CL) from a simultaneous fit of the four coefficients corresponding to the eigenvector combinations.

Coefficient	Expected	Observed
c_{EA}	$0.000^{+0.030}_{-0.027}$	$-0.010^{+0.027}_{-0.025}$
c_{EB}	$0.00^{+0.20}_{-0.19}$	$-0.21^{+0.19}_{-0.20}$
c_{EC}	$0.00^{+0.71}_{-0.67}$	$-0.62^{+0.70}_{-0.66}$
c_{ED}	$0.0^{+2.8}_{-2.7}$	$0.4^{+2.8}_{-2.7}$

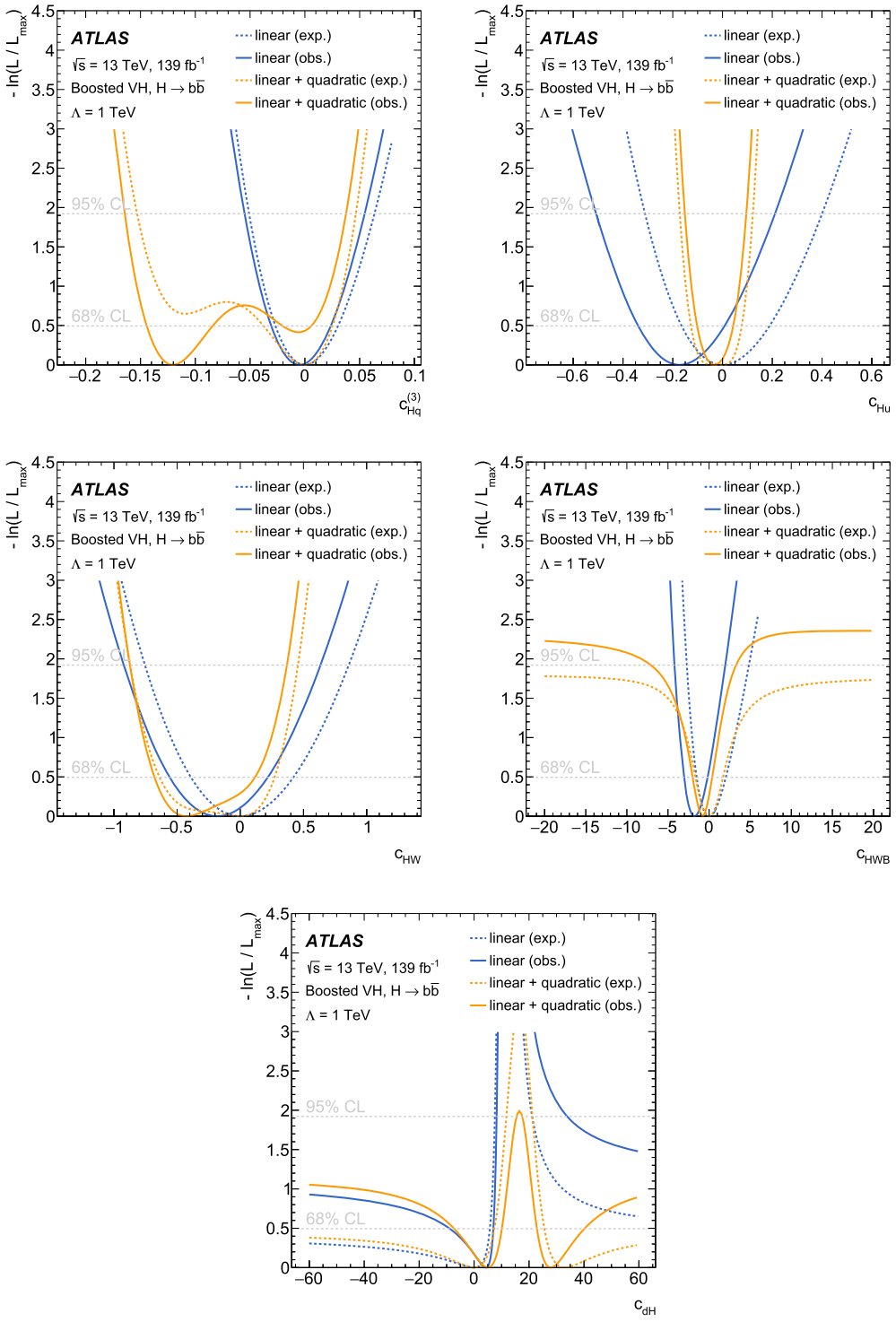

Fig. 7. The negative log-likelihood profile as a function of the variations of single Wilson coefficients $c_{Hq}^{(3)}$, c_{Hu}, c_{HW}, c_{HWB} and c_{dH}. Wilson coefficients of all other operators are set to zero. The fits are performed using a linear-only parametrisation of the VH production cross section and the Higgs decay branching fraction (blue lines), and using a parametrisation that includes both linear and quadratic terms into account (orange lines). Observed results are drawn in thick solid lines, thin dashed lines indicate expected results. The 68% and 95% CL lines are also indicated.

c_{Hu}, and c_{Hd} Wilson coefficients. The c_{EC} and c_{ED} combinations have a larger impact from the c_{HW} and c_{HWB} coefficients, respectively, with a non-negligible sensitivity to $c_{Hq}^{(1)}$. The impact of the variations corresponding to the measurement of each eigenvector combination on the expected cross-sections in the reduced STXS measurement bins is shown in Fig. 6. The results of the simultaneous fit are given in Table 9. No significant deviation from their expected SM value is observed.

10. Conclusion

Measurements of a Higgs boson decaying into a b-quark pair, produced in association with a vector boson at high transverse momentum subsequently decaying into a pair of leptons (electrons, muons and/or neutrinos) are performed. The results are based on the Run 2 dataset of pp collision data collected at $\sqrt{s} = 13$ TeV by the ATLAS detector at the LHC, corresponding to an inte-

grated luminosity of 139 fb^{-1}. These are the most precise measurements currently available in the high transverse momentum regime for this process. The Higgs boson is reconstructed from a single large-R jet to enhance the sensitivity in the high-p_{T} regime.

The significance of the measurement of the SM VH process is 2.1 standard deviations. The expected significance corresponding to the production of the SM VH process is 2.7 standard deviations. For the diboson process (VZ), which is measured simultaneously, the observed significance is 5.4 standard deviations, in good agreement with the expected diboson significance of 5.7 standard deviations. The cross-sections for the associated production of a Higgs boson decaying into a b-quark pair with an electroweak gauge boson W or Z decaying into leptons are measured in the simplified template cross-section framework in two p_{T}^{V} regions: 250 GeV $< p_{\mathrm{T}}^{V} <$ 400 GeV and $p_{\mathrm{T}}^{V} \geq$ 400 GeV. All results are in agreement with SM predictions and are interpreted in terms of constraints on anomalous couplings in the framework of a Standard Model effective field theory.

Declaration of competing interest

The authors declare that they have no known competing financial interests or personal relationships that could have appeared to influence the work reported in this paper.

Acknowledgements

We thank CERN for the very successful operation of the LHC, as well as the support staff from our institutions without whom ATLAS could not be operated efficiently.

We acknowledge the support of ANPCyT, Argentina; YerPhI, Armenia; ARC, Australia; BMWFW and FWF, Austria; ANAS, Azerbaijan; SSTC, Belarus; CNPq and FAPESP, Brazil; NSERC, NRC and CFI, Canada; CERN; ANID, Chile; CAS, MOST and NSFC, China; COLCIENCIAS, Colombia; MSMT CR, MPO CR and VSC CR, Czech Republic; DNRF and DNSRC, Denmark; IN2P3-CNRS and CEA-DRF/IRFU, France; SRNSFG, Georgia; BMBF, HGF and MPG, Germany; GSRT, Greece; RGC and Hong Kong SAR, China; ISF and Benoziyo Center, Israel; INFN, Italy; MEXT and JSPS, Japan; CNRST, Morocco; NWO, Netherlands; RCN, Norway; MNiSW and NCN, Poland; FCT, Portugal; MNE/IFA, Romania; JINR; MES of Russia and NRC KI, Russian Federation; MESTD, Serbia; MSSR, Slovakia; ARRS and MIZŠ, Slovenia; DST/NRF, South Africa; MICINN, Spain; SRC and Wallenberg Foundation, Sweden; SERI, SNSF and Cantons of Bern and Geneva, Switzerland; MOST, Taiwan; TAEK, Turkey; STFC, United Kingdom; DOE and NSF, United States of America. In addition, individual groups and members have received support from BCKDF, CANARIE, Compute Canada, CRC and IVADO, Canada; Beijing Municipal Science & Technology Commission, China; COST, ERC, ERDF, Horizon 2020 and Marie Skłodowska-Curie Actions, European Union; Investissements d'Avenir Labex, Investissements d'Avenir Idex and ANR, France; DFG and AvH Foundation, Germany; Herakleitos, Thales and Aristeia programmes co-financed by EU-ESF and the Greek NSRF, Greece; BSF-NSF and GIF, Israel; La Caixa Banking Foundation, CERCA Programme Generalitat de Catalunya and PROMETEO and GenT Programmes Generalitat Valenciana, Spain; Göran Gustafssons Stiftelse, Sweden; The Royal Society and Leverhulme Trust, United Kingdom.

The crucial computing support from all WLCG partners is acknowledged gratefully, in particular from CERN, the ATLAS Tier-1 facilities at TRIUMF (Canada), NDGF (Denmark, Norway, Sweden), CC-IN2P3 (France), KIT/GridKA (Germany), INFN-CNAF (Italy), NL-T1 (Netherlands), PIC (Spain), ASGC (Taiwan), RAL (UK) and BNL (USA), the Tier-2 facilities worldwide and large non-WLCG resource providers. Major contributors of computing resources are listed in Ref. [115].

Appendix A

This appendix contains the negative log-likelihood profile for the individual fits of the Wilson coefficients (Fig. 7). In each fit all coefficients other than the one individually varied are set to zero. Each fit is performed twice, once with and once without the quadratic terms taken into account, as described in Section 9.

References

[1] F. Englert, R. Brout, Broken symmetry and the mass of gauge vector mesons, Phys. Rev. Lett. 13 (1964) 321.
[2] P.W. Higgs, Broken symmetries, massless particles and gauge fields, Phys. Lett. 12 (1964) 132.
[3] P.W. Higgs, Broken symmetries and the masses of gauge bosons, Phys. Rev. Lett. 13 (1964) 508.
[4] G.S. Guralnik, C.R. Hagen, T.W.B. Kibble, Global conservation laws and massless particles, Phys. Rev. Lett. 13 (1964) 585.
[5] ATLAS Collaboration, CMS Collaboration, Combined measurement of the Higgs boson mass in pp collisions at $\sqrt{s} = 7$ and 8 TeV with the ATLAS and CMS experiments, Phys. Rev. Lett. 114 (2015) 191803, arXiv:1503.07589 [hep-ex].
[6] ATLAS Collaboration, Observation of a new particle in the search for the Standard Model Higgs boson with the ATLAS detector at the LHC, Phys. Lett. B 716 (2012) 1, arXiv:1207.7214 [hep-ex].
[7] CMS Collaboration, Observation of a new boson at a mass of 125 GeV with the CMS experiment at the LHC, Phys. Lett. B 716 (2012) 30, arXiv:1207.7235 [hep-ex].
[8] L. Evans, P. Bryant, LHC machine, J. Instrum. 3 (2008) S08001.
[9] ATLAS Collaboration, Observation of $H \to b\bar{b}$ decays and VH production with the ATLAS detector, Phys. Lett. B 786 (2018) 59, arXiv:1808.08238 [hep-ex].
[10] CMS Collaboration, Observation of Higgs boson decay to bottom quarks, Phys. Rev. Lett. 121 (2018) 121801, arXiv:1808.08242 [hep-ex].
[11] ATLAS Collaboration, Measurement of VH, $H \to b\bar{b}$ production as a function of the vector-boson transverse momentum in 13 TeV pp collisions with the ATLAS detector, J. High Energy Phys. 05 (2019) 141, arXiv:1903.04618 [hep-ex].
[12] J.M. Butterworth, A.R. Davison, M. Rubin, G.P. Salam, Jet substructure as a new Higgs search channel at the large hadron collider, Phys. Rev. Lett. 100 (2008) 242001, arXiv:0802.2470 [hep-ph].
[13] K. Mimasu, V. Sanz, C. Williams, Higher order QCD predictions for associated Higgs production with anomalous couplings to gauge bosons, J. High Energy Phys. 08 (2016) 039, arXiv:1512.02572 [hep-ph].
[14] ATLAS Collaboration, The ATLAS experiment at the CERN large hadron collider, J. Instrum. 3 (2008) S08003.
[15] ATLAS Collaboration, Measurements of WH and ZH production in the $H \to b\bar{b}$ decay channel in pp collisions at 13 TeV with the ATLAS detector, arXiv:2007.02873 [hep-ex], 2020.
[16] LHC Higgs Cross Section Working Group, Handbook of LHC Higgs cross sections: 4. Deciphering the nature of the Higgs sector, CERN-2017-002, arXiv:1610.07922 [hep-ph], 2017.
[17] J.R. Andersen, et al., Les Houches 2015: physics at TeV colliders standard model working group report, in: 9th Les Houches Workshop on Physics at TeV Colliders, PhysTeV 2015, Les Houches, France, June 1–19, 2015, 2016, arXiv:1605.04692 [hep-ph].
[18] R. Contino, M. Ghezzi, C. Grojean, M. Mühlleitner, M. Spira, Effective Lagrangian for a light Higgs-like scalar, J. High Energy Phys. 07 (2013) 035, arXiv:1303.3876 [hep-ph].
[19] ATLAS Collaboration, ATLAS insertable B-layer technical design report, ATLAS-TDR-19, 2010, https://cds.cern.ch/record/1291633, Addendum: ATLAS-TDR-19-ADD-1, 2012, https://cds.cern.ch/record/1451888.
[20] B. Abbott, et al., Production and integration of the ATLAS insertable B-layer, J. Instrum. 13 (2018) T05008, arXiv:1803.00844 [physics.ins-det].
[21] ATLAS Collaboration, Performance of the ATLAS trigger system in 2015, Eur. Phys. J. C 77 (2017) 317, arXiv:1611.09661 [hep-ex].
[22] ATLAS Collaboration, ATLAS data quality operations and performance for 2015-2018 data-taking, J. Instrum. 15 (2020) P04003, arXiv:1911.04632 [physics.ins-det].
[23] ATLAS Collaboration, Luminosity determination in pp collisions at $\sqrt{s} = 13$ TeV using the ATLAS detector at the LHC, ATLAS-CONF-2019-021, https://cds.cern.ch/record/2677054, 2019.
[24] G. Avoni, et al., The new LUCID-2 detector for luminosity measurement and monitoring in ATLAS, J. Instrum. 13 (2018) P07017.
[25] ATLAS Collaboration, The ATLAS simulation infrastructure, Eur. Phys. J. C 70 (2010) 823, arXiv:1005.4568 [physics.ins-det].
[26] S. Agostinelli, et al., GEANT4 - a simulation toolkit, Nucl. Instrum. Methods A 506 (2003) 250.
[27] T. Sjöstrand, S. Mrenna, P. Skands, A brief introduction to PYTHIA 8.1, Comput. Phys. Commun. 178 (2008) 852, arXiv:0710.3820 [hep-ph].

[28] ATLAS Collaboration, The Pythia 8 A3 tune description of ATLAS minimum bias and inelastic measurements incorporating the Donnachie-Landshoff diffractive model, ATL-PHYS-PUB-2016-017, 2016, https://cds.cern.ch/record/2206965.

[29] R.D. Ball, et al., Parton distributions with LHC data, Nucl. Phys. B 867 (2013) 244, arXiv:1207.1303 [hep-ph].

[30] ATLAS Collaboration, Measurement of the Z/γ^* boson transverse momentum distribution in pp collisions at $\sqrt{s} = 7$ TeV with the ATLAS detector, J. High Energy Phys. 09 (2014) 145, arXiv:1406.3660 [hep-ex].

[31] ATLAS Collaboration, ATLAS Pythia 8 tunes to 7 TeV data, ATL-PHYS-PUB-2014-021, https://cds.cern.ch/record/1966419, 2014.

[32] T. Gleisberg, et al., Event generation with SHERPA 1.1, J. High Energy Phys. 02 (2009) 007, arXiv:0811.4622 [hep-ph].

[33] E. Bothmann, et al., Event generation with Sherpa 2.2, SciPost Phys. 7 (2019) 034, arXiv:1905.09127 [hep-ph].

[34] F. Cascioli, P. Maierhofer, S. Pozzorini, Scattering amplitudes with open loops, Phys. Rev. Lett. 108 (2012) 111601, arXiv:1111.5206 [hep-ph].

[35] T. Gleisberg, S. Höche, Comix, a new matrix element generator, J. High Energy Phys. 12 (2008) 039, arXiv:0808.3674 [hep-ph].

[36] D.J. Lange, The EvtGen particle decay simulation package, Nucl. Instrum. Methods A 462 (2001) 152.

[37] R.D. Ball, et al., Parton distributions for the LHC run II, J. High Energy Phys. 04 (2015) 040, arXiv:1410.8849 [hep-ph].

[38] J. Butterworth, et al., PDF4LHC recommendations for LHC Run II, J. Phys. G 43 (2016) 023001, arXiv:1510.03865 [hep-ph].

[39] A. Denner, S. Dittmaier, S. Kallweit, A. Mück, Electroweak corrections to Higgs-strahlung off W/Z bosons at the tevatron and the LHC with Hawk, J. High Energy Phys. 03 (2012) 075, arXiv:1112.5142 [hep-ph].

[40] A. Denner, S. Dittmaier, S. Kallweit, A. Mück, HAWK 2.0: a Monte Carlo program for Higgs production in vector-boson fusion and Higgs strahlung at hadron colliders, Comput. Phys. Commun. 195 (2015) 161, arXiv:1412.5390 [hep-ph].

[41] S. Alioli, P. Nason, C. Oleari, E. Re, A general framework for implementing NLO calculations in shower Monte Carlo programs: the POWHEG BOX, J. High Energy Phys. 06 (2010) 043, arXiv:1200.2581 [hep-ph].

[42] T. Sjöstrand, et al., An introduction to PYTHIA 8.2, Comput. Phys. Commun. 191 (2015) 159, arXiv:1410.3012 [hep-ph].

[43] G. Cullen, et al., Automated one-loop calculations with GOSAM, Eur. Phys. J. C 72 (2012) 1889, arXiv:1111.2034 [hep-ph].

[44] K. Hamilton, P. Nason, G. Zanderighi, MINLO: multi-scale improved NLO, J. High Energy Phys. 10 (2012) 155, arXiv:1206.3572 [hep-ph].

[45] G. Luisoni, P. Nason, C. Oleari, F. Tramontano, $HW \pm /HZ + 0$ and 1 jet at NLO with the POWHEG BOX interfaced to GoSam and their merging within MiNLO, J. High Energy Phys. 10 (2013) 083, arXiv:1306.2542 [hep-ph].

[46] M.L. Ciccolini, S. Dittmaier, M. Krämer, Electroweak radiative corrections to associated WH and ZH production at hadron colliders, Phys. Rev. D 68 (2003) 073003, arXiv:hep-ph/0306234.

[47] O. Brein, A. Djouadi, R. Harlander, NNLO QCD corrections to the Higgs-strahlung processes at hadron colliders, Phys. Lett. B 579 (2004) 149, arXiv:hep-ph/0307206.

[48] G. Ferrera, M. Grazzini, F. Tramontano, Associated Higgs-W-boson production at hadron colliders: a fully exclusive QCD calculation at NNLO, Phys. Rev. Lett. 107 (2011) 152003, arXiv:1107.1164 [hep-ph].

[49] O. Brein, R.V. Harlander, M. Wiesemann, T. Zirke, Top-quark mediated effects in hadronic Higgs-Strahlung, Eur. Phys. J. C 72 (2012) 1868, arXiv:1111.0761 [hep-ph].

[50] G. Ferrera, M. Grazzini, F. Tramontano, Higher-order QCD effects for associated WH production and decay at the LHC, J. High Energy Phys. 04 (2014) 039, arXiv:1312.1669 [hep-ph].

[51] G. Ferrera, M. Grazzini, F. Tramontano, Associated ZH production at hadron colliders: the fully differential NNLO QCD calculation, Phys. Lett. B 740 (2015) 51, arXiv:1407.4747 [hep-ph].

[52] J.M. Campbell, R.K. Ellis, C. Williams, Associated production of a Higgs boson at NNLO, J. High Energy Phys. 06 (2016) 179, arXiv:1601.00658 [hep-ph].

[53] L. Altenkamp, S. Dittmaier, R.V. Harlander, H. Rzehak, T.J.E. Zirke, Gluon-induced Higgs-strahlung at next-to-leading order QCD, J. High Energy Phys. 02 (2013) 078, arXiv:1211.5015 [hep-ph].

[54] B. Hespel, F. Maltoni, E. Vryonidou, Higgs and Z boson associated production via gluon fusion in the SM and the 2HDM, J. High Energy Phys. 06 (2015) 065, arXiv:1503.01656 [hep-ph].

[55] R.V. Harlander, A. Kulesza, V. Theeuwes, T. Zirke, Soft gluon resummation for gluon-induced Higgs Strahlung, J. High Energy Phys. 11 (2014) 082, arXiv:1410.0217 [hep-ph].

[56] R.V. Harlander, S. Liebler, T. Zirke, Higgs Strahlung at the large hadron collider in the 2-Higgs-doublet model, J. High Energy Phys. 02 (2014) 023, arXiv:1307.8122 [hep-ph].

[57] O. Brein, R.V. Harlander, T.J.E. Zirke, vh@nnlo — Higgs Strahlung at hadron colliders, Comput. Phys. Commun. 184 (2013) 998, arXiv:1210.5347 [hep-ph].

[58] S. Frixione, G. Ridolfi, P. Nason, A positive-weight next-to-leading-order Monte Carlo for heavy flavour hadroproduction, J. High Energy Phys. 09 (2007) 126, arXiv:0707.3088 [hep-ph].

[59] M. Czakon, A. Mitov, Top++: a program for the calculation of the top-pair cross-section at hadron colliders, Comput. Phys. Commun. 185 (2014) 2930, arXiv:1112.5675 [hep-ph].

[60] S. Alioli, P. Nason, C. Oleari, E. Re, NLO single-top production matched with shower in POWHEG: s- and t-channel contributions, J. High Energy Phys. 09 (2009) 111, arXiv:0907.4076 [hep-ph], Erratum: NLO single-top production matched with shower in POWHEG: s- and t-channel contributions, J. High Energy Phys. 02 (2010) 011.

[61] N. Kidonakis, Next-to-next-to-leading logarithm resummation for s-channel single top quark production, Phys. Rev. D 81 (2010) 054028, arXiv:1001.5034 [hep-ph].

[62] N. Kidonakis, Next-to-next-to-leading-order collinear and soft gluon corrections for t-channel single top quark production, Phys. Rev. D 83 (2011) 091503, arXiv:1103.2792 [hep-ph].

[63] E. Re, Single-top Wt-channel production matched with parton showers using the POWHEG method, Eur. Phys. J. C 71 (2011) 1547, arXiv:1009.2450 [hep-ph].

[64] N. Kidonakis, Two-loop soft anomalous dimensions for single top quark associated production with a W^- or H^-, Phys. Rev. D 82 (2010) 054018, arXiv:1005.4451 [hep-ph].

[65] S. Schumann, F. Krauss, A parton shower algorithm based on Catani-Seymour dipole factorisation, J. High Energy Phys. 03 (2008) 038, arXiv:0709.1027 [hep-ph].

[66] S. Höche, F. Krauss, M. Schönherr, F. Siegert, QCD matrix elements + parton showers. The NLO case, J. High Energy Phys. 04 (2013) 027, arXiv:1207.5030 [hep-ph].

[67] S. Catani, L. Cieri, G. Ferrera, D. de Florian, M. Grazzini, Vector boson production at hadron colliders: a fully exclusive QCD calculation at NNLO, Phys. Rev. Lett. 103 (2009) 082001, arXiv:0903.2120 [hep-ph].

[68] S. Frixione, E. Laenen, P. Motylinski, C. White, B.R. Webber, Single-top hadroproduction in association with a W boson, J. High Energy Phys. 07 (2008) 029, arXiv:0805.3067 [hep-ph].

[69] ATLAS Collaboration, Vertex reconstruction performance of the ATLAS detector at $\sqrt{s} = 13$ TeV, ATL-PHYS-PUB-2015-026, https://cds.cern.ch/record/2037717, 2015.

[70] ATLAS Collaboration, Electron and photon reconstruction and performance in ATLAS using a dynamical, topological cell clustering-based approach, ATL-PHYS-PUB-2017-022, 2017, https://cds.cern.ch/record/2298955.

[71] ATLAS Collaboration, Electron and photon performance measurements with the ATLAS detector using the 2015-2017 LHC proton-proton collision data, J. Instrum. 14 (2019) P12006, arXiv:1908.0005 [hep-ex].

[72] ATLAS Collaboration, Muon reconstruction performance of the ATLAS detector in proton-proton collision data at $\sqrt{s} = 13$ TeV, Eur. Phys. J. C 76 (2016) 292, arXiv:1603.05598 [hep-ex].

[73] ATLAS Collaboration, Topological cell clustering in the ATLAS calorimeters and its performance in LHC Run 1, Eur. Phys. J. C 77 (2017) 490, arXiv:1603.02934 [hep-ex].

[74] M. Cacciari, G.P. Salam, G. Soyez, The anti-k_t jet clustering algorithm, J. High Energy Phys. 04 (2008) 063, arXiv:0802.1189 [hep-ph].

[75] M. Cacciari, G.P. Salam, G. Soyez, FastJet user manual, Eur. Phys. J. C 72 (2012) 1896, arXiv:1111.6097 [hep-ph].

[76] ATLAS Collaboration, Jet energy scale measurements and their systematic uncertainties in proton-proton collisions at $\sqrt{s} = 13$ TeV with the ATLAS detector, Phys. Rev. D 96 (2017) 072002, arXiv:1703.09665 [hep-ex].

[77] D. Krohn, J. Thaler, L.-T. Wang, Jet trimming, J. High Energy Phys. 02 (2010) 084, arXiv:0912.1342 [hep-ph].

[78] ATLAS Collaboration, Performance of jet substructure techniques for large-R jets in proton-proton collisions at $\sqrt{s} = 7$ TeV using the ATLAS detector, J. High Energy Phys. 09 (2013) 076, arXiv:1306.4945 [hep-ex].

[79] S. Catani, Y.L. Dokshitzer, M.H. Seymour, B.R. Webber, Longitudinally-invariant $k_\perp$-clustering algorithms for hadron-hadron collisions, Nucl. Phys. B 406 (1993) 187.

[80] S.D. Ellis, D.E. Soper, Successive combination jet algorithm for hadron collisions, Phys. Rev. D 48 (1993) 3160, arXiv:hep-ph/9305266.

[81] ATLAS Collaboration, In situ calibration of large-radius jet energy and mass in 13 TeV proton-proton collisions with the ATLAS detector, Eur. Phys. J. C 79 (2019) 135, arXiv:1807.09477 [hep-ex].

[82] ATLAS Collaboration, Performance of pile-up mitigation techniques for jets in pp collisions at $\sqrt{s} = 8$ TeV using the ATLAS detector, Eur. Phys. J. C 76 (2016) 581, arXiv:1510.03823 [hep-ex].

[83] D. Krohn, J. Thaler, L.-T. Wang, Jets with variable R, J. High Energy Phys. 06 (2009) 059, arXiv:0903.0392 [hep-ph].

[84] ATLAS Collaboration, Variable radius, exclusive-k_T, and center-of-mass subjet reconstruction for Higgs($\to b\bar{b}$) tagging in ATLAS, ATL-PHYS-PUB-2017-010, 2017, https://cds.cern.ch/record/2268678.

[85] ATLAS Collaboration, Identification of boosted Higgs bosons decaying into b-quark pairs with the ATLAS detector at 13 TeV, Eur. Phys. J. C 79 (2019) 836, arXiv:1906.11005 [hep-ex].

[86] ATLAS Collaboration, Measurements of b-jet tagging efficiency with the ATLAS detector using $t\bar{t}$ events at $\sqrt{s} = 13$ TeV, J. High Energy Phys. 08 (2018) 089, arXiv:1805.01845 [hep-ex].

[87] M. Cacciari, G.P. Salam, G. Soyez, The catchment area of jets, J. High Energy Phys. 04 (2008) 005, arXiv:0802.1188 [hep-ph].
[88] ATLAS Collaboration, ATLAS b-jet identification performance and efficiency measurement with tt events in pp collisions at $\sqrt{s} = 13$ TeV, Eur. Phys. J. C 79 (2019) 970, arXiv:1907.05120 [hep-ex].
[89] ATLAS Collaboration, Optimisation and performance studies of the ATLAS b-tagging algorithms for the 2017-18 LHC run, ATL-PHYS-PUB-2017-013, 2017, https://cds.cern.ch/record/2273281.
[90] ATLAS Collaboration, Calibration of light-flavour b-jet mistagging rates using ATLAS proton-proton collision data at $\sqrt{s} = 13$ TeV, ATLAS-CONF-2018-006, 2018, https://cds.cern.ch/record/2314418.
[91] ATLAS Collaboration, Measurement of b-tagging efficiency of c-jets in tt events using a likelihood approach with the ATLAS detector, ATLAS-CONF-2018-001, 2018, https://cds.cern.ch/record/2306649.
[92] ATLAS Collaboration, Evidence for the $H \to b\bar{b}$ decay with the ATLAS detector, J. High Energy Phys. 12 (2017) 024, arXiv:1708.03299 [hep-ex].
[93] ATLAS Collaboration, Performance of missing transverse momentum reconstruction with the ATLAS detector using proton-proton collisions at $\sqrt{s} = 13$ TeV, Eur. Phys. J. C 78 (2018) 903, arXiv:1802.08168 [hep-ex].
[94] ATLAS Collaboration, Reconstruction of hadronic decay products of tau leptons with the ATLAS experiment, Eur. Phys. J. C 76 (2016) 295, arXiv1512.05955.
[95] D. Gonçalves, J. Nakamura, Role of the Z polarization in the $H \to b\bar{b}$ measurement, Phys. Rev. D 98 (2018) 093005, arXiv:1805.06385 [hep-ph].
[96] ATLAS Collaboration, ATLAS sensitivity to the standard model Higgs in the HW, and HZ channels at high transverse momenta, ATL-PHYS-PUB-2009-088, 2009, https://cds.cern.ch/record/1201444.
[97] ATLAS Collaboration, Jet mass and substructure of inclusive jets in $\sqrt{s} = 7$ TeV pp collisions with the ATLAS experiment, J. High Energy Phys. 05 (2012) 128, arXiv:1203.4606 [hep-ex].
[98] ATLAS Collaboration, Jet mass reconstruction with the ATLAS detector in early Run 2 data, ATLAS-CONF-2016-035, 2016, https://cds.cern.ch/record/2200211.
[99] ATLAS Collaboration, Measurement of the inelastic proton-proton cross section at $\sqrt{s} = 13$ TeV with the ATLAS detector at the LHC, Phys. Rev. Lett. 117 (2016) 182002, arXiv:1606.02625 [hep-ex].
[100] ATLAS Collaboration, Evaluation of theoretical uncertainties for simplified template cross section measurements of V-associated production of the Higgs boson, ATL-PHYS-PUB-2018-035, 2018, https://cds.cern.ch/record/2649241.
[101] Les Houches 2017: physics at TeV colliders standard model working group report, 2018, arXiv:1803.07977 [hep-ph].
[102] LHC Higgs Cross Section Working Group, S. Dittmaier, C. Mariotti, G. Passarino, R. Tanaka (Eds.), Handbook of LHC Higgs Cross Sections: 1. Inclusive Observables, 2011, CERN-2011-002, arXiv:1101.0593 [hep-ph].
[103] LHC Higgs Cross Section Working Group, S. Dittmaier, C. Mariotti, G. Passarino, R. Tanaka (Eds.), Handbook of LHC Higgs Cross Sections: 2. Differential Distributions, 2012, CERN-2012-002, arXiv:1201.3084 [hep-ph].
[104] LHC Higgs Cross Section Working Group, Handbook of LHC Higgs Cross Sections: 3. Higgs Properties, 2013, CERN-2013-004, arXiv:1307.1347 [hep-ph].
[105] J. Bellm, et al., Herwig 7.0/Herwig++ 3.0 release note, Eur. Phys. J. C 76 (2016) 196, arXiv:1512.01178 [hep-ph].
[106] W. Verkerke, D. Kirkby, The RooFit toolkit for data modeling, arXiv:physics/0306116 [physics.data-an], 2003.
[107] L. Moneta, et al., The RooStats project, in: Proceedings of the 13th International Workshop on Advanced Computing and Analysis Techniques in Physics Research, February 22-27, 2010, arXiv:1009.1003 [physics.data-an].
[108] ATLAS Collaboration, Search for the bb decay of the Standard Model Higgs boson in associated $(W/Z)H$ production with the ATLAS detector, J. High Energy Phys. 01 (2015) 069, arXiv:1409.6212 [hep-ex].
[109] R. Barlow, C. Beeston, Fitting using finite Monte Carlo samples, Comput. Phys. Commun. 77 (1993) 219.
[110] ATLAS Collaboration, Measurement of $W^{\pm}Z$ production cross sections and gauge boson polarisation in pp collisions at $\sqrt{s} = 13$ TeV with the ATLAS detector, Eur. Phys. J. C 79 (2019) 535, arXiv:1902.05759 [hep-ex].
[111] N. Berger, et al., Simplified template cross sections - stage 1.1, arXiv:1906.02754 [hep-ph], 2019.
[112] B. Grzadkowski, M. Iskrzyński, M. Misiak, J. Rosiek, Dimension-six terms in the standard model Lagrangian, J. High Energy Phys. 10 (2010) 085, arXiv:1008.4884 [hep-ph].
[113] I. Brivio, Y. Jiang, M. Trott, The SMEFTsim package, theory and tools, J. High Energy Phys. 12 (2017) 070, arXiv:1709.06492 [hep-ph].
[114] ATLAS Collaboration, Methodology for EFT interpretation of Higgs boson simplified template cross-section results in ATLAS, ATL-PHYS-PUB-2019-042, 2019, https://cds.cern.ch/record/2694284.
[115] ATLAS Collaboration, ATLAS computing acknowledgements, ATL-SOFT-PUB-2020-001, 2020, https://cds.cern.ch/record/2717821.

The ATLAS Collaboration

G. Aad [102], B. Abbott [128], D.C. Abbott [103], A. Abed Abud [36], K. Abeling [53], D.K. Abhayasinghe [94], S.H. Abidi [167], O.S. AbouZeid [40], N.L. Abraham [156], H. Abramowicz [161], H. Abreu [160], Y. Abulaiti [6], B.S. Acharya [67a,67b,n], B. Achkar [53], L. Adam [100], C. Adam Bourdarios [5], L. Adamczyk [84a], L. Adamek [167], J. Adelman [121], M. Adersberger [114], A. Adiguzel [12c,ae], S. Adorni [54], T. Adye [143], A.A. Affolder [145], Y. Afik [160], C. Agapopoulou [65], M.N. Agaras [38], A. Aggarwal [119], C. Agheorghiesei [27c], J.A. Aguilar-Saavedra [139f,139a,ad], A. Ahmad [36], F. Ahmadov [80], W.S. Ahmed [104], X. Ai [18], G. Aielli [74a,74b], S. Akatsuka [86], M. Akbiyik [100], T.P.A. Åkesson [97], E. Akilli [54], A.V. Akimov [111], K. Al Khoury [65], G.L. Alberghi [23b,23a], J. Albert [176], M.J. Alconada Verzini [161], S. Alderweireldt [36], M. Aleksa [36], I.N. Aleksandrov [80], C. Alexa [27b], T. Alexopoulos [10], A. Alfonsi [120], F. Alfonsi [23b,23a], M. Alhroob [128], B. Ali [141], S. Ali [158], M. Aliev [166], G. Alimonti [69a], C. Allaire [36], B.M.M. Allbrooke [156], B.W. Allen [131], P.P. Allport [21], A. Aloisio [70a,70b], F. Alonso [89], C. Alpigiani [148], E. Alunno Camelia [74a,74b], M. Alvarez Estevez [99], M.G. Alviggi [70a,70b], Y. Amaral Coutinho [81b], A. Ambler [104], L. Ambroz [134], C. Amelung [26], D. Amidei [106], S.P. Amor Dos Santos [139a], S. Amoroso [46], C.S. Amrouche [54], F. An [79], C. Anastopoulos [149], N. Andari [144], T. Andeen [11], J.K. Anders [20], S.Y. Andrean [45a,45b], A. Andreazza [69a,69b], V. Andrei [61a], C.R. Anelli [176], S. Angelidakis [9], A. Angerami [39], A.V. Anisenkov [122b,122a], A. Annovi [72a], C. Antel [54], M.T. Anthony [149], E. Antipov [129], M. Antonelli [51], D.J.A. Antrim [171], F. Anulli [73a], M. Aoki [82], J.A. Aparisi Pozo [174], M.A. Aparo [156], L. Aperio Bella [46], N. Aranzabal [36], V. Araujo Ferraz [81a], R. Araujo Pereira [81b], C. Arcangeletti [51], A.T.H. Arce [49], F.A. Arduh [89], J-F. Arguin [110], S. Argyropoulos [52], J.-H. Arling [46], A.J. Armbruster [36], A. Armstrong [171], O. Arnaez [167], H. Arnold [120], Z.P. Arrubarrena Tame [114], G. Artoni [134], K. Asai [126], S. Asai [163], T. Asawatavonvanich [165], N. Asbah [59], E.M. Asimakopoulou [172], L. Asquith [156], J. Assahsah [35e], K. Assamagan [29], R. Astalos [28a], R.J. Atkin [33a], M. Atkinson [173], N.B. Atlay [19], H. Atmani [65], K. Augsten [141], V.A. Austrup [182], G. Avolio [36], M.K. Ayoub [15a], G. Azuelos [110,am], H. Bachacou [144], K. Bachas [162], M. Backes [134], F. Backman [45a,45b], P. Bagnaia [73a,73b], M. Bahmani [85], H. Bahrasemani [152], A.J. Bailey [174], V.R. Bailey [173], J.T. Baines [143], C. Bakalis [10], O.K. Baker [183], P.J. Bakker [120], E. Bakos [16],

D. Bakshi Gupta [8], S. Balaji [157], E.M. Baldin [122b,122a], P. Balek [180], F. Balli [144], W.K. Balunas [134], J. Balz [100], E. Banas [85], M. Bandieramonte [138], A. Bandyopadhyay [24], Sw. Banerjee [181,i], L. Barak [161], W.M. Barbe [38], E.L. Barberio [105], D. Barberis [55b,55a], M. Barbero [102], G. Barbour [95], T. Barillari [115], M-S. Barisits [36], J. Barkeloo [131], T. Barklow [153], R. Barnea [160], B.M. Barnett [143], R.M. Barnett [18], Z. Barnovska-Blenessy [60a], A. Baroncelli [60a], G. Barone [29], A.J. Barr [134], L. Barranco Navarro [45a,45b], F. Barreiro [99], J. Barreiro Guimarães da Costa [15a], U. Barron [161], S. Barsov [137], F. Bartels [61a], R. Bartoldus [153], G. Bartolini [102], A.E. Barton [90], P. Bartos [28a], A. Basalaev [46], A. Basan [100], A. Bassalat [65,aj], M.J. Basso [167], R.L. Bates [57], S. Batlamous [35f], J.R. Batley [32], B. Batool [151], M. Battaglia [145], M. Bauce [73a,73b], F. Bauer [144,*], K.T. Bauer [171], P. Bauer [24], H.S. Bawa [31], A. Bayirli [12c], J.B. Beacham [49], T. Beau [135], P.H. Beauchemin [170], F. Becherer [52], P. Bechtle [24], H.C. Beck [53], H.P. Beck [20,p], K. Becker [178], C. Becot [46], A. Beddall [12d], A.J. Beddall [12a], V.A. Bednyakov [80], M. Bedognetti [120], C.P. Bee [155], T.A. Beermann [182], M. Begalli [81b], M. Begel [29], A. Behera [155], J.K. Behr [46], F. Beisiegel [24], M. Belfkir [5], A.S. Bell [95], G. Bella [161], L. Bellagamba [23b], A. Bellerive [34], P. Bellos [9], K. Beloborodov [122b,122a], K. Belotskiy [112], N.L. Belyaev [112], D. Benchekroun [35a], N. Benekos [10], Y. Benhammou [161], D.P. Benjamin [6], M. Benoit [54], J.R. Bensinger [26], S. Bentvelsen [120], L. Beresford [134], M. Beretta [51], D. Berge [19], E. Bergeaas Kuutmann [172], N. Berger [5], B. Bergmann [141], L.J. Bergsten [26], J. Beringer [18], S. Berlendis [7], G. Bernardi [135], C. Bernius [153], F.U. Bernlochner [24], T. Berry [94], P. Berta [100], C. Bertella [15a], A. Berthold [48], I.A. Bertram [90], O. Bessidskaia Bylund [182], N. Besson [144], A. Bethani [101], S. Bethke [115], A. Betti [42], A.J. Bevan [93], J. Beyer [115], D.S. Bhattacharya [177], P. Bhattarai [26], V.S. Bhopatkar [6], R. Bi [138], R.M. Bianchi [138], O. Biebel [114], D. Biedermann [19], R. Bielski [36], K. Bierwagen [100], N.V. Biesuz [72a,72b], M. Biglietti [75a], T.R.V. Billoud [110], M. Bindi [53], A. Bingul [12d], C. Bini [73a,73b], S. Biondi [23b,23a], C.J. Birch-sykes [101], M. Birman [180], T. Bisanz [36], J.P. Biswal [3], D. Biswas [181,i], A. Bitadze [101], C. Bittrich [48], K. Bjørke [133], T. Blazek [28a], I. Bloch [46], C. Blocker [26], A. Blue [57], U. Blumenschein [93], G.J. Bobbink [120], V.S. Bobrovnikov [122b,122a], S.S. Bocchetta [97], D. Bogavac [14], A.G. Bogdanchikov [122b,122a], C. Bohm [45a], V. Boisvert [94], P. Bokan [53], T. Bold [84a], A.E. Bolz [61b], M. Bomben [135], M. Bona [93], J.S. Bonilla [131], M. Boonekamp [144], C.D. Booth [94], A.G. Borbély [57], H.M. Borecka-Bielska [91], L.S. Borgna [95], A. Borisov [123], G. Borissov [90], D. Bortoletto [134], D. Boscherini [23b], M. Bosman [14], J.D. Bossio Sola [104], K. Bouaouda [35a], J. Boudreau [138], E.V. Bouhova-Thacker [90], D. Boumediene [38], S.K. Boutle [57], A. Boveia [127], J. Boyd [36], D. Boye [33c], I.R. Boyko [80], A.J. Bozson [94], J. Bracinik [21], N. Brahimi [60d,60c], G. Brandt [182], O. Brandt [32], F. Braren [46], B. Brau [103], J.E. Brau [131], W.D. Breaden Madden [57], K. Brendlinger [46], R. Brener [160], L. Brenner [36], R. Brenner [172], S. Bressler [180], B. Brickwedde [100], D.L. Briglin [21], D. Britton [57], D. Britzger [115], I. Brock [24], R. Brock [107], G. Brooijmans [39], W.K. Brooks [146d], E. Brost [29], P.A. Bruckman de Renstrom [85], B. Brüers [46], D. Bruncko [28b], A. Bruni [23b], G. Bruni [23b], L.S. Bruni [120], S. Bruno [74a,74b], M. Bruschi [23b], N. Bruscino [73a,73b], L. Bryngemark [153], T. Buanes [17], Q. Buat [155], P. Buchholz [151], A.G. Buckley [57], I.A. Budagov [80], M.K. Bugge [133], F. Bührer [52], O. Bulekov [112], B.A. Bullard [59], T.J. Burch [121], S. Burdin [91], C.D. Burgard [120], A.M. Burger [129], B. Burghgrave [8], J.T.P. Burr [46], C.D. Burton [11], J.C. Burzynski [103], V. Büscher [100], E. Buschmann [53], P.J. Bussey [57], J.M. Butler [25], C.M. Buttar [57], J.M. Butterworth [95], P. Butti [36], W. Buttinger [36], C.J. Buxo Vazquez [107], A. Buzatu [158], A.R. Buzykaev [122b,122a], G. Cabras [23b,23a], S. Cabrera Urbán [174], D. Caforio [56], H. Cai [138], V.M.M. Cairo [153], O. Cakir [4a], N. Calace [36], P. Calafiura [18], G. Calderini [135], P. Calfayan [66], G. Callea [57], L.P. Caloba [81b], A. Caltabiano [74a,74b], S. Calvente Lopez [99], D. Calvet [38], S. Calvet [38], T.P. Calvet [102], M. Calvetti [72a,72b], R. Camacho Toro [135], S. Camarda [36], D. Camarero Munoz [99], P. Camarri [74a,74b], M.T. Camerlingo [75a,75b], D. Cameron [133], C. Camincher [36], S. Campana [36], M. Campanelli [95], A. Camplani [40], V. Canale [70a,70b], A. Canesse [104], M. Cano Bret [78], J. Cantero [129], T. Cao [161], Y. Cao [173], M.D.M. Capeans Garrido [36], M. Capua [41b,41a], R. Cardarelli [74a], F. Cardillo [149], G. Carducci [41b,41a], I. Carli [142], T. Carli [36], G. Carlino [70a], B.T. Carlson [138], E.M. Carlson [176,168a], L. Carminati [69a,69b], R.M.D. Carney [153], S. Caron [119], E. Carquin [146d], S. Carrá [46], G. Carratta [23b,23a], J.W.S. Carter [167], T.M. Carter [50], M.P. Casado [14,f], A.F. Casha [167], F.L. Castillo [174], L. Castillo Garcia [14], V. Castillo Gimenez [174], N.F. Castro [139a,139e], A. Catinaccio [36], J.R. Catmore [133], A. Cattai [36], V. Cavaliere [29], V. Cavasinni [72a,72b], E. Celebi [12b], F. Celli [134], K. Cerny [130], A.S. Cerqueira [81a], A. Cerri [156], L. Cerrito [74a,74b], F. Cerutti [18], A. Cervelli [23b,23a], S.A. Cetin [12b], Z. Chadi [35a], D. Chakraborty [121], J. Chan [181], W.S. Chan [120], W.Y. Chan [91], J.D. Chapman [32], B. Chargeishvili [159b], D.G. Charlton [21], T.P. Charman [93], C.C. Chau [34], S. Che [127], S. Chekanov [6], S.V. Chekulaev [168a], G.A. Chelkov [80,ah], B. Chen [79], C. Chen [60a], C.H. Chen [79], H. Chen [29], J. Chen [60a], J. Chen [39], J. Chen [26], S. Chen [136], S.J. Chen [15c], X. Chen [15b], Y. Chen [60a],

Y-H. Chen [46], H.C. Cheng [63a], H.J. Cheng [15a], A. Cheplakov [80], E. Cheremushkina [123], R. Cherkaoui El Moursli [35f], E. Cheu [7], K. Cheung [64], T.J.A. Chevalérias [144], L. Chevalier [144], V. Chiarella [51], G. Chiarelli [72a], G. Chiodini [68a], A.S. Chisholm [21], A. Chitan [27b], I. Chiu [163], Y.H. Chiu [176], M.V. Chizhov [80], K. Choi [11], A.R. Chomont [73a,73b], Y.S. Chow [120], L.D. Christopher [33e], M.C. Chu [63a], X. Chu [15a,15d], J. Chudoba [140], J.J. Chwastowski [85], L. Chytka [130], D. Cieri [115], K.M. Ciesla [85], D. Cinca [47], V. Cindro [92], I.A. Cioară [27b], A. Ciocio [18], F. Cirotto [70a,70b], Z.H. Citron [180,j], M. Citterio [69a], D.A. Ciubotaru [27b], B.M. Ciungu [167], A. Clark [54], M.R. Clark [39], P.J. Clark [50], S.E. Clawson [101], C. Clement [45a,45b], Y. Coadou [102], M. Cobal [67a,67c], A. Coccaro [55b], J. Cochran [79], R.F. Coelho Barrue [139a], R. Coelho Lopes De Sa [103], H. Cohen [161], A.E.C. Coimbra [36], B. Cole [39], A.P. Colijn [120], J. Collot [58], P. Conde Muiño [139a,139h], S.H. Connell [33c], I.A. Connelly [57], S. Constantinescu [27b], F. Conventi [70a,an], A.M. Cooper-Sarkar [134], F. Cormier [175], K.J.R. Cormier [167], L.D. Corpe [95], M. Corradi [73a,73b], E.E. Corrigan [97], F. Corriveau [104,ab], M.J. Costa [174], F. Costanza [5], D. Costanzo [149], G. Cowan [94], J.W. Cowley [32], J. Crane [101], K. Cranmer [125], R.A. Creager [136], S. Crépé-Renaudin [58], F. Crescioli [135], M. Cristinziani [24], V. Croft [170], G. Crosetti [41b,41a], A. Cueto [5], T. Cuhadar Donszelmann [171], H. Cui [15a,15d], A.R. Cukierman [153], W.R. Cunningham [57], S. Czekierda [85], P. Czodrowski [36], M.M. Czurylo [61b], M.J. Da Cunha Sargedas De Sousa [60b], J.V. Da Fonseca Pinto [81b], C. Da Via [101], W. Dabrowski [84a], F. Dachs [36], T. Dado [47], S. Dahbi [33e], T. Dai [106], C. Dallapiccola [103], M. Dam [40], G. D'amen [29], V. D'Amico [75a,75b], J. Damp [100], J.R. Dandoy [136], M.F. Daneri [30], M. Danninger [152], V. Dao [36], G. Darbo [55b], O. Dartsi [5], A. Dattagupta [131], T. Daubney [46], S. D'Auria [69a,69b], C. David [168b], T. Davidek [142], D.R. Davis [49], I. Dawson [149], K. De [8], R. De Asmundis [70a], M. De Beurs [120], S. De Castro [23b,23a], N. De Groot [119], P. de Jong [120], H. De la Torre [107], A. De Maria [15c], D. De Pedis [73a], A. De Salvo [73a], U. De Sanctis [74a,74b], M. De Santis [74a,74b], A. De Santo [156], J.B. De Vivie De Regie [65], C. Debenedetti [145], D.V. Dedovich [80], A.M. Deiana [42], J. Del Peso [99], Y. Delabat Diaz [46], D. Delgove [65], F. Deliot [144], C.M. Delitzsch [7], M. Della Pietra [70a,70b], D. Della Volpe [54], A. Dell'Acqua [36], L. Dell'Asta [74a,74b], M. Delmastro [5], C. Delporte [65], P.A. Delsart [58], D.A. DeMarco [167], S. Demers [183], M. Demichev [80], G. Demontigny [110], S.P. Denisov [123], L. D'Eramo [121], D. Derendarz [85], J.E. Derkaoui [35e], F. Derue [135], P. Dervan [91], K. Desch [24], K. Dette [167], C. Deutsch [24], M.R. Devesa [30], P.O. Deviveiros [36], F.A. Di Bello [73a,73b], A. Di Ciaccio [74a,74b], L. Di Ciaccio [5], W.K. Di Clemente [136], C. Di Donato [70a,70b], A. Di Girolamo [36], G. Di Gregorio [72a,72b], B. Di Micco [75a,75b], R. Di Nardo [75a,75b], K.F. Di Petrillo [59], R. Di Sipio [167], C. Diaconu [102], F.A. Dias [120], T. Dias Do Vale [139a], M.A. Diaz [146a], F.G. Diaz Capriles [24], J. Dickinson [18], M. Didenko [166], E.B. Diehl [106], J. Dietrich [19], S. Díez Cornell [46], C. Diez Pardos [151], A. Dimitrievska [18], W. Ding [15b], J. Dingfelder [24], S.J. Dittmeier [61b], F. Dittus [36], F. Djama [102], T. Djobava [159b], J.I. Djuvsland [17], M.A.B. Do Vale [147], M. Dobre [27b], D. Dodsworth [26], C. Doglioni [97], J. Dolejsi [142], Z. Dolezal [142], M. Donadelli [81c], B. Dong [60c], J. Donini [38], A. D'onofrio [15c], M. D'Onofrio [91], J. Dopke [143], A. Doria [70a], M.T. Dova [89], A.T. Doyle [57], E. Drechsler [152], E. Dreyer [152], T. Dreyer [53], A.S. Drobac [170], D. Du [60b], T.A. du Pree [120], Y. Duan [60d], F. Dubinin [111], M. Dubovsky [28a], A. Dubreuil [54], E. Duchovni [180], G. Duckeck [114], O.A. Ducu [36,27b], D. Duda [115], A. Dudarev [36], A.C. Dudder [100], E.M. Duffield [18], M. D'uffizi [101], L. Duflot [65], M. Dührssen [36], C. Dülsen [182], M. Dumancic [180], A.E. Dumitriu [27b], M. Dunford [61a], A. Duperrin [102], H. Duran Yildiz [4a], M. Düren [56], A. Durglishvili [159b], D. Duschinger [48], B. Dutta [46], D. Duvnjak [1], G.I. Dyckes [136], M. Dyndal [36], S. Dysch [101], B.S. Dziedzic [85], M.G. Eggleston [49], T. Eifert [8], G. Eigen [17], K. Einsweiler [18], T. Ekelof [172], H. El Jarrari [35f], V. Ellajosyula [172], M. Ellert [172], F. Ellinghaus [182], A.A. Elliot [93], N. Ellis [36], J. Elmsheuser [29], M. Elsing [36], D. Emeliyanov [143], A. Emerman [39], Y. Enari [163], M.B. Epland [49], J. Erdmann [47], A. Ereditato [20], P.A. Erland [85], M. Errenst [182], M. Escalier [65], C. Escobar [174], O. Estrada Pastor [174], E. Etzion [161], H. Evans [66], M.O. Evans [156], A. Ezhilov [137], F. Fabbri [57], L. Fabbri [23b,23a], V. Fabiani [119], G. Facini [178], R.M. Fakhrutdinov [123], S. Falciano [73a], P.J. Falke [24], S. Falke [36], J. Faltova [142], Y. Fang [15a], Y. Fang [15a], G. Fanourakis [44], M. Fanti [69a,69b], M. Faraj [67a,67c,q], A. Farbin [8], A. Farilla [75a], E.M. Farina [71a,71b], T. Farooque [107], S.M. Farrington [50], P. Farthouat [36], F. Fassi [35f], P. Fassnacht [36], D. Fassouliotis [9], M. Faucci Giannelli [50], W.J. Fawcett [32], L. Fayard [65], O.L. Fedin [137,o], W. Fedorko [175], A. Fehr [20], M. Feickert [173], L. Feligioni [102], A. Fell [149], C. Feng [60b], M. Feng [49], M.J. Fenton [171], A.B. Fenyuk [123], S.W. Ferguson [43], J. Ferrando [46], A. Ferrante [173], A. Ferrari [172], P. Ferrari [120], R. Ferrari [71a], D.E. Ferreira de Lima [61b], A. Ferrer [174], D. Ferrere [54], C. Ferretti [106], F. Fiedler [100], A. Filipčič [92], F. Filthaut [119], K.D. Finelli [25], M.C.N. Fiolhais [139a,139c,a], L. Fiorini [174], F. Fischer [114], J. Fischer [100], W.C. Fisher [107], T. Fitschen [21], I. Fleck [151], P. Fleischmann [106], T. Flick [182], B.M. Flierl [114], L. Flores [136],

L.R. Flores Castillo [63a], F.M. Follega [76a,76b], N. Fomin [17], J.H. Foo [167], G.T. Forcolin [76a,76b], B.C. Forland [66], A. Formica [144], F.A. Förster [14], A.C. Forti [101], E. Fortin [102], M.G. Foti [134], D. Fournier [65], H. Fox [90], P. Francavilla [72a,72b], S. Francescato [73a,73b], M. Franchini [23b,23a], S. Franchino [61a], D. Francis [36], L. Franco [5], L. Franconi [20], M. Franklin [59], G. Frattari [73a,73b], A.N. Fray [93], P.M. Freeman [21], B. Freund [110], W.S. Freund [81b], E.M. Freundlich [47], D.C. Frizzell [128], D. Froidevaux [36], J.A. Frost [134], M. Fujimoto [126], C. Fukunaga [164], E. Fullana Torregrosa [174], T. Fusayasu [116], J. Fuster [174], A. Gabrielli [23b,23a], A. Gabrielli [36], S. Gadatsch [54], P. Gadow [115], G. Gagliardi [55b,55a], L.G. Gagnon [110], G.E. Gallardo [134], E.J. Gallas [134], B.J. Gallop [143], R. Gamboa Goni [93], K.K. Gan [127], S. Ganguly [180], J. Gao [60a], Y. Gao [50], Y.S. Gao [31,l], F.M. Garay Walls [146a], C. García [174], J.E. García Navarro [174], J.A. García Pascual [15a], C. Garcia-Argos [52], M. Garcia-Sciveres [18], R.W. Gardner [37], N. Garelli [153], S. Gargiulo [52], C.A. Garner [167], V. Garonne [133], S.J. Gasiorowski [148], P. Gaspar [81b], A. Gaudiello [55b,55a], G. Gaudio [71a], I.L. Gavrilenko [111], A. Gavrilyuk [124], C. Gay [175], G. Gaycken [46], E.N. Gazis [10], A.A. Geanta [27b], C.M. Gee [145], C.N.P. Gee [143], J. Geisen [97], M. Geisen [100], C. Gemme [55b], M.H. Genest [58], C. Geng [106], S. Gentile [73a,73b], S. George [94], T. Geralis [44], L.O. Gerlach [53], P. Gessinger-Befurt [100], G. Gessner [47], S. Ghasemi [151], M. Ghasemi Bostanabad [176], M. Ghneimat [151], A. Ghosh [65], A. Ghosh [78], B. Giacobbe [23b], S. Giagu [73a,73b], N. Giangiacomi [23b,23a], P. Giannetti [72a], A. Giannini [70a,70b], G. Giannini [14], S.M. Gibson [94], M. Gignac [145], D.T. Gil [84b], B.J. Gilbert [39], D. Gillberg [34], G. Gilles [182], D.M. Gingrich [3,am], M.P. Giordani [67a,67c], P.F. Giraud [144], G. Giugliarelli [67a,67c], D. Giugni [69a], F. Giuli [74a,74b], S. Gkaitatzis [162], I. Gkialas [9,g], E.L. Gkougkousis [14], P. Gkountoumis [10], L.K. Gladilin [113], C. Glasman [99], J. Glatzer [14], P.C.F. Glaysher [46], A. Glazov [46], G.R. Gledhill [131], I. Gnesi [41b,b], M. Goblirsch-Kolb [26], D. Godin [110], S. Goldfarb [105], T. Golling [54], D. Golubkov [123], A. Gomes [139a,139b], R. Goncalves Gama [53], R. Gonçalo [139a,139c], G. Gonella [131], L. Gonella [21], A. Gongadze [80], F. Gonnella [21], J.L. Gonski [39], S. González de la Hoz [174], S. Gonzalez Fernandez [14], R. Gonzalez Lopez [91], C. Gonzalez Renteria [18], R. Gonzalez Suarez [172], S. Gonzalez-Sevilla [54], G.R. Gonzalvo Rodriguez [174], L. Goossens [36], N.A. Gorasia [21], P.A. Gorbounov [124], H.A. Gordon [29], B. Gorini [36], E. Gorini [68a,68b], A. Gorišek [92], A.T. Goshaw [49], M.I. Gostkin [80], C.A. Gottardo [119], M. Gouighri [35b], A.G. Goussiou [148], N. Govender [33c], C. Goy [5], I. Grabowska-Bold [84a], E.C. Graham [91], J. Gramling [171], E. Gramstad [133], S. Grancagnolo [19], M. Grandi [156], V. Gratchev [137], P.M. Gravila [27f], F.G. Gravili [68a,68b], C. Gray [57], H.M. Gray [18], C. Grefe [24], K. Gregersen [97], I.M. Gregor [46], P. Grenier [153], K. Grevtsov [46], C. Grieco [14], N.A. Grieser [128], A.A. Grillo [145], K. Grimm [31,k], S. Grinstein [14,w], J.-F. Grivaz [65], S. Groh [100], E. Gross [180], J. Grosse-Knetter [53], Z.J. Grout [95], C. Grud [106], A. Grummer [118], J.C. Grundy [134], L. Guan [106], W. Guan [181], C. Gubbels [175], J. Guenther [36], A. Guerguichon [65], J.G.R. Guerrero Rojas [174], F. Guescini [115], D. Guest [171], R. Gugel [100], A. Guida [46], T. Guillemin [5], S. Guindon [36], U. Gul [57], J. Guo [60c], W. Guo [106], Y. Guo [60a], Z. Guo [102], R. Gupta [46], S. Gurbuz [12c], G. Gustavino [128], M. Guth [52], P. Gutierrez [128], C. Gutschow [95], C. Guyot [144], C. Gwenlan [134], C.B. Gwilliam [91], E.S. Haaland [133], A. Haas [125], C. Haber [18], H.K. Hadavand [8], A. Hadef [60a], M. Haleem [177], J. Haley [129], J.J. Hall [149], G. Halladjian [107], G.D. Hallewell [102], K. Hamano [176], H. Hamdaoui [35f], M. Hamer [24], G.N. Hamity [50], J. Han [60b], K. Han [60a,v], L. Han [60a], S. Han [18], Y.F. Han [167], K. Hanagaki [82,t], M. Hance [145], D.M. Handl [114], M.D. Hank [37], R. Hankache [135], E. Hansen [97], J.B. Hansen [40], J.D. Hansen [40], M.C. Hansen [24], P.H. Hansen [40], E.C. Hanson [101], K. Hara [169], T. Harenberg [182], S. Harkusha [108], P.F. Harrison [178], N.M. Hartman [153], N.M. Hartmann [114], Y. Hasegawa [150], A. Hasib [50], S. Hassani [144], S. Haug [20], R. Hauser [107], L.B. Havener [39], M. Havranek [141], C.M. Hawkes [21], R.J. Hawkings [36], S. Hayashida [117], D. Hayden [107], C. Hayes [106], R.L. Hayes [175], C.P. Hays [134], J.M. Hays [93], H.S. Hayward [91], S.J. Haywood [143], F. He [60a], Y. He [165], M.P. Heath [50], V. Hedberg [97], S. Heer [24], A.L. Heggelund [133], C. Heidegger [52], K.K. Heidegger [52], W.D. Heidorn [79], J. Heilman [34], S. Heim [46], T. Heim [18], B. Heinemann [46,ak], J.G. Heinlein [136], J.J. Heinrich [131], L. Heinrich [36], J. Hejbal [140], L. Helary [46], A. Held [125], S. Hellesund [133], C.M. Helling [145], S. Hellman [45a,45b], C. Helsens [36], R.C.W. Henderson [90], Y. Heng [181], L. Henkelmann [32], A.M. Henriques Correia [36], H. Herde [26], Y. Hernández Jiménez [33e], H. Herr [100], M.G. Herrmann [114], T. Herrmann [48], G. Herten [52], R. Hertenberger [114], L. Hervas [36], T.C. Herwig [136], G.G. Hesketh [95], N.P. Hessey [168a], H. Hibi [83], A. Higashida [163], S. Higashino [82], E. Higón-Rodriguez [174], K. Hildebrand [37], J.C. Hill [32], K.K. Hill [29], K.H. Hiller [46], S.J. Hillier [21], M. Hils [48], I. Hinchliffe [18], F. Hinterkeuser [24], M. Hirose [132], S. Hirose [52], D. Hirschbuehl [182], B. Hiti [92], O. Hladik [140], D.R. Hlaluku [33e], J. Hobbs [155], N. Hod [180], M.C. Hodgkinson [149], A. Hoecker [36], D. Hohn [52], D. Hohov [65], T. Holm [24], T.R. Holmes [37], M. Holzbock [114], L.B.A.H. Hommels [32], T.M. Hong [138], J.C. Honig [52], A. Hönle [115], B.H. Hooberman [173], W.H. Hopkins [6], Y. Horii [117], P. Horn [48], L.A. Horyn [37], S. Hou [158], A. Hoummada [35a],

J. Howarth [57], J. Hoya [89], M. Hrabovsky [130], J. Hrdinka [77], J. Hrivnac [65], A. Hrynevich [109], T. Hryn'ova [5], P.J. Hsu [64], S.-C. Hsu [148], Q. Hu [29], S. Hu [60c], Y.F. Hu [15a,15d,ao], D.P. Huang [95], Y. Huang [60a], Y. Huang [15a], Z. Hubacek [141], F. Hubaut [102], M. Huebner [24], F. Huegging [24], T.B. Huffman [134], M. Huhtinen [36], R. Hulsken [58], R.F.H. Hunter [34], P. Huo [155], N. Huseynov [80,ac], J. Huston [107], J. Huth [59], R. Hyneman [153], S. Hyrych [28a], G. Iacobucci [54], G. Iakovidis [29], I. Ibragimov [151], L. Iconomidou-Fayard [65], P. Iengo [36], R. Ignazzi [40], O. Igonkina [120,y,*], R. Iguchi [163], T. Iizawa [54], Y. Ikegami [82], M. Ikeno [82], N. Ilic [119,167,ab], F. Iltzsche [48], H. Imam [35a], G. Introzzi [71a,71b], M. Iodice [75a], K. Iordanidou [168a], V. Ippolito [73a,73b], M.F. Isacson [172], M. Ishino [163], W. Islam [129], C. Issever [19,46], S. Istin [160], F. Ito [169], J.M. Iturbe Ponce [63a], R. Iuppa [76a,76b], A. Ivina [180], H. Iwasaki [82], J.M. Izen [43], V. Izzo [70a], P. Jacka [140], P. Jackson [1], R.M. Jacobs [46], B.P. Jaeger [152], V. Jain [2], G. Jäkel [182], K.B. Jakobi [100], K. Jakobs [52], T. Jakoubek [180], J. Jamieson [57], K.W. Janas [84a], R. Jansky [54], M. Janus [53], P.A. Janus [84a], G. Jarlskog [97], A.E. Jaspan [91], N. Javadov [80,ac], T. Javůrek [36], M. Javurkova [103], F. Jeanneau [144], L. Jeanty [131], J. Jejelava [159a], P. Jenni [52,c], N. Jeong [46], S. Jézéquel [5], H. Ji [181], J. Jia [155], H. Jiang [79], Y. Jiang [60a], Z. Jiang [153], S. Jiggins [52], F.A. Jimenez Morales [38], J. Jimenez Pena [115], S. Jin [15c], A. Jinaru [27b], O. Jinnouchi [165], H. Jivan [33e], P. Johansson [149], K.A. Johns [7], C.A. Johnson [66], R.W.L. Jones [90], S.D. Jones [156], T.J. Jones [91], J. Jongmanns [61a], J. Jovicevic [36], X. Ju [18], J.J. Junggeburth [115], A. Juste Rozas [14,w], A. Kaczmarska [85], M. Kado [73a,73b], H. Kagan [127], M. Kagan [153], A. Kahn [39], C. Kahra [100], T. Kaji [179], E. Kajomovitz [160], C.W. Kalderon [29], A. Kaluza [100], A. Kamenshchikov [123], M. Kaneda [163], N.J. Kang [145], S. Kang [79], Y. Kano [117], J. Kanzaki [82], L.S. Kaplan [181], D. Kar [33e], K. Karava [134], M.J. Kareem [168b], I. Karkanias [162], S.N. Karpov [80], Z.M. Karpova [80], V. Kartvelishvili [90], A.N. Karyukhin [123], E. Kasimi [162], A. Kastanas [45a,45b], C. Kato [60d,60c], J. Katzy [46], K. Kawade [150], K. Kawagoe [88], T. Kawaguchi [117], T. Kawamoto [144], G. Kawamura [53], E.F. Kay [176], S. Kazakos [14], V.F. Kazanin [122b,122a], R. Keeler [176], R. Kehoe [42], J.S. Keller [34], E. Kellermann [97], D. Kelsey [156], J.J. Kempster [21], J. Kendrick [21], K.E. Kennedy [39], O. Kepka [140], S. Kersten [182], B.P. Kerševan [92], S. Ketabchi Haghighat [167], M. Khader [173], F. Khalil-Zada [13], M. Khandoga [144], A. Khanov [129], A.G. Kharlamov [122b,122a], T. Kharlamova [122b,122a], E.E. Khoda [175], A. Khodinov [166], T.J. Khoo [54], G. Khoriauli [177], E. Khramov [80], J. Khubua [159b], S. Kido [83], M. Kiehn [36], C.R. Kilby [94], E. Kim [165], Y.K. Kim [37], N. Kimura [95], A. Kirchhoff [53], D. Kirchmeier [48], J. Kirk [143], A.E. Kiryunin [115], T. Kishimoto [163], D.P. Kisliuk [167], V. Kitali [46], C. Kitsaki [10], O. Kivernyk [24], T. Klapdor-Kleingrothaus [52], M. Klassen [61a], C. Klein [34], M.H. Klein [106], M. Klein [91], U. Klein [91], K. Kleinknecht [100], P. Klimek [121], A. Klimentov [29], T. Klingl [24], T. Klioutchnikova [36], F.F. Klitzner [114], P. Kluit [120], S. Kluth [115], E. Kneringer [77], E.B.F.G. Knoops [102], A. Knue [52], D. Kobayashi [88], M. Kobel [48], M. Kocian [153], T. Kodama [163], P. Kodys [142], D.M. Koeck [156], P.T. Koenig [24], T. Koffas [34], N.M. Köhler [36], M. Kolb [144], I. Koletsou [5], T. Komarek [130], T. Kondo [82], K. Köneke [52], A.X.Y. Kong [1], A.C. König [119], T. Kono [126], V. Konstantinides [95], N. Konstantinidis [95], B. Konya [97], R. Kopeliansky [66], S. Koperny [84a], K. Korcyl [85], K. Kordas [162], G. Koren [161], A. Korn [95], I. Korolkov [14], E.V. Korolkova [149], N. Korotkova [113], O. Kortner [115], S. Kortner [115], V.V. Kostyukhin [149,166], A. Kotsokechagia [65], A. Kotwal [49], A. Koulouris [10], A. Kourkoumeli-Charalampidi [71a,71b], C. Kourkoumelis [9], E. Kourlitis [6], V. Kouskoura [29], R. Kowalewski [176], W. Kozanecki [101], A.S. Kozhin [123], V.A. Kramarenko [113], G. Kramberger [92], D. Krasnopevtsev [60a], M.W. Krasny [135], A. Krasznahorkay [36], D. Krauss [115], J.A. Kremer [100], J. Kretzschmar [91], P. Krieger [167], F. Krieter [114], A. Krishnan [61b], M. Krivos [142], K. Krizka [18], K. Kroeninger [47], H. Kroha [115], J. Kroll [140], J. Kroll [136], K.S. Krowpman [107], U. Kruchonak [80], H. Krüger [24], N. Krumnack [79], M.C. Kruse [49], J.A. Krzysiak [85], A. Kubota [165], O. Kuchinskaia [166], S. Kuday [4b], D. Kuechler [46], J.T. Kuechler [46], S. Kuehn [36], T. Kuhl [46], V. Kukhtin [80], Y. Kulchitsky [108,af], S. Kuleshov [146b], Y.P. Kulinich [173], M. Kuna [58], T. Kunigo [86], A. Kupco [140], T. Kupfer [47], O. Kuprash [52], H. Kurashige [83], L.L. Kurchaninov [168a], Y.A. Kurochkin [108], A. Kurova [112], M.G. Kurth [15a,15d], E.S. Kuwertz [36], M. Kuze [165], A.K. Kvam [148], J. Kvita [130], T. Kwan [104], F. La Ruffa [41b,41a], C. Lacasta [174], F. Lacava [73a,73b], D.P.J. Lack [101], H. Lacker [19], D. Lacour [135], E. Ladygin [80], R. Lafaye [5], B. Laforge [135], T. Lagouri [146c], S. Lai [53], I.K. Lakomiec [84a], J.E. Lambert [128], S. Lammers [66], W. Lampl [7], C. Lampoudis [162], E. Lançon [29], U. Landgraf [52], M.P.J. Landon [93], M.C. Lanfermann [54], V.S. Lang [52], J.C. Lange [53], R.J. Langenberg [103], A.J. Lankford [171], F. Lanni [29], K. Lantzsch [24], A. Lanza [71a], A. Lapertosa [55b,55a], J.F. Laporte [144], T. Lari [69a], F. Lasagni Manghi [23b,23a], M. Lassnig [36], T.S. Lau [63a], A. Laudrain [65], A. Laurier [34], M. Lavorgna [70a,70b], S.D. Lawlor [94], M. Lazzaroni [69a,69b], B. Le [101], E. Le Guirriec [102], A. Lebedev [79], M. LeBlanc [7], T. LeCompte [6], F. Ledroit-Guillon [58], A.C.A. Lee [95], C.A. Lee [29], G.R. Lee [17], L. Lee [59], S.C. Lee [158], S. Lee [79], B. Lefebvre [168a], H.P. Lefebvre [94], M. Lefebvre [176],

C. Leggett [18], K. Lehmann [152], N. Lehmann [20], G. Lehmann Miotto [36], W.A. Leight [46], A. Leisos [162,u], M.A.L. Leite [81c], C.E. Leitgeb [114], R. Leitner [142], D. Lellouch [180,*], K.J.C. Leney [42], T. Lenz [24], S. Leone [72a], C. Leonidopoulos [50], A. Leopold [135], C. Leroy [110], R. Les [107], C.G. Lester [32], M. Levchenko [137], J. Levêque [5], D. Levin [106], L.J. Levinson [180], D.J. Lewis [21], B. Li [15b], B. Li [106], C-Q. Li [60a], F. Li [60c], H. Li [60a], H. Li [60b], J. Li [60c], K. Li [148], L. Li [60c], M. Li [15a,15d], Q. Li [15a,15d], Q.Y. Li [60a], S. Li [60d,60c], X. Li [46], Y. Li [46], Z. Li [60b], Z. Li [134], Z. Li [104], Z. Liang [15a], M. Liberatore [46], B. Liberti [74a], A. Liblong [167], K. Lie [63c], S. Lim [29], C.Y. Lin [32], K. Lin [107], R.A. Linck [66], R.E. Lindley [7], J.H. Lindon [21], A. Linss [46], A.L. Lionti [54], E. Lipeles [136], A. Lipniacka [17], T.M. Liss [173,al], A. Lister [175], J.D. Little [8], B. Liu [79], B.X. Liu [6], H.B. Liu [29], J.B. Liu [60a], J.K.K. Liu [37], K. Liu [60d,60c], M. Liu [60a], P. Liu [15a], X. Liu [60a], Y. Liu [46], Y. Liu [15a,15d], Y.L. Liu [106], Y.W. Liu [60a], M. Livan [71a,71b], A. Lleres [58], J. Llorente Merino [152], S.L. Lloyd [93], C.Y. Lo [63b], E.M. Lobodzinska [46], P. Loch [7], S. Loffredo [74a,74b], T. Lohse [19], K. Lohwasser [149], M. Lokajicek [140], J.D. Long [173], R.E. Long [90], I. Longarini [73a,73b], L. Longo [36], K.A. Looper [127], I. Lopez Paz [101], A. Lopez Solis [149], J. Lorenz [114], N. Lorenzo Martinez [5], A.M. Lory [114], P.J. Lösel [114], A. Lösle [52], X. Lou [46], X. Lou [15a], A. Lounis [65], J. Love [6], P.A. Love [90], J.J. Lozano Bahilo [174], M. Lu [60a], Y.J. Lu [64], H.J. Lubatti [148], C. Luci [73a,73b], F.L. Lucio Alves [15c], A. Lucotte [58], F. Luehring [66], I. Luise [135], L. Luminari [73a], B. Lund-Jensen [154], M.S. Lutz [161], D. Lynn [29], H. Lyons [91], R. Lysak [140], E. Lytken [97], F. Lyu [15a], V. Lyubushkin [80], T. Lyubushkina [80], H. Ma [29], L.L. Ma [60b], Y. Ma [95], D.M. Mac Donell [176], G. Maccarrone [51], A. Macchiolo [115], C.M. Macdonald [149], J.C. MacDonald [149], J. Machado Miguens [136], D. Madaffari [174], R. Madar [38], W.F. Mader [48], M. Madugoda Ralalage Don [129], N. Madysa [48], J. Maeda [83], T. Maeno [29], M. Maerker [48], V. Magerl [52], N. Magini [79], J. Magro [67a,67c,q], D.J. Mahon [39], C. Maidantchik [81b], T. Maier [114], A. Maio [139a,139b,139d], K. Maj [84a], O. Majersky [28a], S. Majewski [131], Y. Makida [82], N. Makovec [65], B. Malaescu [135], Pa. Malecki [85], V.P. Maleev [137], F. Malek [58], D. Malito [41b,41a], U. Mallik [78], D. Malon [6], C. Malone [32], S. Maltezos [10], S. Malyukov [80], J. Mamuzic [174], G. Mancini [70a,70b], I. Mandić [92], L. Manhaes de Andrade Filho [81a], I.M. Maniatis [162], J. Manjarres Ramos [48], K.H. Mankinen [97], A. Mann [114], A. Manousos [77], B. Mansoulie [144], I. Manthos [162], S. Manzoni [120], A. Marantis [162], G. Marceca [30], L. Marchese [134], G. Marchiori [135], M. Marcisovsky [140], L. Marcoccia [74a,74b], C. Marcon [97], C.A. Marin Tobon [36], M. Marjanovic [128], Z. Marshall [18], M.U.F. Martensson [172], S. Marti-Garcia [174], C.B. Martin [127], T.A. Martin [178], V.J. Martin [50], B. Martin dit Latour [17], L. Martinelli [75a,75b], M. Martinez [14,w], P. Martinez Agullo [174], V.I. Martinez Outschoorn [103], S. Martin-Haugh [143], V.S. Martoiu [27b], A.C. Martyniuk [95], A. Marzin [36], S.R. Maschek [115], L. Masetti [100], T. Mashimo [163], R. Mashinistov [111], J. Masik [101], A.L. Maslennikov [122b,122a], L. Massa [23b,23a], P. Massarotti [70a,70b], P. Mastrandrea [72a,72b], A. Mastroberardino [41b,41a], T. Masubuchi [163], D. Matakias [29], A. Matic [114], N. Matsuzawa [163], P. Mättig [24], J. Maurer [27b], B. Maček [92], D.A. Maximov [122b,122a], R. Mazini [158], I. Maznas [162], S.M. Mazza [145], J.P. Mc Gowan [104], S.P. Mc Kee [106], T.G. McCarthy [115], W.P. McCormack [18], E.F. McDonald [105], J.A. Mcfayden [36], G. Mchedlidze [159b], M.A. McKay [42], K.D. McLean [176], S.J. McMahon [143], P.C. McNamara [105], C.J. McNicol [178], R.A. McPherson [176,ab], J.E. Mdhluli [33e], Z.A. Meadows [103], S. Meehan [36], T. Megy [38], S. Mehlhase [114], A. Mehta [91], B. Meirose [43], D. Melini [160], B.R. Mellado Garcia [33e], J.D. Mellenthin [53], M. Melo [28a], F. Meloni [46], A. Melzer [24], E.D. Mendes Gouveia [139a,139e], L. Meng [36], X.T. Meng [106], S. Menke [115], E. Meoni [41b,41a], S. Mergelmeyer [19], S.A.M. Merkt [138], C. Merlassino [134], P. Mermod [54], L. Merola [70a,70b], C. Meroni [69a], G. Merz [106], O. Meshkov [113,111], J.K.R. Meshreki [151], J. Metcalfe [6], A.S. Mete [6], C. Meyer [66], J-P. Meyer [144], M. Michetti [19], R.P. Middleton [143], L. Mijović [50], G. Mikenberg [180], M. Mikestikova [140], M. Mikuž [92], H. Mildner [149], A. Milic [167], C.D. Milke [42], D.W. Miller [37], A. Milov [180], D.A. Milstead [45a,45b], R.A. Mina [153], A.A. Minaenko [123], I.A. Minashvili [159b], A.I. Mincer [125], B. Mindur [84a], M. Mineev [80], Y. Minegishi [163], L.M. Mir [14], M. Mironova [134], A. Mirto [68a,68b], K.P. Mistry [136], T. Mitani [179], J. Mitrevski [114], V.A. Mitsou [174], M. Mittal [60c], O. Miu [167], A. Miucci [20], P.S. Miyagawa [93], A. Mizukami [82], J.U. Mjörnmark [97], T. Mkrtchyan [61a], M. Mlynarikova [142], T. Moa [45a,45b], S. Mobius [53], K. Mochizuki [110], P. Mogg [114], S. Mohapatra [39], R. Moles-Valls [24], K. Mönig [46], E. Monnier [102], A. Montalbano [152], J. Montejo Berlingen [36], M. Montella [95], F. Monticelli [89], S. Monzani [69a], N. Morange [65], A.L. Moreira De Carvalho [139a], D. Moreno [22a], M. Moreno Llácer [174], C. Moreno Martinez [14], P. Morettini [55b], M. Morgenstern [160], S. Morgenstern [48], D. Mori [152], M. Morii [59], M. Morinaga [179], V. Morisbak [133], A.K. Morley [36], G. Mornacchi [36], A.P. Morris [95], L. Morvaj [155], P. Moschovakos [36], B. Moser [120], M. Mosidze [159b], T. Moskalets [144], J. Moss [31,m], E.J.W. Moyse [103], S. Muanza [102], J. Mueller [138], R.S.P. Mueller [114], D. Muenstermann [90], G.A. Mullier [97], D.P. Mungo [69a,69b], J.L. Munoz Martinez [14], F.J. Munoz Sanchez [101],

P. Murin [28b], W.J. Murray [178,143], A. Murrone [69a,69b], J.M. Muse [128], M. Muškinja [18], C. Mwewa [33a], A.G. Myagkov [123,ah], A.A. Myers [138], G. Myers [66], J. Myers [131], M. Myska [141], B.P. Nachman [18], O. Nackenhorst [47], A. Nag Nag [48], K. Nagai [134], K. Nagano [82], Y. Nagasaka [62], J.L. Nagle [29], E. Nagy [102], A.M. Nairz [36], Y. Nakahama [117], K. Nakamura [82], T. Nakamura [163], H. Nanjo [132], F. Napolitano [61a], R.F. Naranjo Garcia [46], R. Narayan [42], I. Naryshkin [137], T. Naumann [46], G. Navarro [22a], P.Y. Nechaeva [111], F. Nechansky [46], T.J. Neep [21], A. Negri [71a,71b], M. Negrini [23b], C. Nellist [119], C. Nelson [104], M.E. Nelson [45a,45b], S. Nemecek [140], M. Nessi [36,e], M.S. Neubauer [173], F. Neuhaus [100], M. Neumann [182], R. Newhouse [175], P.R. Newman [21], C.W. Ng [138], Y.S. Ng [19], Y.W.Y. Ng [171], B. Ngair [35f], H.D.N. Nguyen [102], T. Nguyen Manh [110], E. Nibigira [38], R.B. Nickerson [134], R. Nicolaidou [144], D.S. Nielsen [40], J. Nielsen [145], M. Niemeyer [53], N. Nikiforou [11], V. Nikolaenko [123,ah], I. Nikolic-Audit [135], K. Nikolopoulos [21], P. Nilsson [29], H.R. Nindhito [54], Y. Ninomiya [82], A. Nisati [73a], N. Nishu [60c], R. Nisius [115], I. Nitsche [47], T. Nitta [179], T. Nobe [163], D.L. Noel [32], Y. Noguchi [86], I. Nomidis [135], M.A. Nomura [29], M. Nordberg [36], J. Novak [92], T. Novak [92], O. Novgorodova [48], R. Novotny [141], L. Nozka [130], K. Ntekas [171], E. Nurse [95], F.G. Oakham [34,am], H. Oberlack [115], J. Ocariz [135], A. Ochi [83], I. Ochoa [39], J.P. Ochoa-Ricoux [146a], K. O'Connor [26], S. Oda [88], S. Odaka [82], S. Oerdek [53], A. Ogrodnik [84a], A. Oh [101], C.C. Ohm [154], H. Oide [165], M.L. Ojeda [167], H. Okawa [169], Y. Okazaki [86], M.W. O'Keefe [91], Y. Okumura [163], T. Okuyama [82], A. Olariu [27b], L.F. Oleiro Seabra [139a], S.A. Olivares Pino [146a], D. Oliveira Damazio [29], J.L. Oliver [1], M.J.R. Olsson [171], A. Olszewski [85], J. Olszowska [85], Ö.O. Öncel [24], D.C. O'Neil [152], A.P. O'neill [134], A. Onofre [139a,139e], P.U.E. Onyisi [11], H. Oppen [133], R.G. Oreamuno Madriz [121], M.J. Oreglia [37], G.E. Orellana [89], D. Orestano [75a,75b], N. Orlando [14], R.S. Orr [167], V. O'Shea [57], R. Ospanov [60a], G. Otero y Garzon [30], H. Otono [88], P.S. Ott [61a], G.J. Ottino [18], M. Ouchrif [35e], J. Ouellette [29], F. Ould-Saada [133], A. Ouraou [144,*], Q. Ouyang [15a], M. Owen [57], R.E. Owen [143], V.E. Ozcan [12c], N. Ozturk [8], J. Pacalt [130], H.A. Pacey [32], K. Pachal [49], A. Pacheco Pages [14], C. Padilla Aranda [14], S. Pagan Griso [18], G. Palacino [66], S. Palazzo [50], S. Palestini [36], M. Palka [84b], P. Palni [84a], C.E. Pandini [54], J.G. Panduro Vazquez [94], P. Pani [46], G. Panizzo [67a,67c], L. Paolozzi [54], C. Papadatos [110], K. Papageorgiou [9,g], S. Parajuli [42], A. Paramonov [6], C. Paraskevopoulos [10], D. Paredes Hernandez [63b], S.R. Paredes Saenz [134], B. Parida [180], T.H. Park [167], A.J. Parker [31], M.A. Parker [32], F. Parodi [55b,55a], E.W. Parrish [121], J.A. Parsons [39], U. Parzefall [52], L. Pascual Dominguez [135], V.R. Pascuzzi [18], J.M.P. Pasner [145], F. Pasquali [120], E. Pasqualucci [73a], S. Passaggio [55b], F. Pastore [94], P. Pasuwan [45a,45b], S. Pataraia [100], J.R. Pater [101], A. Pathak [181,i], J. Patton [91], T. Pauly [36], J. Pearkes [153], B. Pearson [115], M. Pedersen [133], L. Pedraza Diaz [119], R. Pedro [139a], T. Peiffer [53], S.V. Peleganchuk [122b,122a], O. Penc [140], H. Peng [60a], B.S. Peralva [81a], M.M. Perego [65], A.P. Pereira Peixoto [139a], L. Pereira Sanchez [45a,45b], D.V. Perepelitsa [29], E. Perez Codina [168a], F. Peri [19], L. Perini [69a,69b], H. Pernegger [36], S. Perrella [36], A. Perrevoort [120], K. Peters [46], R.F.Y. Peters [101], B.A. Petersen [36], T.C. Petersen [40], E. Petit [102], V. Petousis [141], A. Petridis [1], C. Petridou [162], F. Petrucci [75a,75b], M. Pettee [183], N.E. Pettersson [103], K. Petukhova [142], A. Peyaud [144], R. Pezoa [146d], L. Pezzotti [71a,71b], T. Pham [105], F.H. Phillips [107], P.W. Phillips [143], M.W. Phipps [173], G. Piacquadio [155], E. Pianori [18], A. Picazio [103], R.H. Pickles [101], R. Piegaia [30], D. Pietreanu [27b], J.E. Pilcher [37], A.D. Pilkington [101], M. Pinamonti [67a,67c], J.L. Pinfold [3], C. Pitman Donaldson [95], M. Pitt [161], L. Pizzimento [74a,74b], A. Pizzini [120], M.-A. Pleier [29], V. Plesanovs [52], V. Pleskot [142], E. Plotnikova [80], P. Podberezko [122b,122a], R. Poettgen [97], R. Poggi [54], L. Poggioli [135], I. Pogrebnyak [107], D. Pohl [24], I. Pokharel [53], G. Polesello [71a], A. Poley [152,168a], A. Policicchio [73a,73b], R. Polifka [142], A. Polini [23b], C.S. Pollard [46], V. Polychronakos [29], D. Ponomarenko [112], L. Pontecorvo [36], S. Popa [27a], G.A. Popeneciu [27d], L. Portales [5], D.M. Portillo Quintero [58], S. Pospisil [141], K. Potamianos [46], I.N. Potrap [80], C.J. Potter [32], H. Potti [11], T. Poulsen [97], J. Poveda [174], T.D. Powell [149], G. Pownall [46], M.E. Pozo Astigarraga [36], P. Pralavorio [102], S. Prell [79], D. Price [101], M. Primavera [68a], M.L. Proffitt [148], N. Proklova [112], K. Prokofiev [63c], F. Prokoshin [80], S. Protopopescu [29], J. Proudfoot [6], M. Przybycien [84a], D. Pudzha [137], A. Puri [173], P. Puzo [65], D. Pyatiizbyantseva [112], J. Qian [106], Y. Qin [101], A. Quadt [53], M. Queitsch-Maitland [36], M. Racko [28a], F. Ragusa [69a,69b], G. Rahal [98], J.A. Raine [54], S. Rajagopalan [29], A. Ramirez Morales [93], K. Ran [15a,15d], D.M. Rauch [46], F. Rauscher [114], S. Rave [100], B. Ravina [149], I. Ravinovich [180], J.H. Rawling [101], M. Raymond [36], A.L. Read [133], N.P. Readioff [149], M. Reale [68a,68b], D.M. Rebuzzi [71a,71b], G. Redlinger [29], K. Reeves [43], J. Reichert [136], D. Reikher [161], A. Reiss [100], A. Rej [151], C. Rembser [36], A. Renardi [46], M. Renda [27b], M.B. Rendel [115], A.G. Rennie [57], S. Resconi [69a], E.D. Resseguie [18], S. Rettie [95], B. Reynolds [127], E. Reynolds [21], O.L. Rezanova [122b,122a], P. Reznicek [142], E. Ricci [76a,76b], R. Richter [115], S. Richter [46],

E. Richter-Was [84b], M. Ridel [135], P. Rieck [115], O. Rifki [46], M. Rijssenbeek [155], A. Rimoldi [71a,71b], M. Rimoldi [46], L. Rinaldi [23b], T.T. Rinn [173], G. Ripellino [154], I. Riu [14], P. Rivadeneira [46], J.C. Rivera Vergara [176], F. Rizatdinova [129], E. Rizvi [93], C. Rizzi [36], S.H. Robertson [104,ab], M. Robin [46], D. Robinson [32], C.M. Robles Gajardo [146d], M. Robles Manzano [100], A. Robson [57], A. Rocchi [74a,74b], E. Rocco [100], C. Roda [72a,72b], S. Rodriguez Bosca [174], A.M. Rodríguez Vera [168b], S. Roe [36], J. Roggel [182], O. Røhne [133], R. Röhrig [115], R.A. Rojas [146d], B. Roland [52], C.P.A. Roland [66], J. Roloff [29], A. Romaniouk [112], M. Romano [23b,23a], N. Rompotis [91], M. Ronzani [125], L. Roos [135], S. Rosati [73a], G. Rosin [103], B.J. Rosser [136], E. Rossi [46], E. Rossi [75a,75b], E. Rossi [70a,70b], L.P. Rossi [55b], L. Rossini [46], R. Rosten [14], M. Rotaru [27b], B. Rottler [52], D. Rousseau [65], G. Rovelli [71a,71b], A. Roy [11], D. Roy [33e], A. Rozanov [102], Y. Rozen [160], X. Ruan [33e], T.A. Ruggeri [1], F. Rühr [52], A. Ruiz-Martinez [174], A. Rummler [36], Z. Rurikova [52], N.A. Rusakovich [80], H.L. Russell [104], L. Rustige [38,47], J.P. Rutherfoord [7], E.M. Rüttinger [149], M. Rybar [142], G. Rybkin [65], E.B. Rye [133], A. Ryzhov [123], J.A. Sabater Iglesias [46], P. Sabatini [53], L. Sabetta [73a,73b], S. Sacerdoti [65], H.F-W. Sadrozinski [145], R. Sadykov [80], F. Safai Tehrani [73a], B. Safarzadeh Samani [156], M. Safdari [153], P. Saha [121], S. Saha [104], M. Sahinsoy [115], A. Sahu [182], M. Saimpert [36], M. Saito [163], T. Saito [163], H. Sakamoto [163], D. Salamani [54], G. Salamanna [75a,75b], A. Salnikov [153], J. Salt [174], A. Salvador Salas [14], D. Salvatore [41b,41a], F. Salvatore [156], A. Salvucci [63a,63b,63c], A. Salzburger [36], J. Samarati [36], D. Sammel [52], D. Sampsonidis [162], D. Sampsonidou [162], J. Sánchez [174], A. Sanchez Pineda [67a,36,67c], H. Sandaker [133], C.O. Sander [46], I.G. Sanderswood [90], M. Sandhoff [182], C. Sandoval [22b], D.P.C. Sankey [143], M. Sannino [55b,55a], Y. Sano [117], A. Sansoni [51], C. Santoni [38], H. Santos [139a,139b], S.N. Santpur [18], A. Santra [174], K.A. Saoucha [149], A. Sapronov [80], J.G. Saraiva [139a,139d], O. Sasaki [82], K. Sato [169], F. Sauerburger [52], E. Sauvan [5], P. Savard [167,am], R. Sawada [163], C. Sawyer [143], L. Sawyer [96,ag], I. Sayago Galvan [174], C. Sbarra [23b], A. Sbrizzi [67a,67c], T. Scanlon [95], J. Schaarschmidt [148], P. Schacht [115], D. Schaefer [37], L. Schaefer [136], S. Schaepe [36], U. Schäfer [100], A.C. Schaffer [65], D. Schaile [114], R.D. Schamberger [155], E. Schanet [114], C. Scharf [19], N. Scharmberg [101], V.A. Schegelsky [137], D. Scheirich [142], F. Schenck [19], M. Schernau [171], C. Schiavi [55b,55a], L.K. Schildgen [24], Z.M. Schillaci [26], E.J. Schioppa [68a,68b], M. Schioppa [41b,41a], K.E. Schleicher [52], S. Schlenker [36], K.R. Schmidt-Sommerfeld [115], K. Schmieden [36], C. Schmitt [100], S. Schmitt [46], J.C. Schmoeckel [46], L. Schoeffel [144], A. Schoening [61b], P.G. Scholer [52], E. Schopf [134], M. Schott [100], J.F.P. Schouwenberg [119], J. Schovancova [36], S. Schramm [54], F. Schroeder [182], A. Schulte [100], H-C. Schultz-Coulon [61a], M. Schumacher [52], B.A. Schumm [145], Ph. Schune [144], A. Schwartzman [153], T.A. Schwarz [106], Ph. Schwemling [144], R. Schwienhorst [107], A. Sciandra [145], G. Sciolla [26], M. Scornajenghi [41b,41a], F. Scuri [72a], F. Scutti [105], L.M. Scyboz [115], C.D. Sebastiani [91], P. Seema [19], S.C. Seidel [118], A. Seiden [145], B.D. Seidlitz [29], T. Seiss [37], C. Seitz [46], J.M. Seixas [81b], G. Sekhniaidze [70a], S.J. Sekula [42], N. Semprini-Cesari [23b,23a], S. Sen [49], C. Serfon [29], L. Serin [65], L. Serkin [67a,67b], M. Sessa [60a], H. Severini [128], S. Sevova [153], F. Sforza [55b,55a], A. Sfyrla [54], E. Shabalina [53], J.D. Shahinian [145], N.W. Shaikh [45a,45b], D. Shaked Renous [180], L.Y. Shan [15a], M. Shapiro [18], A. Sharma [134], A.S. Sharma [1], P.B. Shatalov [124], K. Shaw [156], S.M. Shaw [101], M. Shehade [180], Y. Shen [128], A.D. Sherman [25], P. Sherwood [95], L. Shi [95], S. Shimizu [82], C.O. Shimmin [183], Y. Shimogama [179], M. Shimojima [116], I.P.J. Shipsey [134], S. Shirabe [165], M. Shiyakova [80,z], J. Shlomi [180], A. Shmeleva [111], M.J. Shochet [37], J. Shojaii [105], D.R. Shope [154], S. Shrestha [127], E.M. Shrif [33e], E. Shulga [180], P. Sicho [140], A.M. Sickles [173], E. Sideras Haddad [33e], O. Sidiropoulou [36], A. Sidoti [23b,23a], F. Siegert [48], Dj. Sijacki [16], M.Jr. Silva [181], M.V. Silva Oliveira [36], S.B. Silverstein [45a], S. Simion [65], R. Simoniello [100], C.J. Simpson-allsop [21], S. Simsek [12b], P. Sinervo [167], V. Sinetckii [113], S. Singh [152], M. Sioli [23b,23a], I. Siral [131], S.Yu. Sivoklokov [113], J. Sjölin [45a,45b], A. Skaf [53], E. Skorda [97], P. Skubic [128], M. Slawinska [85], K. Sliwa [170], R. Slovak [142], V. Smakhtin [180], B.H. Smart [143], J. Smiesko [28b], N. Smirnov [112], S.Yu. Smirnov [112], Y. Smirnov [112], L.N. Smirnova [113,r], O. Smirnova [97], E.A. Smith [37], H.A. Smith [134], M. Smizanska [90], K. Smolek [141], A. Smykiewicz [85], A.A. Snesarev [111], H.L. Snoek [120], I.M. Snyder [131], S. Snyder [29], R. Sobie [176,ab], A. Soffer [161], A. Søgaard [50], F. Sohns [53], C.A. Solans Sanchez [36], E.Yu. Soldatov [112], U. Soldevila [174], A.A. Solodkov [123], A. Soloshenko [80], O.V. Solovyanov [123], V. Solovyev [137], P. Sommer [149], H. Son [170], W. Song [143], W.Y. Song [168b], A. Sopczak [141], A.L. Sopio [95], F. Sopkova [28b], S. Sottocornola [71a,71b], R. Soualah [67a,67c], A.M. Soukharev [122b,122a], D. South [46], S. Spagnolo [68a,68b], M. Spalla [115], M. Spangenberg [178], F. Spanò [94], D. Sperlich [52], T.M. Spieker [61a], G. Spigo [36], M. Spina [156], D.P. Spiteri [57], M. Spousta [142], A. Stabile [69a,69b], B.L. Stamas [121], R. Stamen [61a], M. Stamenkovic [120], E. Stanecka [85], B. Stanislaus [134], M.M. Stanitzki [46], M. Stankaityte [134], B. Stapf [120], E.A. Starchenko [123], G.H. Stark [145],

J. Stark [58], P. Staroba [140], P. Starovoitov [61a], S. Stärz [104], R. Staszewski [85], G. Stavropoulos [44], M. Stegler [46], P. Steinberg [29], A.L. Steinhebel [131], B. Stelzer [152,168a], H.J. Stelzer [138], O. Stelzer-Chilton [168a], H. Stenzel [56], T.J. Stevenson [156], G.A. Stewart [36], M.C. Stockton [36], G. Stoicea [27b], M. Stolarski [139a], S. Stonjek [115], A. Straessner [48], J. Strandberg [154], S. Strandberg [45a,45b], M. Strauss [128], T. Strebler [102], P. Strizenec [28b], R. Ströhmer [177], D.M. Strom [131], R. Stroynowski [42], A. Strubig [50], S.A. Stucci [29], B. Stugu [17], J. Stupak [128], N.A. Styles [46], D. Su [153], W. Su [60c,148], X. Su [60a], V.V. Sulin [111], M.J. Sullivan [91], D.M.S. Sultan [54], S. Sultansoy [4c], T. Sumida [86], S. Sun [106], X. Sun [101], K. Suruliz [156], C.J.E. Suster [157], M.R. Sutton [156], S. Suzuki [82], M. Svatos [140], M. Swiatlowski [168a], S.P. Swift [2], T. Swirski [177], A. Sydorenko [100], I. Sykora [28a], M. Sykora [142], T. Sykora [142], D. Ta [100], K. Tackmann [46,x], J. Taenzer [161], A. Taffard [171], R. Tafirout [168a], E. Tagiev [123], R. Takashima [87], K. Takeda [83], T. Takeshita [150], E.P. Takeva [50], Y. Takubo [82], M. Talby [102], A.A. Talyshev [122b,122a], K.C. Tam [63b], N.M. Tamir [161], J. Tanaka [163], R. Tanaka [65], S. Tapia Araya [173], S. Tapprogge [100], A. Tarek Abouelfadl Mohamed [107], S. Tarem [160], K. Tariq [60b], G. Tarna [27b,d], G.F. Tartarelli [69a], P. Tas [142], M. Tasevsky [140], T. Tashiro [86], E. Tassi [41b,41a], A. Tavares Delgado [139a], Y. Tayalati [35f], A.J. Taylor [50], G.N. Taylor [105], W. Taylor [168b], H. Teagle [91], R. Teixeira De Lima [153], P. Teixeira-Dias [94], H. Ten Kate [36], J.J. Teoh [120], S. Terada [82], K. Terashi [163], J. Terron [99], S. Terzo [14], M. Testa [51], R.J. Teuscher [167,ab], S.J. Thais [183], N. Themistokleous [50], T. Theveneaux-Pelzer [46], F. Thiele [40], D.W. Thomas [94], J.O. Thomas [42], J.P. Thomas [21], E.A. Thompson [46], P.D. Thompson [21], E. Thomson [136], E.J. Thorpe [93], R.E. Ticse Torres [53], V.O. Tikhomirov [111,ai], Yu.A. Tikhonov [122b,122a], S. Timoshenko [112], P. Tipton [183], S. Tisserant [102], K. Todome [23b,23a], S. Todorova-Nova [142], S. Todt [48], J. Tojo [88], S. Tokár [28a], K. Tokushuku [82], E. Tolley [127], R. Tombs [32], K.G. Tomiwa [33e], M. Tomoto [117], L. Tompkins [153], P. Tornambe [103], E. Torrence [131], H. Torres [48], E. Torró Pastor [148], C. Tosciri [134], J. Toth [102,aa], D.R. Tovey [149], A. Traeet [17], C.J. Treado [125], T. Trefzger [177], F. Tresoldi [156], A. Tricoli [29], I.M. Trigger [168a], S. Trincaz-Duvoid [135], D.A. Trischuk [175], W. Trischuk [167], B. Trocmé [58], A. Trofymov [65], C. Troncon [69a], F. Trovato [156], L. Truong [33c], M. Trzebinski [85], A. Trzupek [85], F. Tsai [46], J.C-L. Tseng [134], P.V. Tsiareshka [108,af], A. Tsirigotis [162,u], V. Tsiskaridze [155], E.G. Tskhadadze [159a], M. Tsopoulou [162], I.I. Tsukerman [124], V. Tsulaia [18], S. Tsuno [82], D. Tsybychev [155], Y. Tu [63b], A. Tudorache [27b], V. Tudorache [27b], T.T. Tulbure [27a], A.N. Tuna [59], S. Turchikhin [80], D. Turgeman [180], I. Turk Cakir [4b,s], R.J. Turner [21], R. Turra [69a], P.M. Tuts [39], S. Tzamarias [162], E. Tzovara [100], K. Uchida [163], F. Ukegawa [169], G. Unal [36], M. Unal [11], A. Undrus [29], G. Unel [171], F.C. Ungaro [105], Y. Unno [82], K. Uno [163], J. Urban [28b], P. Urquijo [105], G. Usai [8], Z. Uysal [12d], V. Vacek [141], B. Vachon [104], K.O.H. Vadla [133], T. Vafeiadis [36], A. Vaidya [95], C. Valderanis [114], E. Valdes Santurio [45a,45b], M. Valente [54], S. Valentinetti [23b,23a], A. Valero [174], L. Valéry [46], R.A. Vallance [21], A. Vallier [36], J.A. Valls Ferrer [174], T.R. Van Daalen [14], P. Van Gemmeren [6], S. Van Stroud [95], I. Van Vulpen [120], M. Vanadia [74a,74b], W. Vandelli [36], M. Vandenbroucke [144], E.R. Vandewall [129], A. Vaniachine [166], D. Vannicola [73a,73b], R. Vari [73a], E.W. Varnes [7], C. Varni [55b,55a], T. Varol [158], D. Varouchas [65], K.E. Varvell [157], M.E. Vasile [27b], G.A. Vasquez [176], F. Vazeille [38], D. Vazquez Furelos [14], T. Vazquez Schroeder [36], J. Veatch [53], V. Vecchio [101], M.J. Veen [120], L.M. Veloce [167], F. Veloso [139a,139c], S. Veneziano [73a], A. Ventura [68a,68b], A. Verbytskyi [115], V. Vercesi [71a], M. Verducci [72a,72b], C.M. Vergel Infante [79], C. Vergis [24], W. Verkerke [120], A.T. Vermeulen [120], J.C. Vermeulen [120], C. Vernieri [153], M.C. Vetterli [152,am], N. Viaux Maira [146d], T. Vickey [149], O.E. Vickey Boeriu [149], G.H.A. Viehhauser [134], L. Vigani [61b], M. Villa [23b,23a], M. Villaplana Perez [3], E.M. Villhauer [50], E. Vilucchi [51], M.G. Vincter [34], G.S. Virdee [21], A. Vishwakarma [50], C. Vittori [23b,23a], I. Vivarelli [156], M. Vogel [182], P. Vokac [141], S.E. von Buddenbrock [33e], E. Von Toerne [24], V. Vorobel [142], K. Vorobev [112], M. Vos [174], J.H. Vossebeld [91], M. Vozak [101], N. Vranjes [16], M. Vranjes Milosavljevic [16], V. Vrba [141,*], M. Vreeswijk [120], R. Vuillermet [36], I. Vukotic [37], S. Wada [169], P. Wagner [24], W. Wagner [182], J. Wagner-Kuhr [114], S. Wahdan [182], H. Wahlberg [89], R. Wakasa [169], V.M. Walbrecht [115], J. Walder [143], R. Walker [114], S.D. Walker [94], W. Walkowiak [151], V. Wallangen [45a,45b], A.M. Wang [59], A.Z. Wang [181], C. Wang [60a], C. Wang [60c], F. Wang [181], H. Wang [18], H. Wang [3], J. Wang [63a], P. Wang [42], Q. Wang [128], R.-J. Wang [100], R. Wang [60a], R. Wang [6], S.M. Wang [158], W.T. Wang [60a], W. Wang [15c], W.X. Wang [60a], Y. Wang [60a], Z. Wang [106], C. Wanotayaroj [46], A. Warburton [104], C.P. Ward [32], D.R. Wardrope [95], N. Warrack [57], A.T. Watson [21], M.F. Watson [21], G. Watts [148], B.M. Waugh [95], A.F. Webb [11], C. Weber [29], M.S. Weber [20], S.A. Weber [34], S.M. Weber [61a], A.R. Weidberg [134], J. Weingarten [47], M. Weirich [100], C. Weiser [52], P.S. Wells [36], T. Wenaus [29], B. Wendland [47], T. Wengler [36], S. Wenig [36], N. Wermes [24], M. Wessels [61a], T.D. Weston [20], K. Whalen [131], A.M. Wharton [90], A.S. White [106], A. White [8], M.J. White [1], D. Whiteson [171], B.W. Whitmore [90], W. Wiedenmann [181], C. Wiel [48],

M. Wielers [143], N. Wieseotte [100], C. Wiglesworth [40], L.A.M. Wiik-Fuchs [52], H.G. Wilkens [36], L.J. Wilkins [94], H.H. Williams [136], S. Williams [32], S. Willocq [103], P.J. Windischhofer [134], I. Wingerter-Seez [5], E. Winkels [156], F. Winklmeier [131], B.T. Winter [52], M. Wittgen [153], M. Wobisch [96], A. Wolf [100], R. Wölker [134], J. Wollrath [52], M.W. Wolter [85], H. Wolters [139a,139c], V.W.S. Wong [175], N.L. Woods [145], S.D. Worm [46], B.K. Wosiek [85], K.W. Woźniak [85], K. Wraight [57], S.L. Wu [181], X. Wu [54], Y. Wu [60a], J. Wuerzinger [134], T.R. Wyatt [101], B.M. Wynne [50], S. Xella [40], J. Xiang [63c], X. Xiao [106], X. Xie [60a], I. Xiotidis [156], D. Xu [15a], H. Xu [60a], H. Xu [60a], L. Xu [29], T. Xu [144], W. Xu [106], Z. Xu [60b], Z. Xu [153], B. Yabsley [157], S. Yacoob [33a], K. Yajima [132], D.P. Yallup [95], N. Yamaguchi [88], Y. Yamaguchi [165], A. Yamamoto [82], M. Yamatani [163], T. Yamazaki [163], Y. Yamazaki [83], J. Yan [60c], Z. Yan [25], H.J. Yang [60c,60d], H.T. Yang [18], S. Yang [60a], T. Yang [63c], X. Yang [60b,58], Y. Yang [163], Z. Yang [60a], W-M. Yao [18], Y.C. Yap [46], Y. Yasu [82], E. Yatsenko [60c], H. Ye [15c], J. Ye [42], S. Ye [29], I. Yeletskikh [80], M.R. Yexley [90], E. Yigitbasi [25], P. Yin [39], K. Yorita [179], K. Yoshihara [79], C.J.S. Young [36], C. Young [153], J. Yu [79], R. Yuan [60b,h], X. Yue [61a], M. Zaazoua [35f], B. Zabinski [85], G. Zacharis [10], E. Zaffaroni [54], J. Zahreddine [135], A.M. Zaitsev [123,ah], T. Zakareishvili [159b], N. Zakharchuk [34], S. Zambito [36], D. Zanzi [36], D.R. Zaripovas [57], S.V. Zeißner [47], C. Zeitnitz [182], G. Zemaityte [134], J.C. Zeng [173], O. Zenin [123], T. Ženiš [28a], D. Zerwas [65], M. Zgubič [134], B. Zhang [15c], D.F. Zhang [15b], G. Zhang [15b], J. Zhang [6], K. Zhang [15a], L. Zhang [15c], L. Zhang [60a], M. Zhang [173], R. Zhang [181], S. Zhang [106], X. Zhang [60c], X. Zhang [60b], Y. Zhang [15a,15d], Z. Zhang [63a], Z. Zhang [65], P. Zhao [49], Z. Zhao [60a], A. Zhemchugov [80], Z. Zheng [106], D. Zhong [173], B. Zhou [106], C. Zhou [181], H. Zhou [7], M.S. Zhou [15a,15d], M. Zhou [155], N. Zhou [60c], Y. Zhou [7], C.G. Zhu [60b], C. Zhu [15a,15d], H.L. Zhu [60a], H. Zhu [15a], J. Zhu [106], Y. Zhu [60a], X. Zhuang [15a], K. Zhukov [111], V. Zhulanov [122b,122a], D. Zieminska [66], N.I. Zimine [80], S. Zimmermann [52,*], Z. Zinonos [115], M. Ziolkowski [151], L. Živković [16], G. Zobernig [181], A. Zoccoli [23b,23a], K. Zoch [53], T.G. Zorbas [149], R. Zou [37], L. Zwalinski [36]

[1] *Department of Physics, University of Adelaide, Adelaide; Australia*
[2] *Physics Department, SUNY Albany, Albany NY; United States of America*
[3] *Department of Physics, University of Alberta, Edmonton AB; Canada*
[4] [(a)] *Department of Physics, Ankara University, Ankara;* [(b)] *Istanbul Aydin University, Application and Research Center for Advanced Studies, Istanbul;* [(c)] *Division of Physics, TOBB University of Economics and Technology, Ankara; Turkey*
[5] *LAPP, Université Grenoble Alpes, Université Savoie Mont Blanc, CNRS/IN2P3, Annecy; France*
[6] *High Energy Physics Division, Argonne National Laboratory, Argonne IL; United States of America*
[7] *Department of Physics, University of Arizona, Tucson AZ; United States of America*
[8] *Department of Physics, University of Texas at Arlington, Arlington TX; United States of America*
[9] *Physics Department, National and Kapodistrian University of Athens, Athens; Greece*
[10] *Physics Department, National Technical University of Athens, Zografou; Greece*
[11] *Department of Physics, University of Texas at Austin, Austin TX; United States of America*
[12] [(a)] *Bahcesehir University, Faculty of Engineering and Natural Sciences, Istanbul;* [(b)] *Istanbul Bilgi University, Faculty of Engineering and Natural Sciences, Istanbul;* [(c)] *Department of Physics, Bogazici University, Istanbul;* [(d)] *Department of Physics Engineering, Gaziantep University, Gaziantep; Turkey*
[13] *Institute of Physics, Azerbaijan Academy of Sciences, Baku; Azerbaijan*
[14] *Institut de Física d'Altes Energies (IFAE), Barcelona Institute of Science and Technology, Barcelona; Spain*
[15] [(a)] *Institute of High Energy Physics, Chinese Academy of Sciences, Beijing;* [(b)] *Physics Department, Tsinghua University, Beijing;* [(c)] *Department of Physics, Nanjing University, Nanjing;* [(d)] *University of Chinese Academy of Science (UCAS), Beijing; China*
[16] *Institute of Physics, University of Belgrade, Belgrade; Serbia*
[17] *Department for Physics and Technology, University of Bergen, Bergen; Norway*
[18] *Physics Division, Lawrence Berkeley National Laboratory and University of California, Berkeley CA; United States of America*
[19] *Institut für Physik, Humboldt Universität zu Berlin, Berlin; Germany*
[20] *Albert Einstein Center for Fundamental Physics and Laboratory for High Energy Physics, University of Bern, Bern; Switzerland*
[21] *School of Physics and Astronomy, University of Birmingham, Birmingham; United Kingdom*
[22] [(a)] *Facultad de Ciencias y Centro de Investigaciónes, Universidad Antonio Nariño, Bogotá;* [(b)] *Departamento de Física, Universidad Nacional de Colombia, Bogotá, Colombia; Colombia*
[23] [(a)] *INFN Bologna and Universita' di Bologna, Dipartimento di Fisica;* [(b)] *INFN Sezione di Bologna; Italy*
[24] *Physikalisches Institut, Universität Bonn, Bonn; Germany*
[25] *Department of Physics, Boston University, Boston MA; United States of America*
[26] *Department of Physics, Brandeis University, Waltham MA; United States of America*
[27] [(a)] *Transilvania University of Brasov, Brasov;* [(b)] *Horia Hulubei National Institute of Physics and Nuclear Engineering, Bucharest;* [(c)] *Department of Physics, Alexandru Ioan Cuza University of Iasi, Iasi;* [(d)] *National Institute for Research and Development of Isotopic and Molecular Technologies, Physics Department, Cluj-Napoca;* [(e)] *University Politehnica Bucharest, Bucharest;* [(f)] *West University in Timisoara, Timisoara; Romania*
[28] [(a)] *Faculty of Mathematics, Physics and Informatics, Comenius University, Bratislava;* [(b)] *Department of Subnuclear Physics, Institute of Experimental Physics of the Slovak Academy of Sciences, Kosice; Slovak Republic*
[29] *Physics Department, Brookhaven National Laboratory, Upton NY; United States of America*
[30] *Departamento de Física, Universidad de Buenos Aires, Buenos Aires; Argentina*
[31] *California State University, CA; United States of America*
[32] *Cavendish Laboratory, University of Cambridge, Cambridge; United Kingdom*
[33] [(a)] *Department of Physics, University of Cape Town, Cape Town;* [(b)] *iThemba Labs, Western Cape;* [(c)] *Department of Mechanical Engineering Science, University of Johannesburg, Johannesburg;* [(d)] *University of South Africa, Department of Physics, Pretoria;* [(e)] *School of Physics, University of the Witwatersrand, Johannesburg; South Africa*
[34] *Department of Physics, Carleton University, Ottawa ON; Canada*
[35] [(a)] *Faculté des Sciences Ain Chock, Réseau Universitaire de Physique des Hautes Energies – Université Hassan II, Casablanca;* [(b)] *Faculté des Sciences, Université Ibn-Tofail, Kénitra;* [(c)] *Faculté des Sciences Semlalia, Université Cadi Ayyad, LPHEA, Marrakech;* [(d)] *Moroccan Foundation for Advanced Science Innovation and Research (MASciR), Rabat;* [(e)] *LPMR, Faculté des Sciences, Université Mohamed Premier, Oujda;* [(f)] *Faculté des sciences, Université Mohammed V, Rabat; Morocco*
[36] *CERN, Geneva; Switzerland*
[37] *Enrico Fermi Institute, University of Chicago, Chicago IL; United States of America*
[38] *LPC, Université Clermont Auvergne, CNRS/IN2P3, Clermont-Ferrand; France*
[39] *Nevis Laboratory, Columbia University, Irvington NY; United States of America*

[40] Niels Bohr Institute, University of Copenhagen, Copenhagen; Denmark
[41] [(a)] Dipartimento di Fisica, Università della Calabria, Rende; [(b)] INFN Gruppo Collegato di Cosenza, Laboratori Nazionali di Frascati; Italy
[42] Physics Department, Southern Methodist University, Dallas TX; United States of America
[43] Physics Department, University of Texas at Dallas, Richardson TX; United States of America
[44] National Centre for Scientific Research "Demokritos", Agia Paraskevi; Greece
[45] [(a)] Department of Physics, Stockholm University; [(b)] Oskar Klein Centre, Stockholm; Sweden
[46] Deutsches Elektronen-Synchrotron DESY, Hamburg and Zeuthen; Germany
[47] Lehrstuhl für Experimentelle Physik IV, Technische Universität Dortmund, Dortmund; Germany
[48] Institut für Kern- und Teilchenphysik, Technische Universität Dresden, Dresden; Germany
[49] Department of Physics, Duke University, Durham NC; United States of America
[50] SUPA – School of Physics and Astronomy, University of Edinburgh, Edinburgh; United Kingdom
[51] INFN e Laboratori Nazionali di Frascati, Frascati; Italy
[52] Physikalisches Institut, Albert-Ludwigs-Universität Freiburg, Freiburg; Germany
[53] II. Physikalisches Institut, Georg-August-Universität Göttingen, Göttingen; Germany
[54] Département de Physique Nucléaire et Corpusculaire, Université de Genève, Genève; Switzerland
[55] [(a)] Dipartimento di Fisica, Università di Genova, Genova; [(b)] INFN Sezione di Genova; Italy
[56] II. Physikalisches Institut, Justus-Liebig-Universität Giessen, Giessen; Germany
[57] SUPA – School of Physics and Astronomy, University of Glasgow, Glasgow; United Kingdom
[58] LPSC, Université Grenoble Alpes, CNRS/IN2P3, Grenoble INP, Grenoble; France
[59] Laboratory for Particle Physics and Cosmology, Harvard University, Cambridge MA; United States of America
[60] [(a)] Department of Modern Physics and State Key Laboratory of Particle Detection and Electronics, University of Science and Technology of China, Hefei; [(b)] Institute of Frontier and Interdisciplinary Science and Key Laboratory of Particle Physics and Particle Irradiation (MOE), Shandong University, Qingdao; [(c)] School of Physics and Astronomy, Shanghai Jiao Tong University, Key Laboratory for Particle Astrophysics and Cosmology (MOE), SKLPPC, Shanghai; [(d)] Tsung-Dao Lee Institute, Shanghai; China
[61] [(a)] Kirchhoff-Institut für Physik, Ruprecht-Karls-Universität Heidelberg, Heidelberg; [(b)] Physikalisches Institut, Ruprecht-Karls-Universität Heidelberg, Heidelberg; Germany
[62] Faculty of Applied Information Science, Hiroshima Institute of Technology, Hiroshima; Japan
[63] [(a)] Department of Physics, Chinese University of Hong Kong, Shatin, N.T., Hong Kong; [(b)] Department of Physics, University of Hong Kong, Hong Kong; [(c)] Department of Physics and Institute for Advanced Study, Hong Kong University of Science and Technology, Clear Water Bay, Kowloon, Hong Kong; China
[64] Department of Physics, National Tsing Hua University, Hsinchu; Taiwan
[65] IJCLab, Université Paris-Saclay, CNRS/IN2P3, 91405, Orsay; France
[66] Department of Physics, Indiana University, Bloomington IN; United States of America
[67] [(a)] INFN Gruppo Collegato di Udine, Sezione di Trieste, Udine; [(b)] ICTP, Trieste; [(c)] Dipartimento Politecnico di Ingegneria e Architettura, Università di Udine, Udine; Italy
[68] [(a)] INFN Sezione di Lecce; [(b)] Dipartimento di Matematica e Fisica, Università del Salento, Lecce; Italy
[69] [(a)] INFN Sezione di Milano; [(b)] Dipartimento di Fisica, Università di Milano, Milano; Italy
[70] [(a)] INFN Sezione di Napoli; [(b)] Dipartimento di Fisica, Università di Napoli, Napoli; Italy
[71] [(a)] INFN Sezione di Pavia; [(b)] Dipartimento di Fisica, Università di Pavia, Pavia; Italy
[72] [(a)] INFN Sezione di Pisa; [(b)] Dipartimento di Fisica E. Fermi, Università di Pisa, Pisa; Italy
[73] [(a)] INFN Sezione di Roma; [(b)] Dipartimento di Fisica, Sapienza Università di Roma, Roma; Italy
[74] [(a)] INFN Sezione di Roma Tor Vergata; [(b)] Dipartimento di Fisica, Università di Roma Tor Vergata, Roma; Italy
[75] [(a)] INFN Sezione di Roma Tre; [(b)] Dipartimento di Matematica e Fisica, Università Roma Tre, Roma; Italy
[76] [(a)] INFN-TIFPA; [(b)] Università degli Studi di Trento, Trento; Italy
[77] Institut für Astro- und Teilchenphysik, Leopold-Franzens-Universität, Innsbruck; Austria
[78] University of Iowa, Iowa City IA; United States of America
[79] Department of Physics and Astronomy, Iowa State University, Ames IA; United States of America
[80] Joint Institute for Nuclear Research, Dubna; Russia
[81] [(a)] Departamento de Engenharia Elétrica, Universidade Federal de Juiz de Fora (UFJF), Juiz de Fora; [(b)] Universidade Federal do Rio De Janeiro COPPE/EE/IF, Rio de Janeiro; [(c)] Instituto de Física, Universidade de São Paulo, São Paulo; Brazil
[82] KEK, High Energy Accelerator Research Organization, Tsukuba; Japan
[83] Graduate School of Science, Kobe University, Kobe; Japan
[84] [(a)] AGH University of Science and Technology, Faculty of Physics and Applied Computer Science, Krakow; [(b)] Marian Smoluchowski Institute of Physics, Jagiellonian University, Krakow; Poland
[85] Institute of Nuclear Physics Polish Academy of Sciences, Krakow; Poland
[86] Faculty of Science, Kyoto University, Kyoto; Japan
[87] Kyoto University of Education, Kyoto; Japan
[88] Research Center for Advanced Particle Physics and Department of Physics, Kyushu University, Fukuoka ; Japan
[89] Instituto de Física La Plata, Universidad Nacional de La Plata and CONICET, La Plata; Argentina
[90] Physics Department, Lancaster University, Lancaster; United Kingdom
[91] Oliver Lodge Laboratory, University of Liverpool, Liverpool; United Kingdom
[92] Department of Experimental Particle Physics, Jožef Stefan Institute and Department of Physics, University of Ljubljana, Ljubljana; Slovenia
[93] School of Physics and Astronomy, Queen Mary University of London, London; United Kingdom
[94] Department of Physics, Royal Holloway University of London, Egham; United Kingdom
[95] Department of Physics and Astronomy, University College London, London; United Kingdom
[96] Louisiana Tech University, Ruston LA; United States of America
[97] Fysiska institutionen, Lunds universitet, Lund; Sweden
[98] Centre de Calcul de l'Institut National de Physique Nucléaire et de Physique des Particules (IN2P3), Villeurbanne; France
[99] Departamento de Física Teorica C-15 and CIAFF, Universidad Autónoma de Madrid, Madrid; Spain
[100] Institut für Physik, Universität Mainz, Mainz; Germany
[101] School of Physics and Astronomy, University of Manchester, Manchester; United Kingdom
[102] CPPM, Aix-Marseille Université, CNRS/IN2P3, Marseille; France
[103] Department of Physics, University of Massachusetts, Amherst MA; United States of America
[104] Department of Physics, McGill University, Montreal QC; Canada
[105] School of Physics, University of Melbourne, Victoria; Australia
[106] Department of Physics, University of Michigan, Ann Arbor MI; United States of America
[107] Department of Physics and Astronomy, Michigan State University, East Lansing MI; United States of America
[108] B.I. Stepanov Institute of Physics, National Academy of Sciences of Belarus, Minsk; Belarus
[109] Research Institute for Nuclear Problems of Byelorussian State University, Minsk; Belarus
[110] Group of Particle Physics, University of Montreal, Montreal QC; Canada
[111] P.N. Lebedev Physical Institute of the Russian Academy of Sciences, Moscow; Russia
[112] National Research Nuclear University MEPhI, Moscow; Russia
[113] D.V. Skobeltsyn Institute of Nuclear Physics, M.V. Lomonosov Moscow State University, Moscow; Russia
[114] Fakultät für Physik, Ludwig-Maximilians-Universität München, München; Germany

[115] Max-Planck-Institut für Physik (Werner-Heisenberg-Institut), München; Germany
[116] Nagasaki Institute of Applied Science, Nagasaki; Japan
[117] Graduate School of Science and Kobayashi-Maskawa Institute, Nagoya University, Nagoya; Japan
[118] Department of Physics and Astronomy, University of New Mexico, Albuquerque NM; United States of America
[119] Institute for Mathematics, Astrophysics and Particle Physics, Radboud University/Nikhef, Nijmegen; Netherlands
[120] Nikhef National Institute for Subatomic Physics and University of Amsterdam, Amsterdam; Netherlands
[121] Department of Physics, Northern Illinois University, DeKalb IL; United States of America
[122] [(a)] Budker Institute of Nuclear Physics and NSU, SB RAS, Novosibirsk; [(b)] Novosibirsk State University Novosibirsk; Russia
[123] Institute for High Energy Physics of the National Research Centre Kurchatov Institute, Protvino; Russia
[124] Institute for Theoretical and Experimental Physics named by A.I. Alikhanov of National Research Centre "Kurchatov Institute", Moscow; Russia
[125] Department of Physics, New York University, New York NY; United States of America
[126] Ochanomizu University, Otsuka, Bunkyo-ku, Tokyo; Japan
[127] Ohio State University, Columbus OH; United States of America
[128] Homer L. Dodge Department of Physics and Astronomy, University of Oklahoma, Norman OK; United States of America
[129] Department of Physics, Oklahoma State University, Stillwater OK; United States of America
[130] Palacký University, RCPTM, Joint Laboratory of Optics, Olomouc; Czech Republic
[131] Institute for Fundamental Science, University of Oregon, Eugene, OR; United States of America
[132] Graduate School of Science, Osaka University, Osaka; Japan
[133] Department of Physics, University of Oslo, Oslo; Norway
[134] Department of Physics, Oxford University, Oxford; United Kingdom
[135] LPNHE, Sorbonne Université, Université de Paris, CNRS/IN2P3, Paris; France
[136] Department of Physics, University of Pennsylvania, Philadelphia PA; United States of America
[137] Konstantinov Nuclear Physics Institute of National Research Centre "Kurchatov Institute", PNPI, St. Petersburg; Russia
[138] Department of Physics and Astronomy, University of Pittsburgh, Pittsburgh PA; United States of America
[139] [(a)] Laboratório de Instrumentação e Física Experimental de Partículas – LIP, Lisboa; [(b)] Departamento de Física, Faculdade de Ciências, Universidade de Lisboa, Lisboa; [(c)] Departamento de Física, Universidade de Coimbra, Coimbra; [(d)] Centro de Física Nuclear da Universidade de Lisboa, Lisboa; [(e)] Departamento de Física, Universidade do Minho, Braga; [(f)] Departamento de Física Teórica y del Cosmos, Universidad de Granada, Granada (Spain); [(g)] Dep Física and CEFITEC of Faculdade de Ciências e Tecnologia, Universidade Nova de Lisboa, Caparica; [(h)] Instituto Superior Técnico, Universidade de Lisboa, Lisboa; Portugal
[140] Institute of Physics of the Czech Academy of Sciences, Prague; Czech Republic
[141] Czech Technical University in Prague, Prague; Czech Republic
[142] Charles University, Faculty of Mathematics and Physics, Prague; Czech Republic
[143] Particle Physics Department, Rutherford Appleton Laboratory, Didcot; United Kingdom
[144] IRFU, CEA, Université Paris-Saclay, Gif-sur-Yvette; France
[145] Santa Cruz Institute for Particle Physics, University of California Santa Cruz, Santa Cruz CA; United States of America
[146] [(a)] Departamento de Física, Pontificia Universidad Católica de Chile, Santiago; [(b)] Universidad Andres Bello, Department of Physics, Santiago; [(c)] Instituto de Alta Investigación, Universidad de Tarapacá; [(d)] Departamento de Física, Universidad Técnica Federico Santa María, Valparaíso; Chile
[147] Universidade Federal de São João del Rei (UFSJ), São João del Rei; Brazil
[148] Department of Physics, University of Washington, Seattle WA; United States of America
[149] Department of Physics and Astronomy, University of Sheffield, Sheffield; United Kingdom
[150] Department of Physics, Shinshu University, Nagano; Japan
[151] Department Physik, Universität Siegen, Siegen; Germany
[152] Department of Physics, Simon Fraser University, Burnaby BC; Canada
[153] SLAC National Accelerator Laboratory, Stanford CA; United States of America
[154] Physics Department, Royal Institute of Technology, Stockholm; Sweden
[155] Departments of Physics and Astronomy, Stony Brook University, Stony Brook NY; United States of America
[156] Department of Physics and Astronomy, University of Sussex, Brighton; United Kingdom
[157] School of Physics, University of Sydney, Sydney; Australia
[158] Institute of Physics, Academia Sinica, Taipei; Taiwan
[159] [(a)] E. Andronikashvili Institute of Physics, Iv. Javakhishvili Tbilisi State University, Tbilisi; [(b)] High Energy Physics Institute, Tbilisi State University, Tbilisi; Georgia
[160] Department of Physics, Technion, Israel Institute of Technology, Haifa; Israel
[161] Raymond and Beverly Sackler School of Physics and Astronomy, Tel Aviv University, Tel Aviv; Israel
[162] Department of Physics, Aristotle University of Thessaloniki, Thessaloniki; Greece
[163] International Center for Elementary Particle Physics and Department of Physics, University of Tokyo, Tokyo; Japan
[164] Graduate School of Science and Technology, Tokyo Metropolitan University, Tokyo; Japan
[165] Department of Physics, Tokyo Institute of Technology, Tokyo; Japan
[166] Tomsk State University, Tomsk; Russia
[167] Department of Physics, University of Toronto, Toronto ON; Canada
[168] [(a)] TRIUMF, Vancouver BC; [(b)] Department of Physics and Astronomy, York University, Toronto ON; Canada
[169] Division of Physics and Tomonaga Center for the History of the Universe, Faculty of Pure and Applied Sciences, University of Tsukuba, Tsukuba; Japan
[170] Department of Physics and Astronomy, Tufts University, Medford MA; United States of America
[171] Department of Physics and Astronomy, University of California Irvine, Irvine CA; United States of America
[172] Department of Physics and Astronomy, University of Uppsala, Uppsala; Sweden
[173] Department of Physics, University of Illinois, Urbana IL; United States of America
[174] Instituto de Física Corpuscular (IFIC), Centro Mixto Universidad de Valencia – CSIC, Valencia; Spain
[175] Department of Physics, University of British Columbia, Vancouver BC; Canada
[176] Department of Physics and Astronomy, University of Victoria, Victoria BC; Canada
[177] Fakultät für Physik und Astronomie, Julius-Maximilians-Universität Würzburg, Würzburg; Germany
[178] Department of Physics, University of Warwick, Coventry; United Kingdom
[179] Waseda University, Tokyo; Japan
[180] Department of Particle Physics and Astrophysics, Weizmann Institute of Science, Rehovot; Israel
[181] Department of Physics, University of Wisconsin, Madison WI; United States of America
[182] Fakultät für Mathematik und Naturwissenschaften, Fachgruppe Physik, Bergische Universität Wuppertal, Wuppertal; Germany
[183] Department of Physics, Yale University, New Haven CT; United States of America

[a] Also at Borough of Manhattan Community College, City University of New York, New York NY; United States of America.
[b] Also at Centro Studi e Ricerche Enrico Fermi; Italy.
[c] Also at CERN, Geneva; Switzerland.
[d] Also at CPPM, Aix-Marseille Université, CNRS/IN2P3, Marseille; France.
[e] Also at Département de Physique Nucléaire et Corpusculaire, Université de Genève, Genève; Switzerland.

[f] Also at Departament de Fisica de la Universitat Autonoma de Barcelona, Barcelona; Spain.
[g] Also at Department of Financial and Management Engineering, University of the Aegean, Chios; Greece.
[h] Also at Department of Physics and Astronomy, Michigan State University, East Lansing MI; United States of America.
[i] Also at Department of Physics and Astronomy, University of Louisville, Louisville, KY; United States of America.
[j] Also at Department of Physics, Ben Gurion University of the Negev, Beer Sheva; Israel.
[k] Also at Department of Physics, California State University, East Bay; United States of America.
[l] Also at Department of Physics, California State University, Fresno; United States of America.
[m] Also at Department of Physics, California State University, Sacramento; United States of America.
[n] Also at Department of Physics, King's College London, London; United Kingdom.
[o] Also at Department of Physics, St. Petersburg State Polytechnical University, St. Petersburg; Russia.
[p] Also at Department of Physics, University of Fribourg, Fribourg; Switzerland.
[q] Also at Dipartimento di Matematica, Informatica e Fisica, Università di Udine, Udine; Italy.
[r] Also at Faculty of Physics, M.V. Lomonosov Moscow State University, Moscow; Russia.
[s] Also at Giresun University, Faculty of Engineering, Giresun; Turkey.
[t] Also at Graduate School of Science, Osaka University, Osaka; Japan.
[u] Also at Hellenic Open University, Patras; Greece.
[v] Also at IJCLab, Université Paris-Saclay, CNRS/IN2P3, 91405, Orsay; France.
[w] Also at Institucio Catalana de Recerca i Estudis Avancats, ICREA, Barcelona; Spain.
[x] Also at Institut für Experimentalphysik, Universität Hamburg, Hamburg; Germany.
[y] Also at Institute for Mathematics, Astrophysics and Particle Physics, Radboud University/Nikhef, Nijmegen; Netherlands.
[z] Also at Institute for Nuclear Research and Nuclear Energy (INRNE) of the Bulgarian Academy of Sciences, Sofia; Bulgaria.
[aa] Also at Institute for Particle and Nuclear Physics, Wigner Research Centre for Physics, Budapest; Hungary.
[ab] Also at Institute of Particle Physics (IPP); Canada.
[ac] Also at Institute of Physics, Azerbaijan Academy of Sciences, Baku; Azerbaijan.
[ad] Also at Instituto de Fisica Teorica, IFT-UAM/CSIC, Madrid; Spain.
[ae] Also at Istanbul University, Dept. of Physics, Istanbul; Turkey.
[af] Also at Joint Institute for Nuclear Research, Dubna; Russia.
[ag] Also at Louisiana Tech University, Ruston LA; United States of America.
[ah] Also at Moscow Institute of Physics and Technology State University, Dolgoprudny; Russia.
[ai] Also at National Research Nuclear University MEPhI, Moscow; Russia.
[aj] Also at Physics Department, An-Najah National University, Nablus; Palestine.
[ak] Also at Physikalisches Institut, Albert-Ludwigs-Universität Freiburg, Freiburg; Germany.
[al] Also at The City College of New York, New York NY; United States of America.
[am] Also at TRIUMF, Vancouver BC; Canada.
[an] Also at Universita di Napoli Parthenope, Napoli; Italy.
[ao] Also at University of Chinese Academy of Sciences (UCAS), Beijing; China.
[*] Deceased.